Generation and Evaluation of Truss Structures for the Strut-and-Tie Model.

Based on Topology Optimization Results for Deep Concrete Beams.

G.P. Argudo Sanchez

Delft University of Technology

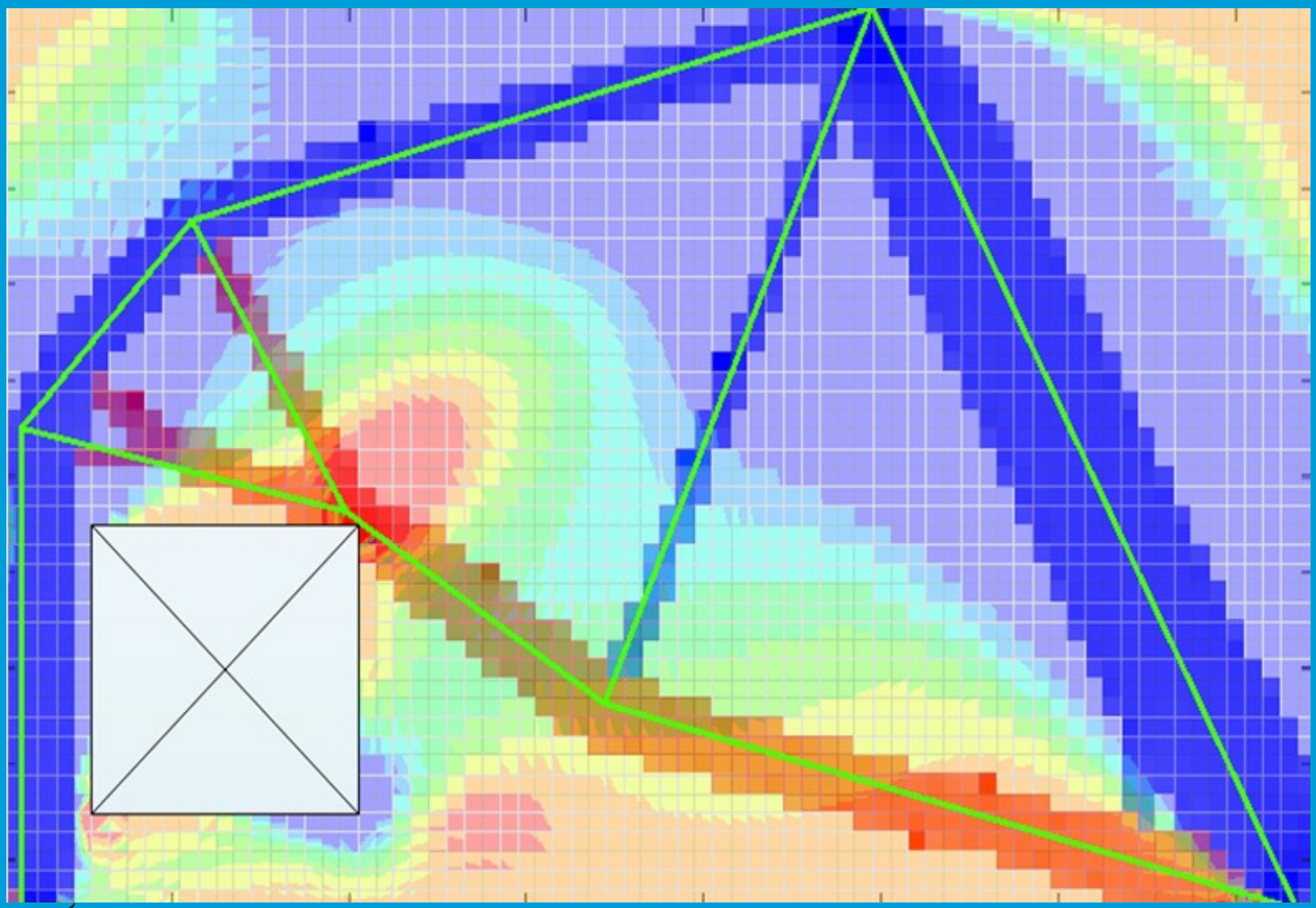

TU Delft

Generation and Evaluation of Truss Structures for the Strut-and-Tie model.

Based on Topology Optimization Results for Deep Concrete Beams.

by

G.P. Argudo Sanchez

to obtain the degree of Master of Science
at the Delft University of Technology,
to be defended publicly on Monday August 19, 2019 at 10:00 AM.

Student number: 4751779

Thesis committee:

Dr. ir. M. Hendriks,	TU Delft, Chair
Dr. ir. M. Lukovic ,	TU Delft, Supervisor
Ir. L. Houben ,	TU Delft, Supervisor
MSc. Y. Xia ,	TU Delft, Daily supervisor

TU Delft

ABSTRACT

The Strut-and-Tie model (STM) is an efficient technique for the design of concrete structures, but the creation of suitable truss structures gets complicated when these structures become more complex. The topology optimization (TO) is a convenient technique that has been used in recent years for the creation of trusses of complex structures for the STM.

This thesis presents a process for the creation of suitable truss structures for the STM using the results obtained with the TO, as well as, an evaluation of them to see which is the most optimal truss structure according to the total amount of tension force present on the full truss, this total amount of tension force is the selected evaluation criterion. Three deep concrete beams were analyzed using two topology optimization (SIMP and BESO approaches) for the generation of stress paths, these approaches are based on the minimization of the strain energy. The procedure starts with the computation of the principal stresses over the results of the topology optimization, then bar elements are placed over the stress paths of these diagrams creating a first (harsh) layout of the trusses. These trusses were not always found stable, but all the trusses were stabilized because, in this way, it is easy to calculate the axial force of in the truss elements, thus satisfy a basic requirement of the STM. To stabilize the truss structures two methods were explored. (i) The addition of new members outside of the stress paths (stabilizers), the essential characteristic of these new elements is that the axial force in them should be zero to not change the stress distribution found during the optimization process. A sensitivity analysis of the stabilizers was performed to track how the axial force changes in these members depending on the position of the nodes connected to them, this process was necessary because when an element outside the stress paths has axial force the stress diagrams have been changed. (ii) The creation of substructures within the stress paths, this process stabilizes the global structure without the addition of members outside the stress paths. Finally, a structural analysis was performed to obtain the axial forces in each member of the truss structure, and through an analysis of these results, the total amount of tension forces in the truss was computed. The truss with the minimum value of total tension force is assumed as the most optimal structure for each case. It is clear through the analysis that the variation of the input parameters does not cause large variations in the results of the topology optimization, but it has an impact in the stabilization process and the performance of the structures according to the evaluation criterion. Furthermore, it has been proved that suitable trusses for the STM can be created using any of the two selected optimization approaches obtaining good results, and a similar performance according to the evaluation criterion.

ACKNOWLEDGEMENTS

I would like to thank all the people who support me during this thesis and these whole two years: First, I would like to thank my thesis supervisor and committee chair Max Hendriks, for allowing me to work in this project, and for all the constructive and positive feedback. To Mladena Lukovic member of my committee, for her friendly attitude and her willingness to answer all my questions, her support during this whole process was very important. Especially, I want to thank MSc. Yi Xia, my daily supervisor for taking this project as his own, for his concern, supervision, and help since the first day that I started working on it. Also, I want to thank all my family, especially to my parents and brother for their support and love, without them, anything of this would have been possible. Finally, I want to thank all my friends for always being there when I needed them, and for making these past two years amazing ones. I would also like to acknowledge the funding of the Ecuadorean government thorough the Secretary of Superior Education, Science, Technology and innovation (SENESCYT)

CONTENTS

LIST OF FIGURES

LIST OF TABLES

1 INTRODUCTION

1.1 GENERAL OVERVIEW

During the design of reinforced concrete structures two types of regions that can be identified, (i) Bernoulli regions (B regions), where the Bernoulli's Hypothesis (plane sections remain plane after the deformation of the structure) is valid, and (ii) Disturbed region (D regions), where the stress or strains have a non-linear or complex distributions. The D regions can happen for two main reasons, (i) openings or sudden changes in the geometry of the structure, and (ii) application of concentrated loads or the presence of point supports [10]. Disturbed regions represent a problem for simple methods of analysis, because in these regions the Bernoulli hypothesis is not valid anymore. Innovative design methods as the Strut-and-Tie method or finite element analysis have been used to design structures with D regions. The Strut-and-Tie method (STM) is used as a basic approach for the design of non-standard concrete structures, especially for structures with disturbed regions. The STM is formed by three types of elements, the struts are elements under compression, the ties are elements under tension, and the nodes are elements created by the intersection of two or more struts/ties. The STM always gives a safe lower bound analysis for the final capacity of a structure, this model assumes that the concrete can carry only compressive stresses, and the tensile stresses will be carried by the reinforcement present on the beam [11].

Optimization processes have been used in many fields of engineering, and of the industry in general. The term optimization refers to find an optimal shape or material distribution for given conditions. In structural engineering, the optimization process has been used in recent years to find the most economical, or optimal shape of structures. These concepts, precisely the Topology Optimization (TO) are applied in this thesis to deep concrete beams, to obtain valid truss structures for the creating of the STM these beams.

This thesis focused on obtaining optimal truss structures for three deep concrete beams (Bernoulli's hypothesis is not valid), that could be used as the STM of these structures. Many approaches can be used to find these truss structures, but in this thesis, two approaches based on the minimization of the strain energy are used, the simplified isotropic material with penalization (SIMP) approach, this approach is the most popular approach for topology optimization, and the bi-directional evolutionary structural optimization (BESO) approach, this approach is a relatively new and it started as an extension of the evolutionary structural optimization approach. The results obtained from the optimization process are compared to see how the created truss structures differ from one approach to the other. Once that,

these truss structures have been created a stability check was performed on them, in case they were non-stable, they were stabilized to perform structural analysis. Having stable trusses is not an essential requirement for the STM, but it makes easier the calculation of the axial force in the elements of the trusses. Finally, to find the most optimal truss structure, according to the evaluation criteria, which satisfy the optimization process, the total amount of tension force in the ties of each truss is determined. It was assumed that the optimal truss structure for each case was the one with minimum total tension force.

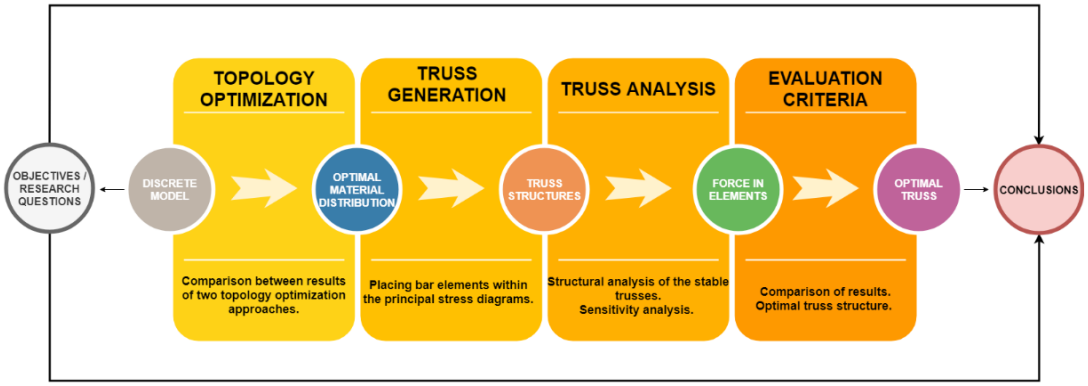

Figure 1.1: Overview

1.2 OBJECTIVES AND RESEARCH QUESTIONS

The main objectives of this thesis are:

1. **Generation of truss structures based on the results obtained during the Topology optimization for each studied case.** The truss structures that are created should be consistent with the results of the topology optimization.

2. **Implementation of the topology optimization to MATLAB scripts for deep concrete beams using different approaches.** Two different approaches of topology optimization are analyzed, the SIMP and BESO approach. The creation of the MATLAB scripts is be based on previous educational scripts.

3. **Determination of the most optimal truss structure for each case based on an specific evaluation criterion.** The determination of the most optimal truss is based on the total minimum tensile force in the truss.

In order to achieve these objectives the following research questions would be answered:

a Can suitable truss structures for the Strut-and-Tie model always be created from the results obtained in the topology optimization ?

b What is the influence of the input parameters for each approach, and to what extent do these approaches differ in the results of the topology optimization, and truss generation ?

c Which aspects should be considered to stabilize the truss structures obtained using topology optimization?

d How sensitive are the stabilizers of the trusses to change the stress diagrams obtained with the topology optimization?

e Which is the most optimal approach (SIMP or BESO) for topology optimization to create truss structures based on the results of the optimization process according to the evaluation criteria?

1.3 RESEARCH STRUCTURE

This study will be divided on five stages, specific results are expected on each stage of the study.

i **Literature Review. -** This first stage of the study consists on the review of previous studies about TO and STMs, familiarization with different approaches of the TO, creation of truss structures based on TO, improving programing skills through the implementation and modification of an educational script.

ii **Topological Optimization implementation. -** In this second stage of the study, MATLAB scripts are created for the SIMP and BESO approaches. They will be based on a well-known educational code which use a SIMP approach for a symmetric simple supported beam. The topology optimization is applied to the three deep concrete beams.

iii **Truss Structure Generation. -** The third stage of the study consists on the generation of truss structures for the STM, they are generated based on the results obtained from the TO. Always considering that the elements of the trusses should be within the stress diagrams of the TO.

iv **Evaluation of Truss Structures. –** In this stage, different trusses for each case are evaluated, to determinate the axial force on its members. These forces will be used to determinate the total amount of tension force in the structure.

v **Conclusions. -** In this final stage, conclusions, recommendations, and further research will be state. Besides, all the parts of the thesis will be putting together.

2 LITERATURE REVIEW

2.1 STRUT-AND-TIE MODEL

2.1.1 Introduction and Principle of the Strut-and-Tie model

The Strut-and-Tie method as is known today was proposed by Schlaich, Schäfer,and Jennewein, (1987), it appeared as a generalization of the truss model proposed by Ritter (1899). The main difference between these methods are, (i) in Ritter truss structures all the elements have inclinations of 0°, 90°, or 45°, while the Strut-and-Tie model allows to its elements have any inclination, (ii)Ritter truss structures are valid only for beam regions (B regions), in B regions the Bernoulli hypothesis of linear strains distribution is valid, B regions are the parts of the structure with constant, or gradually changes in depth, and where the load is evenly distributed. Whereas the Strut-and-Tie model is valid for B regions and for disturbed regions (D regions), D regions have two origins. (i) Geometrical, due to the presence of holes or discontinuities in the beam, and large relations h/l (deep beams) (ii) Mechanical, for the application of point loads, or support reactions of the beam [10] [12]. In these kind of regions the Bernoulli hypothesis of linear strains is not valid anymore, because the strains, and stresses have non-linear distributions, Figure 2.1 shows B and D regions for a simply supported beam under distributed load.

The Strut-and-Tie method uses a generalized design concept that could be applied to all kinds of structures, and to all the parts of a structure. The Strut-and-Tie method can also be applied to prestressed concrete structures. [3] [8]. Truss models represent an idealized scheme where the stress distribution of a structure can be represented by struts, ties, and nodes (Figure 2.2). The struts are compression fields that are idealized as compression members, the ties are tension members that in most of cases are resisted by the reinforcement, and the nodes are points where the struts, ties, and external forces intersect, for equilibrium conditions in a node at least three forces should be present [8].

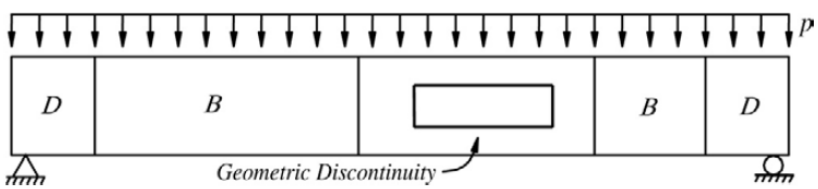

Figure 2.1: Different regions in a beam [1].

The main objective of the Strut-and-Tie model is describing the structural behavior in a fully cracked state of a RC structure. The Strut-and-Tie model

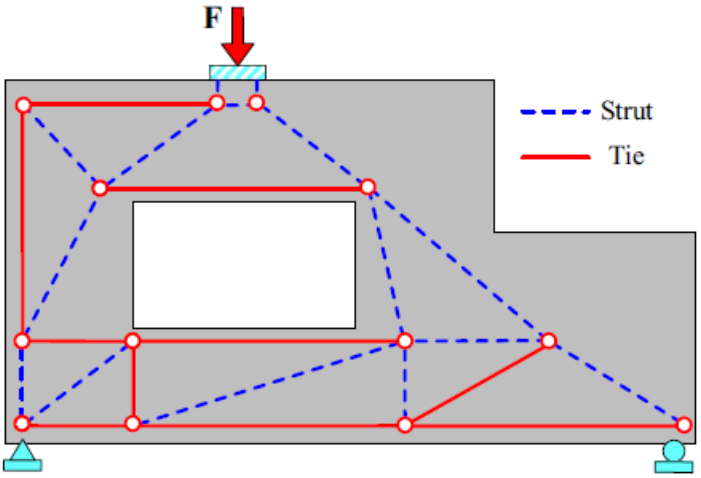

Figure 2.2: Elements of the Strut-and-Tie model [2].

is based on the concept that the inner forces of a structure could be represented as stress trajectories, or load paths. However, placing truss elements for the Strut-and-Tie model within the load paths neglects some capacity of the structure at the moment of determining the ultimate load capacity. On the other hand, an advantage of this procedure is that one model can be used for serviceability capacity, and ultimate capacity applying the theory of plasticity. Since disturbed regions (D regions) can have many load paths, the Strut-and-Tie model for a RC structure is not unique, the models would depend on the desire and expertise of the designer, for instance, the safest model will vary from the cheapest one, etc. [1] [3].

The Strut-and-Tie model gives always a lower bound limit for the analysis of a structure, because it is based on the lower-bound theorem. The lower-bound theorem states that "if an equilibrium distribution of stress can be found which balances the applied loads, and is everywhere below yield or at yield, the structure will not collapse or will be just at the point of collapse." The use of limit analysis theorems for the Strut-and-Tie model comes from two assumptions. (i) Perfect plastic material, the material of the structure has not hardened or softening. (ii) Small deformations, the structure suffers only small deformations, thus the geometry of the structure does not change, for this reason, the principle of virtual work can be used to calculate the limit theorems. [8] [13] . Since, the Strut-and-Tie model analyze the structure at the moment of collapse, the model should satisfy two conditions for considering a model acceptable, (i) equilibrium condition, and (ii) yield criterion. This method can be used with different materials, being specially useful for materials with a low tension capacity [8].

2.1.2 Truss Structures Generation

The generation of truss structures are essential for the creation of Strut-and-Tie models (STMs), but this truss structures are not unique, meaning that for a specific beam, several truss structures can be found. The Strut-and-Tie model changes depending on the loading, and support conditions, in other words, a simple supported beam would have different a STM, if the beam is

under the action of a point load, than if the same beam is under the action of a distributed load. The trusses that would be used for the creation of the Strut-and-Tie should be *statically admissible like systems* [14], it means that the structure should satisfy equilibrium conditions under the applied force.

Several authors have chosen as the best Strut-and-Tie model the one that provides maximum stiffness for a given volume constrains, for concrete structures, since this material allows only limited plastic deformations, the internal structure (truss structure) should be one that keeps the deformations within this limit[3] [14]. On the other hand, Schlaich et al. [15] proposed that the best Strut-and-Tie model is the one with shortest ties. However, the best Strut-and-Tie model model will depend on the needs of the designer.

The most popular technique to find Strut-and-Tie models is using an elastic stress distribution, and the load paths method. This method oriented the struts and ties in the direction of the principal stress trajectories. Following the load paths will produce trusses with smoothly curved elements, in order to obtain a truss like structure these curved elements should be replaced by straight elements forming polygons. Once that all the curved elements have been replaced, it would be necessary to add some extra elements (struts or ties) to the truss structure to guarantee transverse equilibrium and truss stability [3] [8]. The final result after the addition of the extra elements is the Strut-and-Tie model. This process is illustrated in Figure 2.3. One drawback of this approach is, that for complex geometries or loading conditions, finding the Strut-and-Tie model becomes complex and time consuming a solution for this cases is using topology optimization to create the Strut-and-Tie model [7].

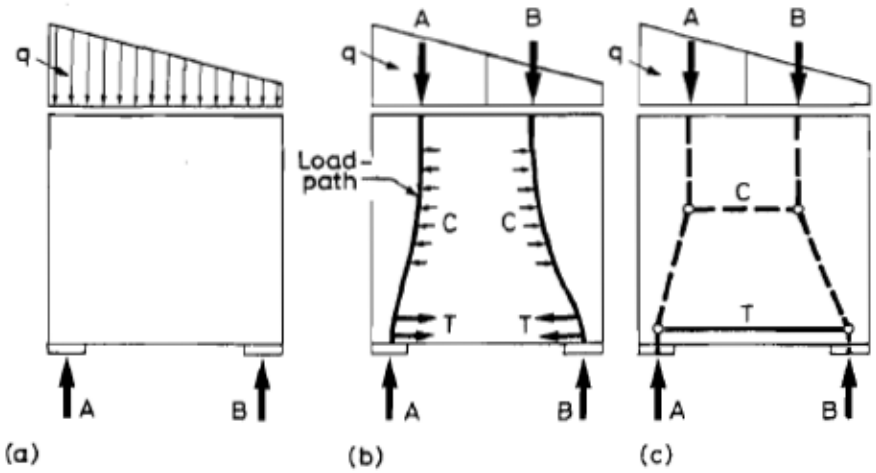

Figure 2.3: Truss generation process: (a) Discrete Model; (b) Load paths of the structure; (c) Structure after elements addition. [3].

A useful technique to find the location and direction of the elements of the trusses within the stress paths is performing an finite element analysis, in this analysis the stresses paths in the principal directions can be calculated. Then according to the load path method to obtain a truss like structure, the truss elements can be placed at the middle of the principal stress diagrams [3][8].

2.1.3 Truss Stability

A truss structure is defined as any structure where its elements resist only axial forces, and the bending moment at the joints is zero. There are three basic types of structures: (i) simple structures, these kind of structures are constructed from a triangle, however, it does not mean that the truss consist of only triangles. (ii) compound structures, they are formed by the connection of multiple simple trusses. (iii) complex structures, this type of trusses can not be classified as a simple or compound structure, but they satisfy force and stability criteria [4].

A important concept in the stability of trusses is the determinacy of a structure, it is given by the relation between the number of unknowns of the system and the number of equations of equilibrium to solve them. In this way, the unknowns of the system are the number *"b"* of forces in every member (one unknown per member), and the number *"r"* of support reactions. On the other hand, the number of equations of equilibrium are function of the number of nodes or joints in the structure. Since, it is necessary to satisfy the equilibrium in both directions, the sum of forces in both directions should be equal to zero, $Fx = 0$ and $Fy = 0$. Based on it, there are two equations of equilibrium per node (*"2j"*). The degree of determinacy is given by the comparison of the total number of unknowns with the total number of equations of equilibrium Equation 2.1 shows the three possible cases that can be expected:

$$\begin{aligned} b + r < 2j \quad & \text{Unstable structure} \\ b + r = 2j \quad & \text{Statically determinate structure} \\ b + r > 2j \quad & \text{Statically indeterminate structure} \end{aligned} \tag{2.1}$$

Although the stability of a truss is not a fundamental requirement for the Strut-and-Tie model, the truss is stabilized to easily obtain the axial forces acting in its members. There are two cases where the structure can be unstable, even if the structure satisfy the determinacy criteria. The first case is known as external stability, the structure is unstable, if all of its reactions are concurrent or parallel, these case is shown in Figure 2.4. The second case is the internal stability, a structure is unstable if its joints do not hold in affixed position. It means that its joints can move in a "rigid body" sense with respect to other joints, the truss of Figure 2.5 is unstable because there are not elements that restrain the movement between joints *"E"* and *"B"*, or between joints *"F"* and *"C"*[4].

In case of having unstable truss structures due to the lack of elements $b + r < 2j$, it is necessary to add the missing number of elements to create a stable truss in which a structural analysis can be performed to obtain the internal axial forces [4]. This is the case in most of trusses of the Strut-and-Tie models, it does not mean that the structure would collapse due to lack of stability, it means that "any movement of the model nodes evokes diagonal compression forces in the concrete, which stabilize the system" Thus, these additional elements in most cases do no help to carry loads of the structures, in other words, the forces in these additional members are zero or close

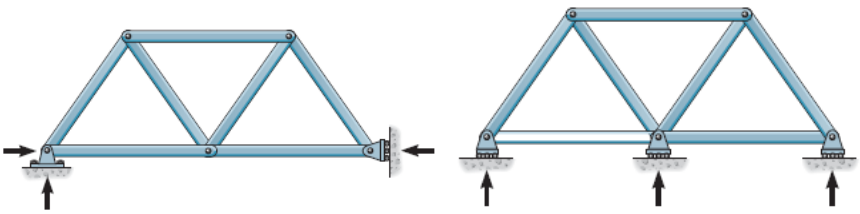

(a) Concurrent reactions (Unstable structure). **(b)** Parallel reactions (Unstable structure)

Figure 2.4: External Stability [4]

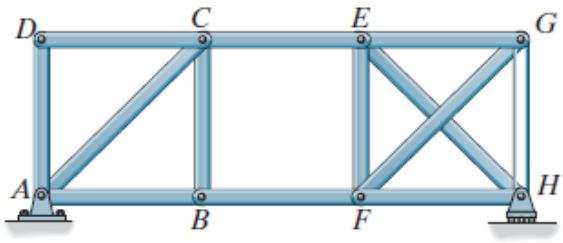

Figure 2.5: Internal Stability [4]

to zero because the function of these additional elements is stabilizing the structure. [8].

2.1.4 Principal Stresses Calculation

The principal stresses of a element are the maximum and minimum normal stress that the elements of a structure experience, these stresses occur in the surfaces where the shear stress is zero [16]. The discretization of the beam was made using four-noded quadrilateral elements, these elements have two degrees of freedom per node. The unknown fields of these elements are found interpolating the polynomial shape functions of each element. To find the element shape functions basic relationships from continuum mechanics were used to. So, the displacement and strain fields for a element of the beam, are give by Equations 2.2 and 2.3 respectively,

$$u^h = Na_e \tag{2.2}$$

$$\epsilon^h = Ba_e \tag{2.3}$$

where the matrix **N** contains the element shape functions for a element, the matrix **B** contains the derivaties of the element shape functions with respect to the unknown fields (displacements in x and y), and a_e represents the elements displacements.

Linear shape functions are used to obtain the matrices **N** and **B**, as quadrilateral elements are being used the shape functions for the ith node on a bi-unit square are given by Equation 2.4.

$$N_i(\xi,\eta) = \frac{1}{4}(1+\xi_i\xi)(1+\eta_i\eta) \tag{2.4}$$

For the calculation of the stresses σ_{xx}, σ_{yy}, numerical integration and isoparametric mapping are used. For the numerical integration a 2x2 Gauss integration scheme is used. The stress is given by Equation 2.5, where matrix D^e is the elastic stiffness matrix for a element. Substituting Equation 2.3 in 2.5, Equation 2.6 is obtained [17] [16]. This equations will be used for the calculation of the stresses of the elements.

$$\sigma = D^e\epsilon \tag{2.5}$$

$$\sigma = DBu \tag{2.6}$$

Since 2D elements are used for the discretization of the beam , the use of Equation 2.6 gives three values of stresses $\sigma_{xx}, \sigma_{yy}, \sigma_{xy}$, the matrix representation of this stress tensor is showed in Equation 2.7. Once that these stresses have been computed, the value of the stresses in the principal directions σ_1, σ_2 can be found. Solving Equation 2.8 for λ the principal stresses are found [17].

$$\Sigma = \begin{bmatrix} \sigma_{xx} & \sigma_{xy} \\ \sigma_{yx} & \sigma_{yy} \end{bmatrix} \tag{2.7}$$

$$\begin{aligned} &det(\Sigma - \lambda I) = 0 \\ &det\begin{bmatrix} \sigma_{xx}-\lambda & \sigma_{xy} \\ \sigma_{yx} & \sigma_{yy}-\lambda \end{bmatrix} = 0 \end{aligned} \tag{2.8}$$

After obtaining the stresses in the principal directions for the results of the topology optimization, bar elements are placed within these stress paths.

2.2 TOPOLOGY OPTIMIZATION

2.2.1 Introduction

In the field of structural optimization, it is necessary to differentiate two types of optimization procedures, (1) shape or macro-structure optimization (geometry optimization), and (2) topology or micro-structure optimization (material optimization). In the former one, the initial domain can change during the optimization process meaning, that at the end of the optimization the geometry of the beam could have changed with respect to the geometry

of the initial problem. Whereas in the latter one the design domain is prescribed at the beginning of the optimization process, it remains unalterable during the optimization process, meaning that the shape of the beam will still be the same, but the internal distribution of the material will not be evenly distributed. [18] Figure 2.6 illustrates the difference between shape and topology optimization.

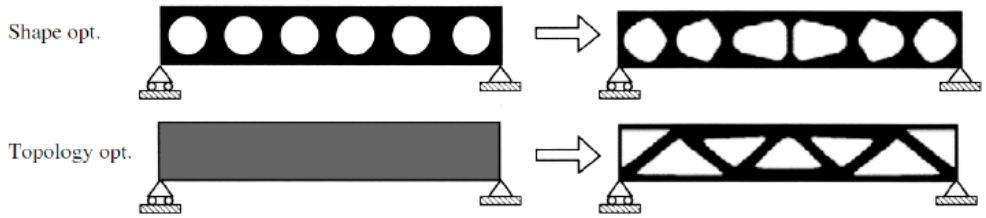

Figure 2.6: Comparison between shape and topology optimization [5]

Topology Optimization is a theoretical and numerical producer, in order to find the most optimal stress trajectory, and load paths for given conditions. The topology optimization deals with the material distribution in a structure for a given loading, and supports conditions. The topology optimization assumes that the initial volume of material in a structure is more than the necessary amount to satisfy the given conditions. So, the load or stress paths of a structure can be taken as the remaining elements after the optimization (elements removing) process.[19] [20]. The topology optimization starts with an even distribution of material over all the continuum domain of the structure, this material is considered porous, in the way that these porous can become larger when this happens areas without material start appearing. Then the optimization itself consists in determining which elements of the domain of the structure should have material and which of them no. The optimization procedure is based on a gradual removal of elements from the domain of the structure that contribute least to carrying the applied loads. Based on this principle, two types of elements are identified, (i) 0 density elements (voids), they are elements that do not contribute to carrying loads, (ii) 1 density elements (solid), they represent the part of the structure that is carrying the loads. Figure 2.7 shows these two types of elements in the result of the topology optimization for a rectangular simple supported beam. The outcome of the optimization process is considered as a harsh description of the boundaries of the structure, it represents the global optimum topology for the given conditions [9] [21] .

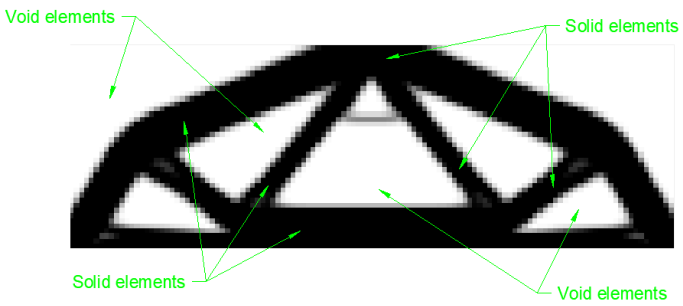

Figure 2.7: Types of elements after the topology optimization

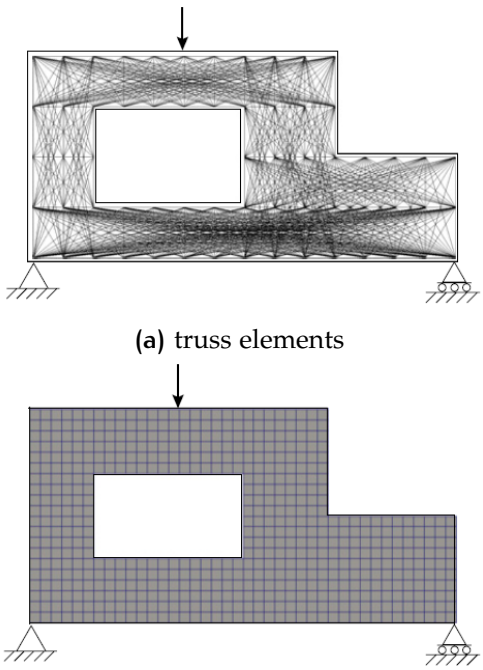

(a) truss elements

(b) four-noded quadrilateral elements

Figure 2.8: Discretization of topology Optimization domains [6].

The principle of the topology optimization is the minimization of an objective function or variable, to find an optimal distribution of material [1]. In order to achieve it, the design domain is discretized using structural elements, the most common elements used for the discretization are truss elements or continuum elements (Figure 2.8).

In this thesis, the optimization process was performed using four-noded quadrilateral plane stress continuum elements. There are many approaches that have been studied in topology optimization the two approaches selected in this thesis are: (i) the Simplified Isotropic Material with Penalization (SIMP) approach, (ii) Bi-directional Evolutionary Structural Optimization (BESO) approach.

2.2.2 Simplified Isotropic Material with Penalization (SIMP) Approach.

The Simplified Isotropic Material with Penalization (SIMP) approach was developed in the late eighties. It was introduced as an alternative to the homogenization approach which simplifies the formulation and improves the convergence of the solutions. This method is also known as power-law, material interpolation, or density approach. Currently, the SIMP approach is the most famous topological optimization approach based on a finite element numerical formulation. The principle of the SIMP approach is the maximization of the stiffness through the minimization of the total strain energy (mean compliance), this method introduces as continuous variable the density (ρ) of the material, with values in the range $0 < \rho \leq 1$. For problems of constant thickness, the variable ρ can be taken as the thickness of the material, density, or cost of the material [18][22].

The relation between the density of the material and the Young's modulus is given by Equation 2.9.

$$E(\rho_i) = g(p_i)E_0 = \rho_i^p E_0, \tag{2.9}$$

where ρ is the density of the material, p is the penalization factor, and E_0 is the Young's modulus of the solid material. If the penalization p is not considered, or its value is assumed as $\rho = 1$, the solution of the optimization problem with respect to the compliance would consist of essentially "grey" elements. "Grey" elements are elements that after the process of optimization have density values within the range 0 - 1. These elements are directly affected by the value of p. Many authors have studied the effect of choosing different values of p, concluding that the value which assures a good convergence is $p = 3$, solutions using $p = 3$ give results with mostly 0 density or 1 density elements (black-and-white results). Too high or too low values of p cause too much grey areas or too fast convergence. [9] [18] [22].

The numerical formulation used for this thesis corresponds to the one used by Sigmund in his educational algorithm for topology optimization [9]. The domain of the structure is assumed to be formed by 2D rectangular four node plane stress elements (Figure 2.8.b). In this case, the topology optimization takes as objective function the compliance of structure which is given by Equation 2.10, and Equation 2.11.

$$c(x) = U^T K U = \sum_{e=1}^{N} (x_e)^p u_e^T k_0 u_e, \tag{2.10}$$

With,

$$\begin{aligned} &\frac{V_{(x)}}{V_0} = f \\ &KU = F \\ &0 < x_{min} \leq 1 \end{aligned} \tag{2.11}$$

where c is the compliance of the structure, U is the variable for global displacements, F is the global external forces applied to the structure, K is global stiffness matrix, u_e is element displacement vector, k_e is local stiffness matrix, x is vector of the design variables, and x_{min} is the vector of minimum densities.

Even though, the density of removed elements, in theory, is zero, for the numerical calculations they should be taken as non-zero values to avoid singularity problems, in the SIMP approach is conceived to provide fading stiffness when the value of the stiffness reaches a pre-established minimum value [9] [20].

The principle of the SIMP approach is based on finding the equilibrium of the external loads for a given amount of material. This amount of material that is a fraction of the volume of the structure before the optimization is known as **Volfrac**. Generally, the use of low values of **Volfrac** grants the achievement of truss-like structures [20]. Figure 2.9 shows the effect in the results of the topology optimization for two different values of **Volfrac**.

(a) $Volfrac = 0.40$ **(b)** $Volfrac = 0.65$

Figure 2.9: Comparison between results for different values of $Volfrac$

Another important parameter in results obtained with the SIMP approach is the minimum radius (**rmin**). It refers to the effect that an element has with its surroundings. This value is normalized by the size of the elements (mesh size) of the beam, "The sensitivity filter modifies element sensitivity values to be weighted averages of their neighbors within a mesh independent radius rmin". The **rmin** can also be consider as a size filter, since it leaves a grey are of a width **rmin** between black elements and white elements. [18]. Figure 2.10 illustrates this difference.

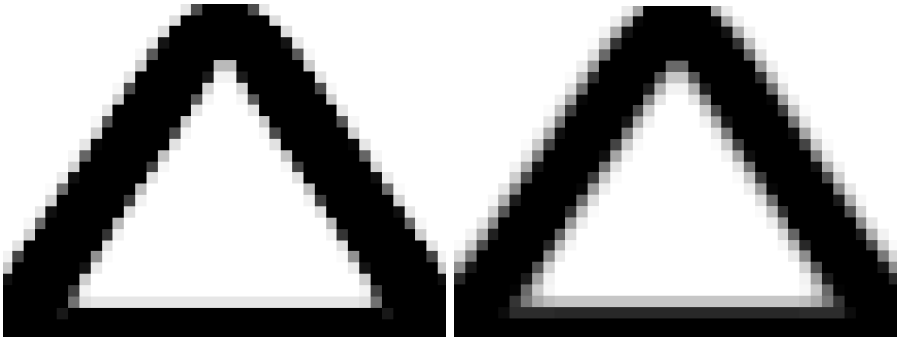

(a) $r_{min} = 1.1$ **(b)** $r_{min} = 2$

Figure 2.10: Comparison between results for different r_{min}

The SIMP approach has a constant volume in every iteration, this value is given as a input input parameter, but the value of the compliance is being optimize (reduce) gradually until it converges to a minimum value that satisfy the loading and support conditions. The process of optimization is shown in Figure 2.11. Huang and Xie proved that the SIMP approach converges to a higher value of compliance than other methods such as the ESO, BESO or continuation method. However, the SIMP approach works better with larger mesh elements size than methods that do not use the mesh-independency filter, such as the ESO approach. [23].

2.2.3 Bi-directional Evolutionary Structural Optimization (BESO) Approach.

The Bi-directional Evolutionary Structural Optimization (BESO) approach, appeared as an extension of the Evolutionary Structural Optimization (ESO) approach, where besides of the hard killing strategies used by the ESO approach, the BESO approach incorporates bi-directional schemes. These types of schemes allow the addition of new elements next to the elements with the highest strain energy. Both methods ESO/BESO are based on the same principle, minimization of total strain energy of the structure. Both methods

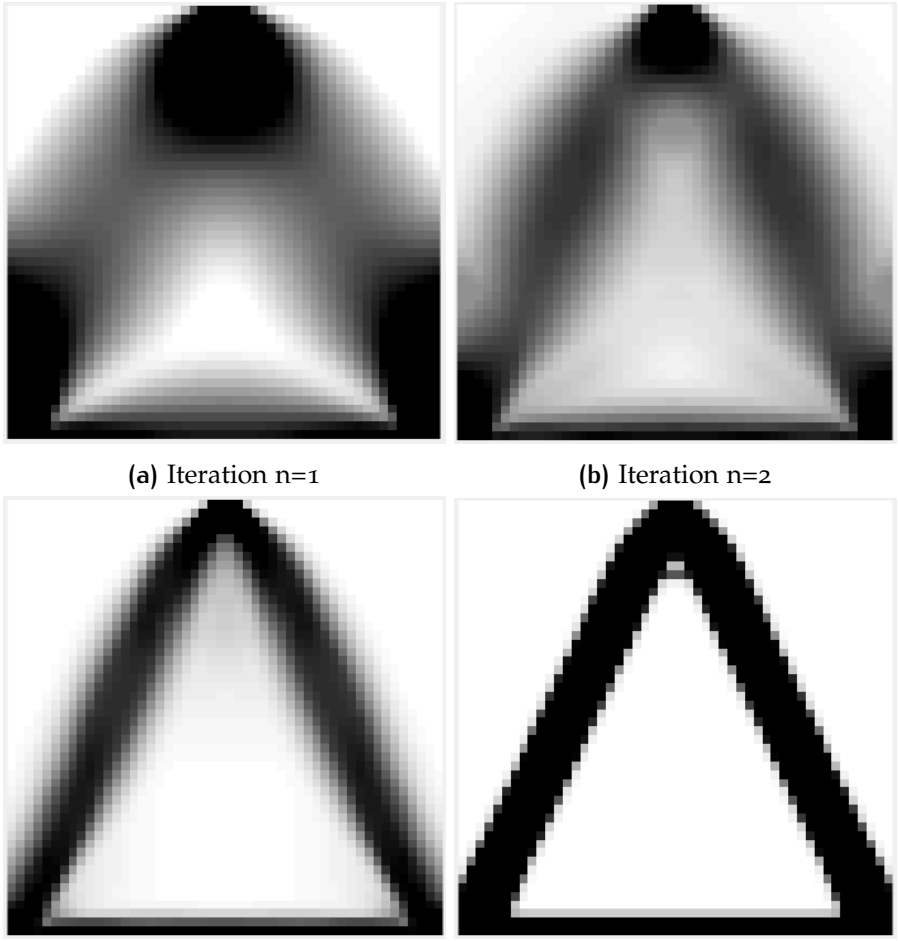

(a) Iteration n=1 **(b)** Iteration n=2

(c) Iteration n=5 **(d)** Iteration n=66

Figure 2.11: Process of optimization SIMP approach. Volfrac=0.3

gradually remove inefficient material (elements with lowest strain energy) from the original domain of the structure, in order to obtain a maximum stiffness. These evolutionary approaches are based on the concept that after the elimination process of inefficient material, the remaining material represents an optimal material distribution for the given loading and support conditions. One benefit of the BESO approach over the ESO approach is that the BESO approach is more stable, and less depended on the selection of parameters because, it uses a mesh-independency filter, similar to the one used in the SIMP approach [18] [23] [24]. In the BESO approach the optimization is given by the minimization of Equation 2.12 subject to Equation 2.13.

$$c(x) = \frac{1}{2} U^T K U \tag{2.12}$$

$$V^* - \sum_{i=1}^{N} (V_e) x_i, \qquad x_i = x_{min} \text{ or } 1 \tag{2.13}$$

where, C is the mean compliance of the structure, K is the global stiffness matrix, u is the vector of global displacements, N is the number of elements,

and x_i is the density of the i element, in the same manner than in the SIMP approach elements with values lower than a prescribed minimum will be assumed as voids (o density) [23].

Reintroducing elements during the optimization process means that elements which at some point of the optimization were assumed as voids (o density elements), can be reintroduced in further steps as solid elements (1 density elements). The criteria used for these optimization approach states that "the strain energy densities of solid elements are always higher than those of soft elements". [23]. During FEM calculations void elements are removed from the global stiffness matrix (K), it is done by assigning a very small value close to zero (theoretically, it should be zero but to avoid singularities in the calculation a very small value is assumed) to the local stiffness matrix of the elements (K_e) that were removed during the optimization. In this way, the algorithm used for assembling the global stiffness matrix does not change during the whole optimization process [24].

The sensitivity number for the *ith* element in the BESO approach is given as α_i, from Equation 2.14 can be seen that if the value of the penalization p goes to infinity, the sensitivity changes to Equation 2.15 which corresponds to the value of the sensitivity for the ESO approach. Thus, the ESO approach can be seen as a special case of the BESO approach, when the value of p tends to infinity [23].

$$\alpha_i = -\frac{1}{p}\frac{\partial C}{\partial x_i} = \begin{cases} \frac{1}{2}u_i^T K_i^0 u_i & \text{when } x_i = 1 \\ \frac{p_{min}^{p-1}}{2}u_i^T K_i^0 u_i & \text{when } x_i = x_{min} \end{cases} \tag{2.14}$$

$$\alpha_i = -\frac{1}{p}\frac{\partial C}{\partial x_i} = \begin{cases} \frac{1}{2}u_i^T K_i^0 u_i & \text{when } x_i = 1 \\ 0 & \text{when } x_i = x_{min} \end{cases} \tag{2.15}$$

An important parameter in the final shape of the optimization process is the element removal ratio **ER**. This value represents the maximum percentage of elements that can be removed from the structure in each iteration. The value of ER remains constant during the whole optimization process. It has been proved that lower values of **ER** (1%-3%) give good solutions to the optimization problem. [23] Figure 2.12 shows a comparison of the optimization results using different values of ER.

(a) $ER = 2\%$ **(b)** $ER = 10\%$

Figure 2.12: Comparison between results for different ER

In contrast with the SIMP approach, the ESO/BESO approach do not have a constant volume during the whole optimization process, where the structure starts with an initial volume of 1 (entire structure domain) and it gradually converges to the desired volume *volfrac* [23]. Figure 2.13 shows this process. Another difference between the results of the BESO and ESO approach is that the BESO approach does not have "grey" elements in its result, all remaining elements have densities of 0 or 1.

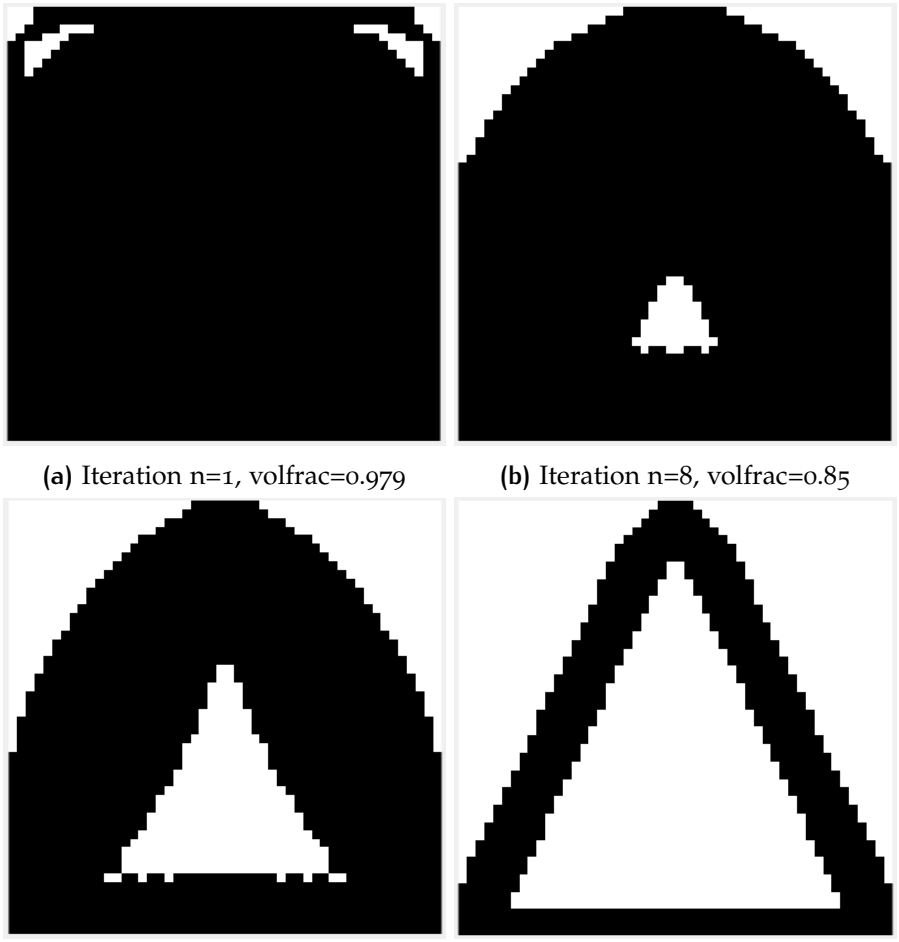

(a) Iteration n=1, volfrac=0.979 **(b)** Iteration n=8, volfrac=0.85

(c) Iteration n=19, volfrac=0.68 **(d)** Iteration n=70, volfrac=0.30

Figure 2.13: Process of optimization BESO approach. Volfrac=0.3, ER=2%

2.3 TOPOLOGICAL OPTIMIZATION FOR STRUT-AND-TIE MODELS

The Strut-and-Tie model is idealized as a mechanism that transfers the load at the ultimate limit state of an RC structure, this load transfer follows the load paths from the point where the load is applied to the supports. There are two main aspects that the Strut-and-Tie model should always satisfy, stress constrains and equilibrium. The Strut-and-Tie models can be found using the elastic stress distribution, frame analysis, load path method, etc. But, the problem with these classical methods arises when the structure has

complex geometry or the loading conditions. A solution for finding the Strut–and-Tie model in these complex cases is the application of topology optimization as a tool for finding truss-like structures [7] [25] [8].

During the creation process of the truss structures for the Strut–and-Tie models, the topology optimization was conceived as a method to find optimal layouts by distributing a given amount of material within the boundaries of the initial domain of the structure. The results obtained from the topology optimization will determine the general configuration of the trusses, these optimization results are taken as the stress paths of the structure for the given load and support conditions. It has been observed that small values of volume constrains, value that in the topology optimization approaches is know as the input parameter *volfrac*, produces better truss structures than large values, because large values produce more branched and articulate trusses. Generally these truss structures can be used as optimal Strut-and-Tie model [14] [20].

The creation process of the Strut-and-Tie model using topology optimization starts with the determination of the optimal topology of the analyzed structure (Figure 2.14.a), here all the inefficient parts of the domain are eliminated, getting an optimal material distribution for the given load and support conditions. Then truss elements are positioned at the compression and tension areas of the topology optimization results. After placing these truss elements the obtained truss structure is assumed to be the Strut-and-Tie model (Figure 2.14.b). This truss structure is used to determine the element's force and the necessary amount of reinforcement for the analyzed structure. The difference between the Strut-and-Tie model created using topology optimization, and using elastic stress with the load path method is shown in Figure 2.14.b and 2.14.c [7].

2.3.1 Evaluation Criteria.

Determining which truss-like structure is the most optimal for each case would always depend on the selected evaluation criteria. For this reason, it is necessary to have well-established the evaluation criteria before deciding which truss-like structure is the best option.

Generally, the most economic RC beam is the one that has the least amount of reinforcement, this reinforcement is linearly related to the tension forces in the elements. Considering this relation, the selected evaluation criterion in this thesis is the total tensile force in the truss structures after the application of the load. To accurately evaluate this criterion, the parameter H was calculated. This parameter is considered as a way to optimize a model because it quantifies the magnitude and the distance that a load has to travel from its application point to the supports of the structure. In this way, the smallest value of H corresponds to the best truss-like structure [3] [26]. Equation 2.16 gives the formulation for the parameter H.

$$H = \sum_{i=1}^{N} T_i L_i \tag{2.16}$$

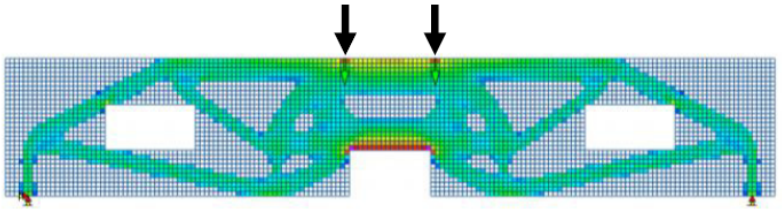

(a) Optimal topology

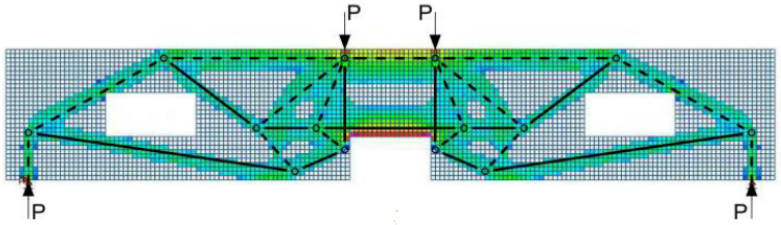

(b) Strut-and-Tie model using Topology optimization

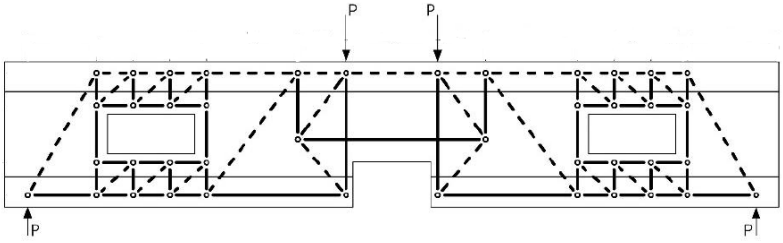

(c) Strut-and-Tie model classical methods

Figure 2.14: Creation process of Strut-and-Tie model using topology optimization, and Strut-and-Tie model using classical methods [7].

where, T_i is the tensile force acting on the i element, L_i is the length of the i member under tensile force.

In addition to the parameter H, the stress in the struts of the structure was computed to check that this stress was smaller than the maximum allowed stress in the concrete f_{cd}. Idealized prismatic struts were assumed to check the stresses in the concrete (Figure 2.15). These types of struts are the simplest type of struts. They are generally used to model compressive stress-blocks of beam elements [8].

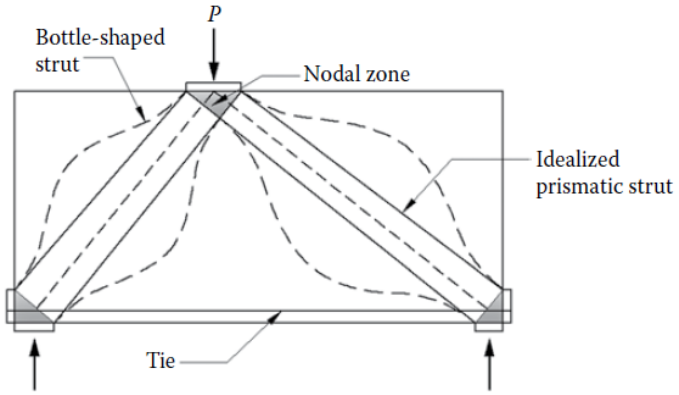

Figure 2.15: Types of struts in a deep beam [8].

Equation 2.17 gives the expression to determine the width of a compressive strut for a general case. Figure 2.16.a shows the layout of a general node zone. Since in this thesis the reinforcement layout was not determined. It was assumed that all the necessary reinforcement is placed in one row of bars ending within the nodal zone (Figure 2.16.b), this makes that $W_T = 0$. Using these assumptions in Equation 2.17 the width of the obtained strut is reduced. Equation 2.18 gives the expression to determinate the reduced width of the strut [8].

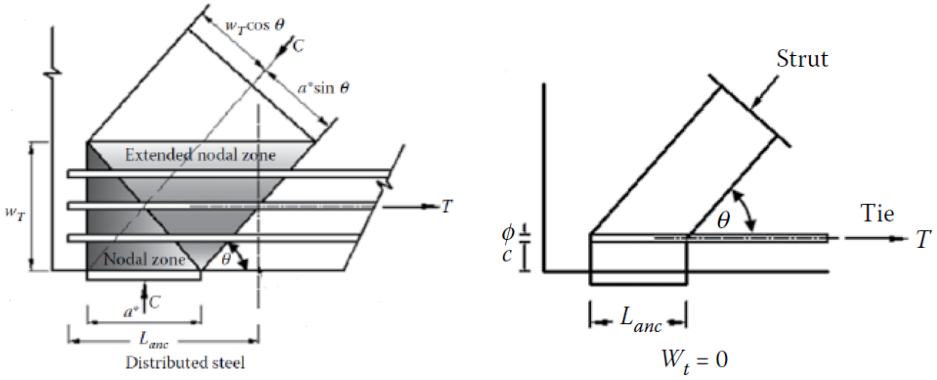

(a) General nodal zone. **(b)** Nodal zone for single row of bars.

Figure 2.16: Nodal zones [8].

$$W_c = W_T cos\theta + a^* sin\theta \tag{2.17}$$

$$w_c = a^* sin\theta \tag{2.18}$$

where a is the length of the supports, θ is the angle of the strut, and w_t is a distance given by the reinforcement layout.

3 METHODS

This chapter contains a description of the methods, procedures, verification, MATLAB scripts, and all considerations used for the generation, and evaluation of the truss-like structures.

3.1 PROCEDURE AND CASE DESCRIPTION

3.1.1 Procedure Description

To check the influence of the input parameters in the different topology optimization approaches three cases were analyzed, (i) a deep concrete beam (Figure 3.2), (ii) a deep concrete beam whit a hole in a side (Figure 3.3), and (iii) a dapped deep concrete beam with a hole in the middle (Figure 3.4). The following procedure was applied to these three studied cases.

The first step in the creation of a truss structure starts with the application of the topology optimization to the full domain of the beam, the obtained results are consider to be the optimal material distribution for the given support and material conditions. MATLAB scripts were used to obtain this optimal material distribution, in all the cases four-noded plane square elements, with an element size of 100 mm were used. This process was done using two different topology optimization approaches, (i) the Simplified Isotropic Material with Penalization (SIMP), (ii) the Bi-directional Evolutionary Structural Optimization (BESO). Then a finite element analysis was performed over the result of the optimization process, to get principal stress diagrams of the new material distribution. This calculation was implemented in the MATLAB scripts used for the topology optimization process. Additionally, a finite element analysis (FEA) over the full domain of the three studied beams was performed using the commercial FEM software DIANA FEA.

Once the principal stress diagrams were obtained, truss elements were placed within these diagrams getting a first truss structure for each case. The stability of these preliminary truss structures should be analyzed to be able to a perform structural analysis on them. In case that a truss structure is unstable, it should be stabilized by adding additional elements or changing the configuration of the elements in the structure. Additionally, to the trusses where stabilizers were added a sensitivity analysis was performed to check how the forces in these additional elements change depending on the position of the nodes of the structure. This analysis was done because when the forces in the stabilizers start to increase, the proposed truss structure does not correspond anymore to the stress diagrams obtained during the optimization process. After the stabilization of the truss structures, a struc-

tural truss analysis to obtain the axial forces in each member was done in the commercial software Rhinoceros, using Grasshopper and Karamba plugins.

Finally, with the results obtained from the structural analysis the total tension force was computed according to the evaluation criterion. The evaluation of the truss structures was also done for some STM from the literature. Based on the evaluation criterion the most optimal truss structure was determinate for each of the studied cases. Figure 3.1 shows all the steps described in this process.

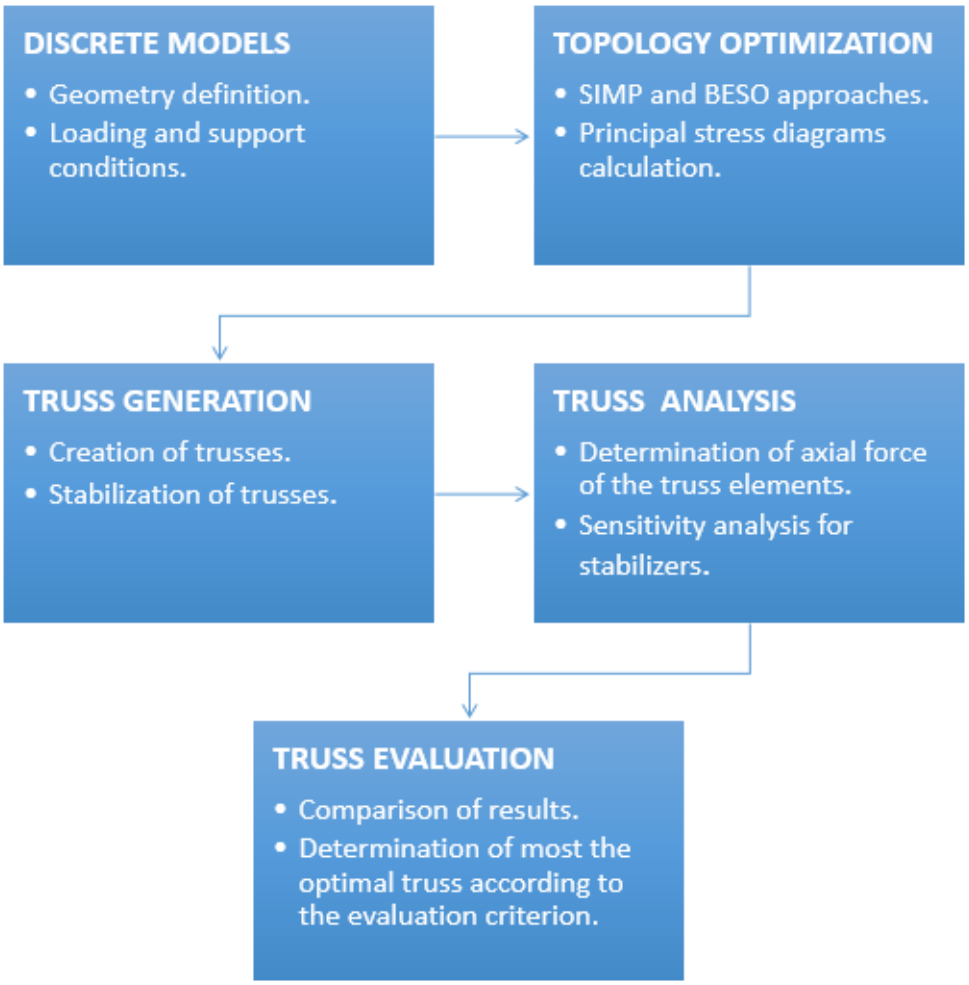

Figure 3.1: Description chart for the generation and evaluation of truss structures.

3.1.2 Case Description

In this section the geometry, position of the loads, and support conditions of the discrete models are described.

Case 1

This first studied case (Figure 3.2) refers to a simply supported deep square concrete beam, these supports have a width of 200 mm. This beam has a side dimension of $l = 4400$ mm, a constant thickness of $t = 100$ mm. It is under the action of two point loads of magnitude $F = 100KN$, the loads are

applied to single points in the model. These loads are located at a distance of 1100 mm from both of the top corners of the beam.

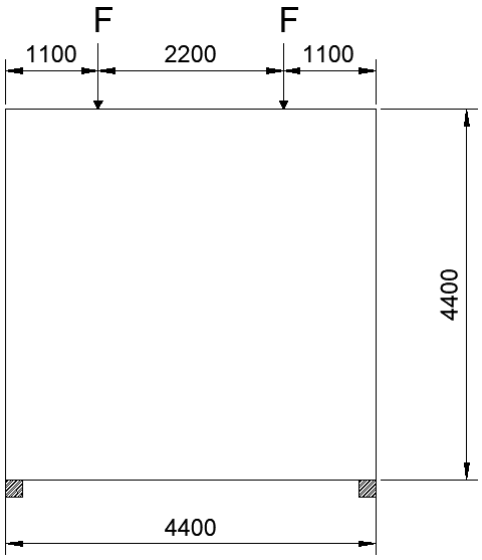

Figure 3.2: Case 1.- Deep concrete beam

Case 2

The second studied case (Figure 3.3) refers to a simply supported deep concrete beam with a square hole. The supports have a width of 200 mm, the square hole is located to a distance of 500 mm in the vertical and horizontal directions from the bottom left corner, it has a side dimension of 1500 mm. The beam dimensions are $l = 7400$ mm by $h = 4700$ mm, with a constant thickness of 100 mm. The beam is under the action of one point load $F = 100kN$, applied to a single point in the model, located to a distance of 4900 mm from the top left corner.

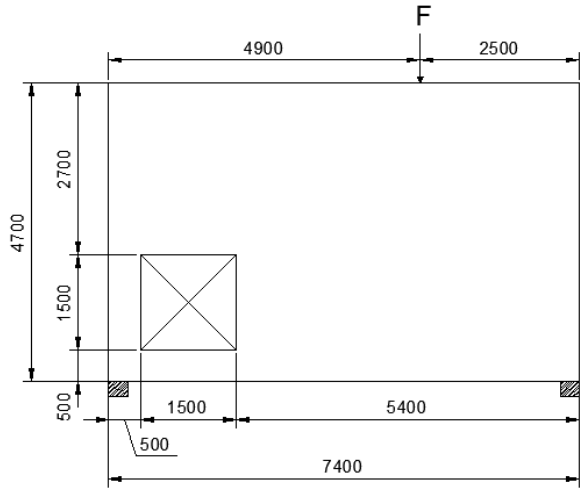

Figure 3.3: Case 2.- Deep concrete beam with a hole

Case 3

The third studied case (Figure 3.4) refers to a simply supported dapped deep concrete beam with a hole. The supports have a width of 100 mm, the beam outer dimensions are $l = 6400$ mm by $h = 3000$ mm with a constant thickness of 100 mm. The beam has a dapped end in the top right corner with dimensions of 1800 mm in the horizontal direction, by 1200 mm in the vertical direction. The beam is under the action of one point load $F = 100kN$ located to a distance of 2200 mm from the top left corner, this load is applied in a single point of the model. The hole is located to a distance of 1200 mm in the horizontal direction, and 1000 mm in the vertical direction from the bottom left corner. The opening has a rectangular shape with dimensions of 2000 mm in the horizontal direction and 1000 mm in the vertical direction.

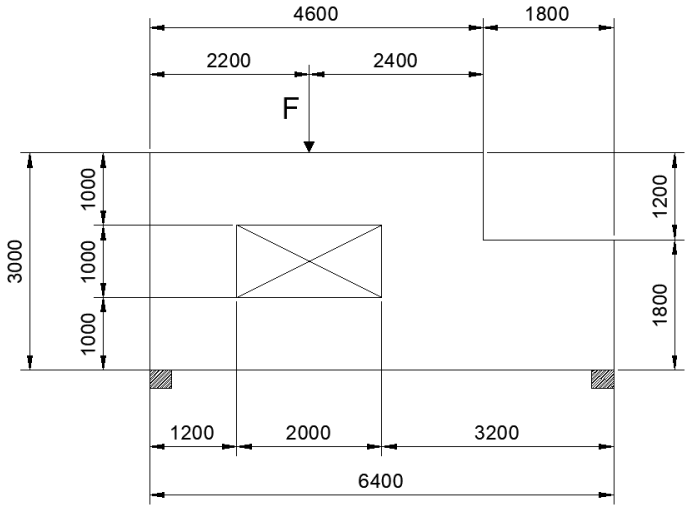

Figure 3.4: Case 3.- Dapped deep concrete beam with an opening

3.2 STRESS PATHS GENERATION USING TOPOLOGY OPTIMIZATION

In this section, the MATLAB scripts used for the generation of the topology optimization of both approaches along their input variables are described.

3.2.1 Simplified Isotropic Material with Penalization (SIMP) Approach

The MATLAB script used for application of topology optimization was based on the educational script proposed by Sigmund [9]. This MATLAB script performs the topology optimization for a simply supported symmetric beam under the action of one point load at the mid-span. Figure 3.5 shows the discrete model used by Sigmund [9], Figure 3.6 shows the result of the topology optimization using this MATLAB script.

General modifications were done to this script. First, the domain of the beam was extended to the full length of it, so the results show the full beam not only one half of it. This modification was necessary because only the first

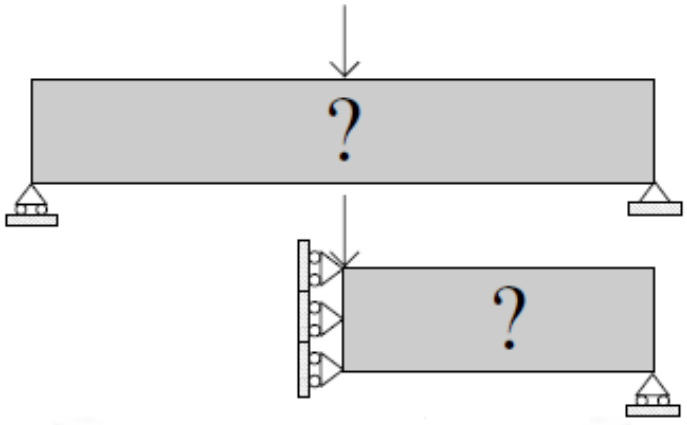

Figure 3.5: Discrete model used for the SIMP approach [9]

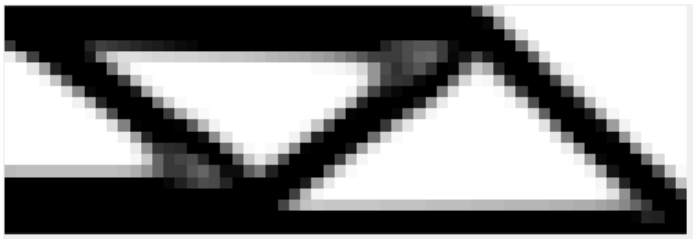

Figure 3.6: Result of the Topology Optimization

studied case is symmetric. Second, the loading conditions were modified to adapt them to any number and position according to each case. The addition of holes within the boundaries of the beam was also done in the script done by Sigmund [9]. However, it was done only for circular holes at a specific position with a given size, the position and size of the hole were changed, given the possibility to define it as input values according to each case. Finally, for the third case, the position and size of the dapped were introduced as input values. Appendix A shows the MATLAB script used for the calculation of the topology optimization using the SIMP approach.

The input parameter $nelx$ and $nely$ refer to the number of elements in x and y directions, respectively. These numbers always refer to the outer perimeter of the beam, which are given by the dimension of the beam in each direction over the size of the used finite element ($100mm$). For instance for Case 2 the number of elements are $nelx = 74$ and $nely = 47$, in the same way for Case 3 are $nelx = 64$ and $nely = 30$. The next input parameter is *volfrac* as it was described in Section 2.2, it defines the fraction of the volume that is desired after the optimization process. To observe the difference in results of the topology optimization several values of this parameter were used. Table 3.1 shows the values selected for *volfrac* at the moment of applying the topology optimization.

The value of the penalization factor p was taken as three for all the studied cases, and for all the different combinations of the other input parameters. This value of p assures a good convergence of results (Section 2.2). As well as *volfrac* the value of the input parameter *rmin* was vary to observe the effect that it produces in every case in the ideal material distribution obtained after

Table 3.1: Values of *volfrac* for Topology Optimization

	SIMP Approach	BESO Approach
volfrac	0.3	0.3
	0.4	0.4
	0.5	0.5

Table 3.2: Values of *rmin* for Topology Optimization

	SIMP	BESO
rmin	1.1	1.1
	1.5	1.5

the topology optimization. Several values of *rmin* were analyzed, but some of them were not considered because of the great similitude among their results. Table shows the selected values for *rmin*.

This variation of values of *volfrac* and *rmin* were used for all the three studied cases.

The input parameters *xdapped* and *ydapped* refers to the dimensions of the dapped measured from the top left corner, in case that the dapped would be in a different position, it would be necessary to adapt the code to the desired position. The values of these two input parameters should be given as a number of elements, in this way for Case 3 the value of *xdapped* and *ydapped* are 18 and 12, respectively. Case 1 and Case 2 have no dapped so the value for these parameters should be defined as zero.

The last four parameters are used for the definition and position of the hole. The first two *xhole* and *yhole* are the dimensions that the hole has in x and y direction respectively. The last two input parameters *xdistance* and *ydistance* refer to the position of the hole in the beam, the values of these parameters should also be given as a number of elements and the reference point for them is the bottom left corner. Table 3.3 shows the values of these four input parameters for the three cases.

3.2.2 Bi-directional Evolutionary Structural Optimization (BESO) Approach

The MATLAB script used for the generation of the optimal topology using the BESO approach is based on the script given by Huang and Xie [23], this code is also based on the educational code developed by Sigmund [9] this is the one used in the SIMP approach. Similar modifications to the ones

Table 3.3: Input parameters for the definition of the hole into the MATLAB

	Case 1	Case 2	Case 3
xhole	0	15	20
yhole	0	15	10
xdistance	0	0	12
ydistance	0	0	10

described for the MATLAB script used in the SIMP approach were done to this script to satisfy the geometry and load conditions of each case. Appendix B shows the MATLAB script used for the calculation of the topology optimization using the BESO approach.

Most of the input parameters used in this approach are the same as the ones used in the SIMP approach, so the definition and values of these parameters are the same. The only difference in the input parameters is that the BESO approach has a new input parameter *er*, it refers to the element removal ratio (Section 2.2), instead of the penalization factor p in the SIMP approach. The value assumed for all the three cases for the *er* is 2%.

3.3 PRINCIPAL STRESS CALCULATION.

The calculation of the principal stress diagrams over the results of the topology optimization is necessary to know which parts of the new material distribution obtained in the optimization process are under compression or tension. This calculation was also performed over the full beam domain using the commercial finite element analysis software DIANA FEA. Having the results of the principal-stresses over the full beam domain and over the optimal material distribution gave the possibility to check if the compression and tension areas are consistent between them.

Principal Stress calculation over the optimal material distribution

The principal stress diagrams were calculated using a MATLAB script. Where, first the shape functions of the four-noded quadrilateral elements are obtained in a symbolic form, then the principal stresses were obtained using numerical integration. Appendix A and Appendix B contain the function *stress* this function was used for calculation of the principal stress. In the obtained diagrams to have concordance with the results obtained from the FEA for the full beam, the blue areas represent areas in compression, these areas are obtained when the value of the principal stress in the elements (Equation 2.8) is smaller than zero. Whereas, the red areas represent areas in tension, in these areas the value of the principal stress is higher than zero. Figure 3.7 shows an example of the principal stress diagrams obtained. Knowing which areas are in compression or tension is more important than the value of the stresses in these areas because for the evaluation process of the trusses bar elements were placed within these paths.

Principal Stress calculation over the full beam domain

Finite element analyses were performed over the three studied cases, these analyses were done using the commercial software DIANA FEA. In these analyses, a linear elastic behavior of the materials was assumed. The full domain of the beams was modeled, the supports and loading conditions correspond to the ones shown in the discrete models (Figure 3.2 to Figure 3.4). To be consistent with the analysis of the material distribution obtained from the optimization process, four-noded quadrilateral elements with a size dimension of 100 mm were used in the FEA models. In the visualization of the

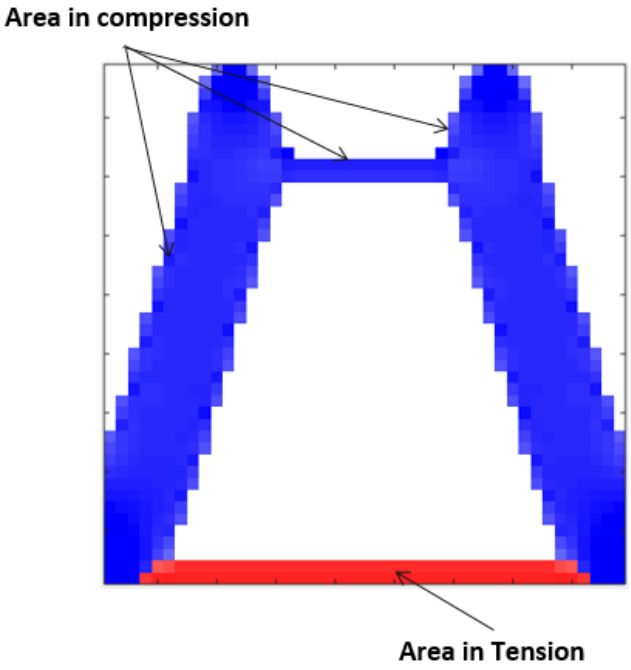

Figure 3.7: Example of principal stress diagrams over the ideal material distribution

results the same color convention than the one used in the MATLAB script was assumed, blue for areas in tension and red for areas in compression. It made clear the comparison and understanding of results. Appendix C shows the principal stress diagrams for all of the studied cases.

3.4 GENERATION AND STABILIZATION OF TRUSS STRUCTURES

The generation of the truss-like structures followed a manual process. This process consist that once the principal stress diagrams are obtained, the bar elements can be located within the stress paths connecting all the branches of the diagrams. At the end of this process, the result is a truss structure that could be used as the skeleton of the Strut-and-Tie model. The generation process started placing elements next to the fixed points of the beams domain. These points are the supports of the beams and the locations of the point loads. The position of these points cannot change because they are taken from the discrete model, this type of nodes are known as external nodes, in all the studied cases these nodes are in the outer perimeter of the beams. The rest of the nodes are the ones formed by the intersection of two or more bar elements. This type of nodes are known as internal nodes. The internal nodes do not have a fixed position, but the constraints for the possible positions are the limits of the stress paths in the principal stress diagrams. Furthermore, it is necessary to consider that at the moment of placing the bar elements they do not have to cross areas that in the discrete model have no material such as holes or the dapped for cases two and three.

In most cases, after placing the bar elements within the stress paths the created truss structures were statically unstable, because of it, it was not possible to perform a truss analysis in these structures yet. Even thought,having a stable truss structure is not an essential condition for the STM, it was necessary to make these structures statically stable to perform an structural analysis on them using only truss elements. In most cases to stabilize a truss structure it was necessary to add some additional elements, which were not given by the results of the topology optimization. These additional elements are called stabilizers, the number of stabilizers required to stabilize a truss structure are given by Equation 2.1. The stabilizers do not change the stress diagrams obtained during the optimization process, because the main characteristic of them is that the axial force of them should always be equal to zero. Therefore, there is no specific rule or procedure for placing the stabilizers, as long as, after the truss analysis the axial force on these elements is zero. Figure 3.8 shows an example of a stable truss structure after placing the bar elements within the stress paths and the addition of the stabilizers for the example shown in Figure 3.7. Applying Equation 2.1 to this example gives $b + r = 7$ and $2j = 8$, so the necessary amount of stabilizers that should been added is one.

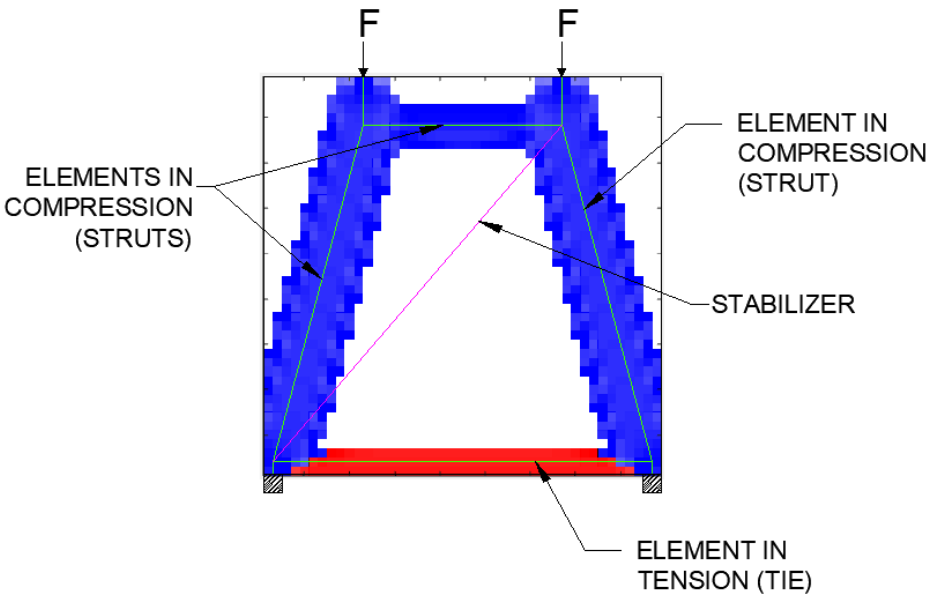

Figure 3.8: Stabilization of truss structures adding stabilizers.

There are also cases in which the simple addition of stabilizer did not lead to a good solution, because the addition of extra elements changed the stress distribution diagrams obtained from the topology optimization, in other words the force in the stabilizer was not zero. In these types of truss structures, it was necessary to add some other elements or create substructures within the stress paths, to create stable truss structures. In the same way than for the case of the stabilizer there is not a exact or unique procedure to do it. Figure 3.9 shows a possible solution for this type of truss structures.

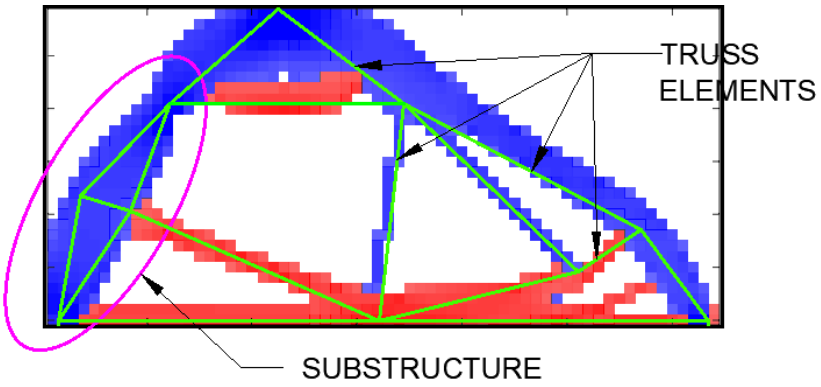

Figure 3.9: Stabilization of trusses without adding of stabilizers.

3.5 TRUSS STRUCTURES ANALYSIS.

3.5.1 Structural Analysis

The structural analysis of the stable truss structures was done in the commercial software Rhinoceros, using Grasshopper with the Karamba plug-in. This software was chosen because of the facility that it provides at the moment of parametrizing the trusses. Parametrizing the proposed trusses saves time in the moment of analyzing the impact that different positions of nodes would have in the truss structure. This aspect was very important because a large number of possible truss structures were analyzed for each case and the different positions that each node can have in every solution. To use the benefits of this software, it was necessary to create a visual script in Grasshopper for each analyzed truss structure. Besides, it was necessary to add a section for evaluation of the truss to the visual scripts. Figure 3.10 shows a visual script used for the evaluation of a specific truss structure.

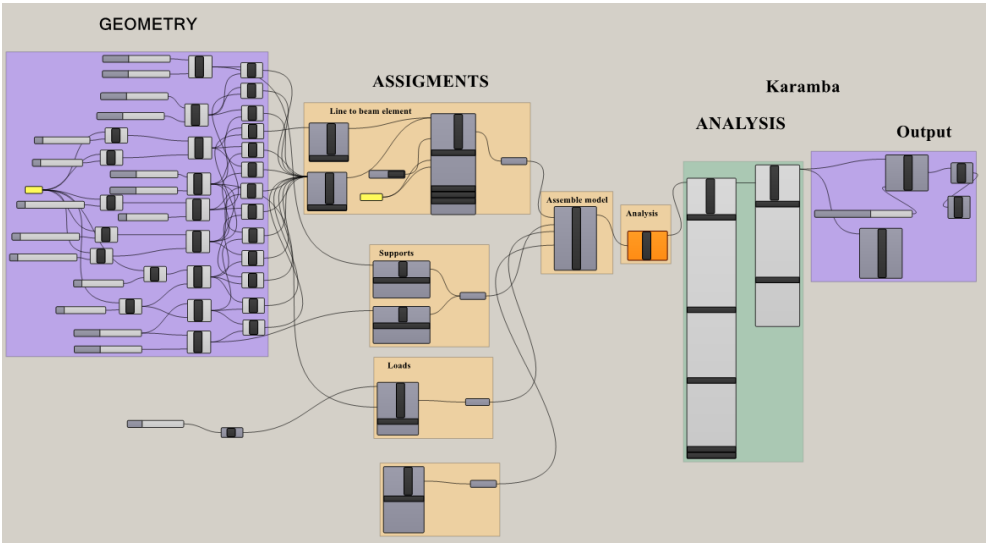

Figure 3.10: Visual script used for the evaluation of a truss structure.

Once that all the visual scripts were created, it was possible to analyze the forces in the members of all the trusses. Besides, all the solutions that were found applying the SIMP and BESO approach, visual scripts were created

for Strut-and-Tie models from literature for each studied case (Figure 3.11). Analyzing these cases from literature gave the possibility to compare their results with the results from the proposed truss structures given a better understanding of the performance of the proposed structures according to the chosen evaluation criteria. Figure 3.11 shows the STM chosen from literature for the three cases. For Case 1 and Case 2 the STM selected are the ones proposed by Schlaich and Schäfer [8], in the Case 3 two models from literarure are used; (i) the STM proposed by Novak-Sprenger, and (ii) the STM proposed by Zhong et al [2]

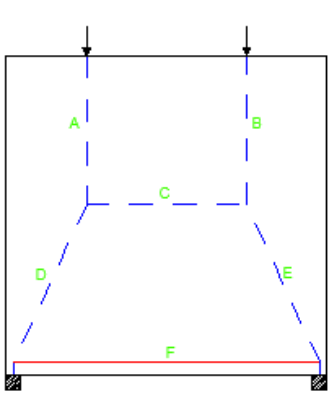

(a) STM for Case 1 [8]

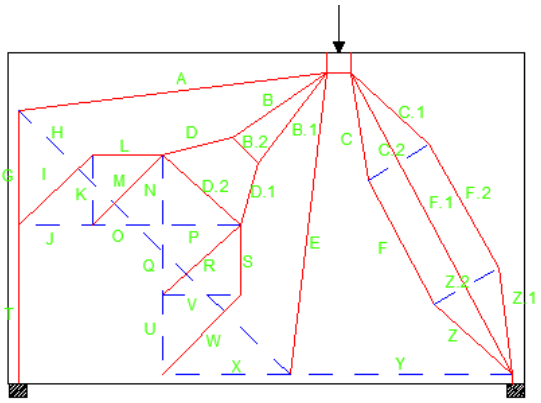

(b) STM for Case 2 [8]

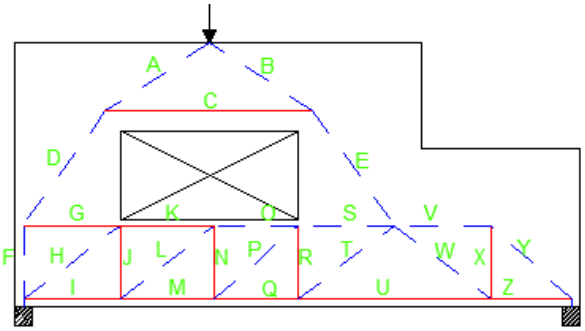

(c) Novak-Sprenger STM for Case 3

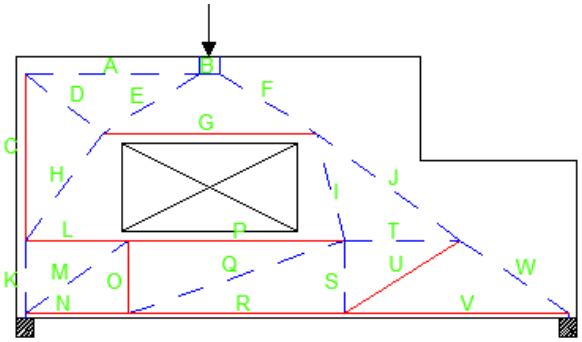

(d) Zhong et al. STM for Case 3

Figure 3.11: STM models from literature for the studied cases.

3.5.2 Sensitivity Analysis

Once the principal stress paths were obtained, and the bar elements were placed within them, some of the obtained truss structures required the addition of extra elements (stabilizers) to create suitable stable truss structures for the structural analysis. The truss analysis showed that the axial force in the stabilizers is zero. But, an inquiry that aroused was, what would happen with the axial force in the stabilizers, if the position of the nodes changes? In order to answer this inquiry, a sensitivity analysis to the stabilizers was performed.

The proposed sensitivity analysis consisted of evaluating the change of the axial force in the stabilizer when the position of the nodes that connect the stabilizers with the truss elements, or the position of the elements that share a node with the stabilizers change. The results of this analysis show when the proposed truss structure is not consistent anymore with the stress diagrams obtained in the optimization process, because the force in the stabilizer starts to increase due to a specific position of some nodes. To check this effect, every time that the position of a node changed respected to the proposed position the force in the stabilizer was registered. Since all the elements of the truss structure must be within the stress paths, this was the restriction for the possible positions of these nodes.

Sensitive analysis Case 1

In Case 1, for both approaches, the stabilizer connects the bottom left node with the one on the top right corner of the truss. The possible positions of these nodes are very limited, due to the horizontal position of both nodes cannot change because their position is given by the location of the point loads and the supports. So, the only possible parameter that would change in a sensitivity analysis is the vertical position of the top horizontal bar. Table 3.4, shows the possible y coordinated of the two nodes that the top bar shares.

Table 3.4: Coordinates for sensitivity analysis Case 1

Y COORDINATES	
SIMP Approach	BESO Approach
4.1	—
3.98	3.6
3.85	3.5
3.72	3.4
3.6	—

Sensitive analysis Case 2

In both approaches, one of the nodes of the stabilizer corresponds to the node where the point load is applied (external node). So, this node cannot move in any direction. On the other hand, the bottom node of the stabilizer can freely move in both directions as long as all the elements that share this

node remain within the stress diagrams. Here not only the position of the node that the truss elements share with the stabilizer has an effect on the forces in the stabilizer, but it is also possible that the change of position of other nodes in the structure causes an effect in the stabilizer. To chose the possible positions of the points, first the areas within the nodes can freely move were determined. Figure 3.12 shows these areas for both approaches.

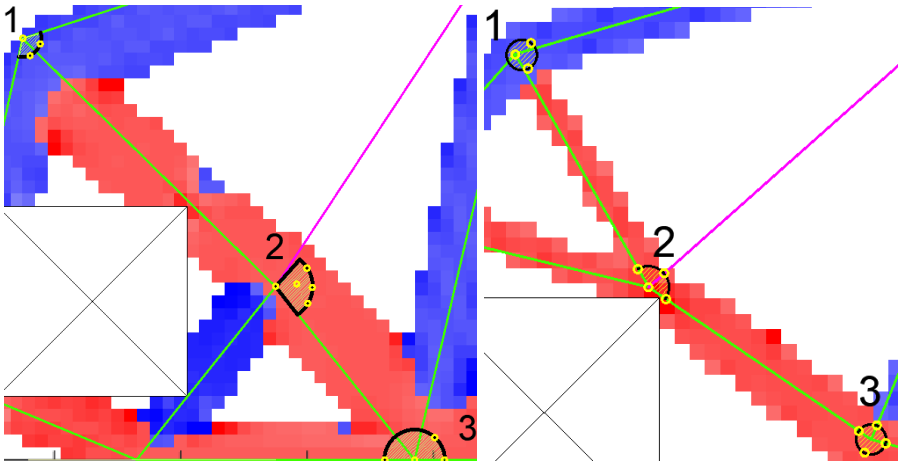

(a) Areas for SIMP approach **(b)** Areas for BESO approach

Figure 3.12: Areas within the nodes can move in Case 2

For a better understanding of how this analysis works, a sensitivity analysis for only node 2 of the BESO approach was performed. Here, the sensitivity analysis consisted of displacing this node in X and Y direction (Figure 3.13) , and register the axial force in the stabilizer for each position of the node.

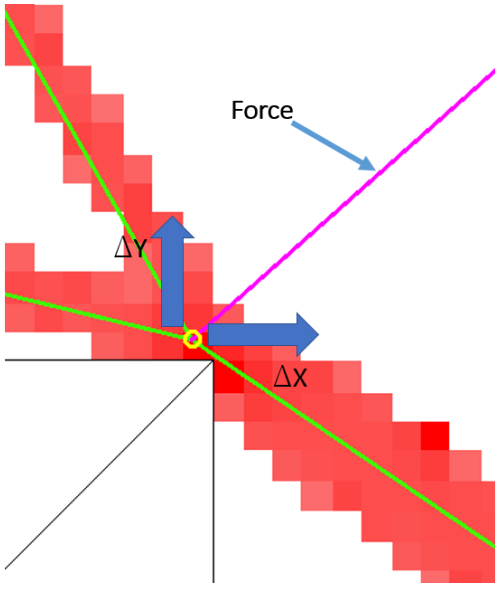

Figure 3.13: Nodal displacements for node 2. Case 2 BESO approach

To analyze the sensitivity of the force in the stabilizer, several positions for each node were selected. Table 3.5 and Table 3.6 show the selected positions

for each analyzed node in both approaches. With these positions all the possible combinations for the three selected nodes were analyzed.

Table 3.5: Coordinates for sensitivity analysis Case 2-SIMP approach (Figure3.12.a)

	NODE 1		NODE 2		NODE 3	
COORDINATE	X	Y	X	Y	X	Y
POSITION 1	0.6	3.33	2.6	1.37	3.7	0
POSITION 2	0.66	3.19	2.86	1.24	3.46	0
POSITION 3	0.74	3.29	2.85	1.51	3.86	0.18
POSITION 4	—	—	2.77	1.39	3.94	0
POSITION 5	—	—	2.89	1.36	—	—

Table 3.6: Coordinates for sensitivity analysis Case 2-BESO approach (Figure3.12.b)

	NODE 1		NODE 2		NODE 3	
COORDINATE	X	Y	X	Y	X	Y
POSITION 1	0.96	3.59	1.83	2.07	3.29	1.08
POSITION 2	1.06	3.66	1.76	2.19	3.24	0.99
POSITION 3	1.04	3.5	1.93	2.16	3.21	1.13
POSITION 4	—	—	1.94	1.99	3.32	1.17
POSITION 5	—	—	—	—	3.38	1.05

Sensitive analysis Case 3

In this case the sensitivity analysis was applied to the truss structure obtained using the SIMP approach only. Here the stabilizer connects two internal nodes of the structure, for the sensitivity analysis a third node was also considered, this additional node was considered because the two elements that share nodes with the stabilizer also share this additional node. Figure 3.14 shows the areas where the selected nodes can move, Table 3.7 shows the position of these nodes, likewise Case 2 all the possible combinations with these nodes were analyzed to check the sensitivity of the force in the stabilizer.

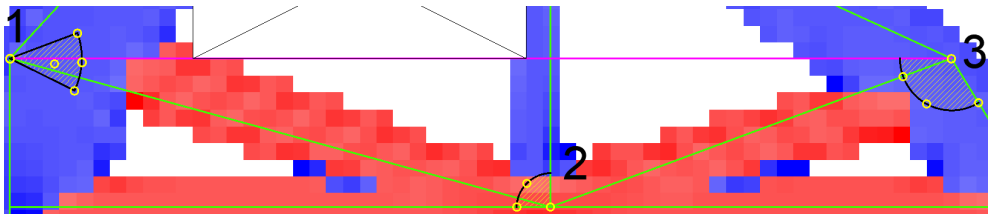

Figure 3.14: Areas within the nodes can move in Case 3.

Table 3.7: Coordinates for sensitivity analysis Case 3-SIMP approach (Figure3.14)

	NODE 1		NODE 2		NODE 3	
COORDINATES	X	Y	X	Y	X	Y
POSITION 1	0	1	3.24	0	5.65	1
POSITION 2	0.39	0.81	3.04	0	5.36	0.89
POSITION 3	0.43	0.98	3.1	0.25	5.5	0.73
POSITION 4	0.4	1.15	—	—	5.81	0.74
POSITION 5	0.27	0.97	—	—	—	—

3.6 EVALUATION CRITERIA.

The selected evaluation criteria for the obtained truss structures after the optimization and stabilization process are (i) the total amount of tension force in the truss structure and (ii) the concrete stress in the struts of the truss structure.

After computing all the evaluation criteria parameters of each truss structure, including the structures taken from the literature, their results were compared to see which approach gives the most optimal truss structure according to these specific criteria. The best approach for each case was taken as the one that gave the lowest total tension force in the structure as long as the value of the stress in the concrete remains smaller than the maximum allowed.

3.6.1 Total Amount of Tension Force and Reinforcement.

The total amount of tension force was taken as the parameter H (Equation 2.16) this parameter corresponds to the summation of the product between the tension force in each member in $[KN]$ and its length in $[m]$. The parameter H was computed for every proposed structure of the three cases, once the parameter H has been calculated for all of these structures, it was possible to determinate the most optimal truss-like structure according to this criterion.

To compute this parameter the axial forces of the truss elements under the loading conditions taken from the discrete models were tabulated, then a sub-table with only the elements under tension force was created, this process was done for all the proposed truss-structures for every studied case and to the truss structures taken from literature. An example of this type of subtable is 3.8. From this table the parameter H was calculated applying Equation 2.16.

The necessary amount of reinforcement is linearly related with the total amount of tension force in the bar elements. This value is calculated for each truss structures as an addition to the tension force. Appendix D shows the necessary amount of reinforcement for each truss structure. The necessary

Table 3.8: Example of subtable to compute H for Case 2 using SIMP Approach

ELEMENT	FORCE (kN)	LENGTH (m)
E	30.34	2.82
G	7.33	1.63
I	30.92	1.76
J	9.04	2.2
K	34.04	3.5

amount of reinforcing steel for a given tension force was compute using Equation3.1:

$$As_{req} = \frac{T_{Ed} * \gamma_s}{fy} \tag{3.1}$$

where T $[KN]$ is the tension force of the demand in a truss element, γ_s is the partial factor for reinforcing steel, according to [27] the value of γ_s should be taken as 1.15, and fy is the characteristic resistance of the reinforcing steel, here it is taken as $fy = 420$ $[MPa]$.

3.6.2 Compressive Stress in the Concrete.

The stress in the concrete was calculated to ensure that the beam do not fail due to compressive stresses in the members in compression of the truss structure (struts). So, as long as the stress in the concrete remains smaller than the maximum permitted value $f_{cd} = 30$ [MPa], the criterion that is consider to determine the optimal truss structure was the minimum total tension force.

The force used to determinate the stress in the concrete was the compression force of each strut, the beams in all the three cases were assumed to have a constant thickness of $100mm$, and as a prismatic shape of the struts were assumed the width of them taken for the calculation is given by Equation 2.18. Then the stress in the concrete was calculated using Equation 3.2 .

$$\sigma_{ci} = \frac{C_i}{A_i} \tag{3.2}$$

where C_i $[N]$ is the compression force of the $i-th$ strut, A_i $[mm^2]$ is the area of the concrete corresponding to the width of the $i-th$ strut.

4 RESULTS AND DISCUSSION.

This chapter consists of the results found in all the stages of the study, from the topology optimization to the evaluation of the final truss structures according to the evaluation criteria, with their respectively discussion and interpretation. Figure 4.1 shows the followed scheme to present the results of the study.

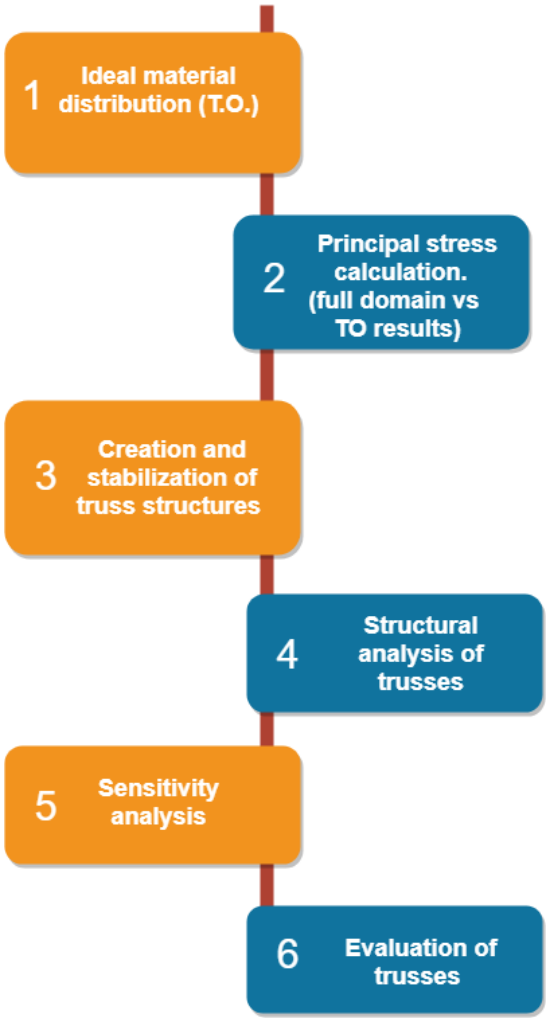

Figure 4.1: Scheme followed for the presentation of results.

4.1 IDEAL MATERIAL DISTRIBUTION

The results obtained after applying the topology optimization to the full domain of a beam are considered to be the ideal material distribution of

it. These material distributions were calculated for both approaches (SIMP and BESO approach). The results shown in this section correspond to the ones obtained with the variation of the input parameters *volfrac* and *rmin*. This variation was done for both approaches of the topology optimization (TO), obtaining six different results per case per approach. To check the effects that the variation of the input parameters produce in the results of the TO, two types of comparisons were made, (i) comparing results from the same approach, here the influence of the input parameters *volfrac* and *rmin* was analyzed, and (ii) a global comparison between the results of the two approaches.

4.1.1 Material Distribution for Case 1

Figure 4.2 and Figure 4.3 show the ideal material distributions for Case 1 using SIMP and BESO approaches, respectively. First, the results of the same approach are compared among them (variation of the input parameters *volfrac* and *rmin*). Then in a more general way, the results obtained using these approaches are compared with each other.

Comparing, Figure 4.2.a with Figure 4.2.b, Figure 4.2.c with Figure 4.2.d, and Figure 4.2.e with Figure 4.2.f, the effect that the variation of *rmin* has on the results of the TO is seen. It is seen that the variation of *rmin* had a small impact in the results of the ideal material distribution, neither the shape nor the thickness of the paths had a significant change in any of these cases. The only visible change is the transition between white (voids) areas to black (solid) areas.

In the same way, making a comparison among Figure 4.2.a, Figure 4.2.b and Figure 4.2.c, and Figure 4.2.d, Figure 4.2.e, and Figure 4.2.f. the effect that the variation of *volfrac* has on the results of the TO is seen. It is seen that the shape of the material distribution did not change, but the thickness of the paths got thicker as the value of *volfrac* increased. The same corresponding comparisons for the BESO approach (Figure 4.3) were made, from them, it is seen that the effects of the input parameters on the variation of results when *volfrac* and *rmin* changed are similar to the ones of the SIMP approach.

Comparing the corresponding results from the SIMP and BESO approaches, it is observed that for Case 1, there is not a big difference in the global shape of the new material distribution and in the thickness of the stress paths. Some factors that might have contributed are given by the characteristics of the discrete model (Figure 3.2): relation height over length $h/l = 1$, symmetric loading conditions, absence of holes on the beam domain, and the simple support conditions.

Due to the large similarity of the results in the material distribution after the variation of the input parameters, for both approaches, it is assumed that every structure created using these results would have similar performance in the Strut-and-Tie model.

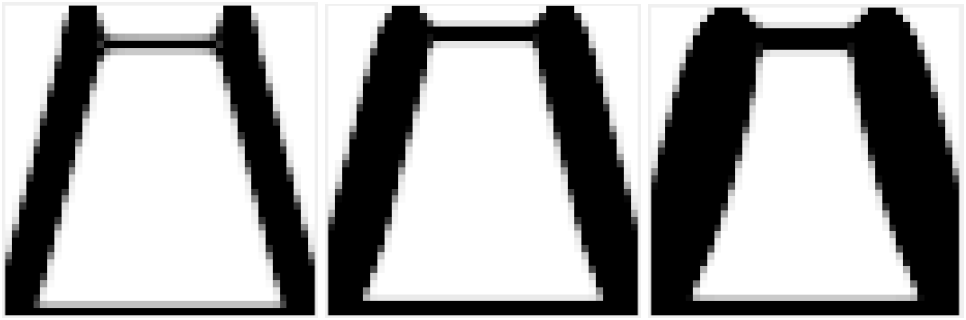

(a) Volfrac=0.3, rmin=1.1 **(b)** Volfrac=0.4, rmin=1.1 **(c)** Volfrac=0.5, rmin=1.1

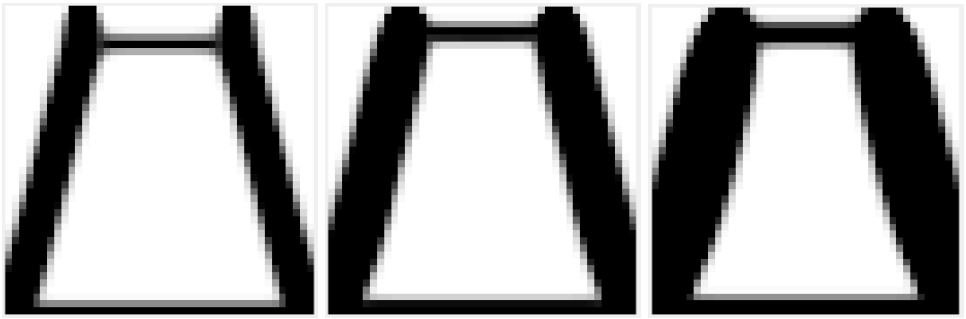

(d) Volfrac=0.3, rmin=1.5 **(e)** Volfrac=0.4, rmin=1.5 **(f)** Volfrac=0.5, rmin=1.5

Figure 4.2: Results of Topology Optimization using SIMP approach Case 1.

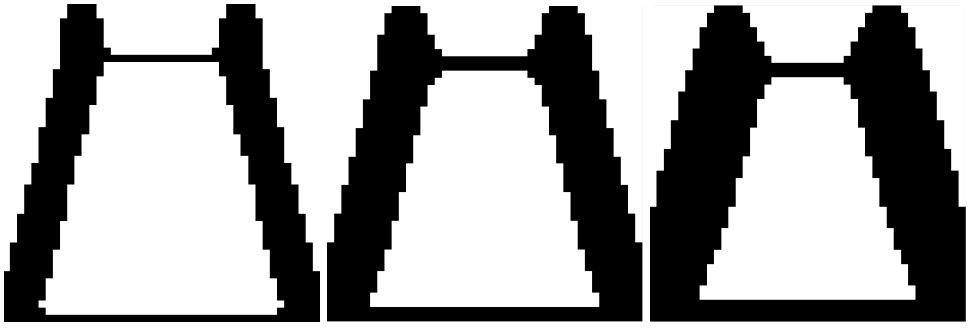

(a) Volfrac=0.3, rmin=1.1 **(b)** Volfrac=0.4, rmin=1.1 **(c)** Volfrac=0.5, rmin=1.1

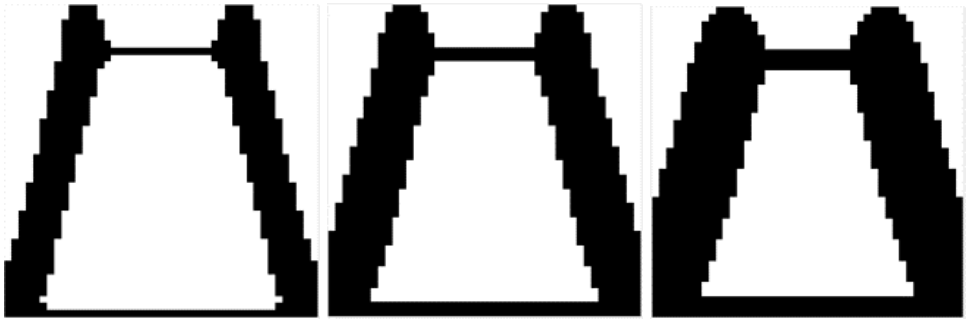

(d) Volfrac=0.3, rmin=1.5 **(e)** Volfrac=0.4, rmin=1.5 **(f)** Volfrac=0.5, rmin=1.5

Figure 4.3: Results of Topology Optimization using BESO approach Case 1.

4.1.2 Material Distribution for Case 2

Figure 4.4 and Figure 4.5 show the ideal material distribution for Case 2 using SIMP and BESO approaches, respectively. In the same way that it was done for Case 1, the results from the same approach are first compared

among them. Then in a more general way, the results obtained using these approaches are compared with each other.

First, only the results of the SIMP approach were compared (Figure 4.4). To see the effect of *rmin* it was compared Figure 4.4.a with Figure 4.4.b, Figure 4.4.c with Figure 4.4.d, and Figure 4.4.e with Figure 4.4.f, from them it is seen that the global shape of the material distribution did not change, but in the results with values of $rmin = 1.5$, the material distribution is less branched than the one obtained using values of $rmin = 1.1$. Also, the thickness of the internal paths is a little thicker when $rmin = 1.5$ than when $rmin = 1.1$, this was expected because larger *rmin* has a bigger influence in the surrounding area of an element. In the case of the results of the BESO approach (Figure 4.5) the same corresponding comparisons that the ones for the SIMP approach were made, these results exhibited a similar behavior than the ones of the SIMP approach having less branched results when $rmin = 1.5$ than when $rmin = 1.1$, the effect is more visible in for values of *volfrac=0.5*

On the other hand, to see the effect of *volfrac* comparisons among Figure 4.4.a, Figure 4.4.c, and Figure 4.4.e for a value of $rmin = 1.1$, and among Figure 4.4.b, Figure 4.4.d, and Figure 4.4.f for a value of $rmin = 1.5$ were made. From these comparisons was observed that the global shape of the results remained almost the same, the paths got ticker and some small branches started appearing as the value of *volfrac* increased. Similar comparisons were made with the results of the BESO approach (Figure 4.4). These results have a larger variation among them than the ones obtained with the SIMP approach. Here the paths got thicker, some more branches appeared. There is a change in the global shape when the value of *volfrac=0.5*, the shape of this result is very similar to the ones obtained using the SIMP approach.

Comparing, the results between the SIMP and BESO approach, it is seen that the difference between the results of the topology optimization is manly appreciate in the area below the hole, the main difference is that in the results from the SIMP approach there are some stress paths surrounding the hole, while , in the results of the BESO approach the area below the hole has no stress paths at all except for only one case (Figure 4.4.e). A consequence of that is that the results of the SIMP approach cover more surface area than the ones of the BESO approach, this characteristic would be useful in the moment of the reinforcement layout design.

In this case, the results obtained with the variation of the input parameters are considerably larger than for Case 1. Here the trusses created based on these results would be different from each other, so it would be expected that the structural performance of them in the Strut-and-Tie would not be similar, this effect is analyzed in Section 4.3.

4.1.3 Material Distribution for Case 3

Figure 4.6 and Figure 4.7 show the results of the ideal material distribution for Case 3 after the topology optimization using the SIMP and BESO approaches, respectively. In the same way that it was done for the other two

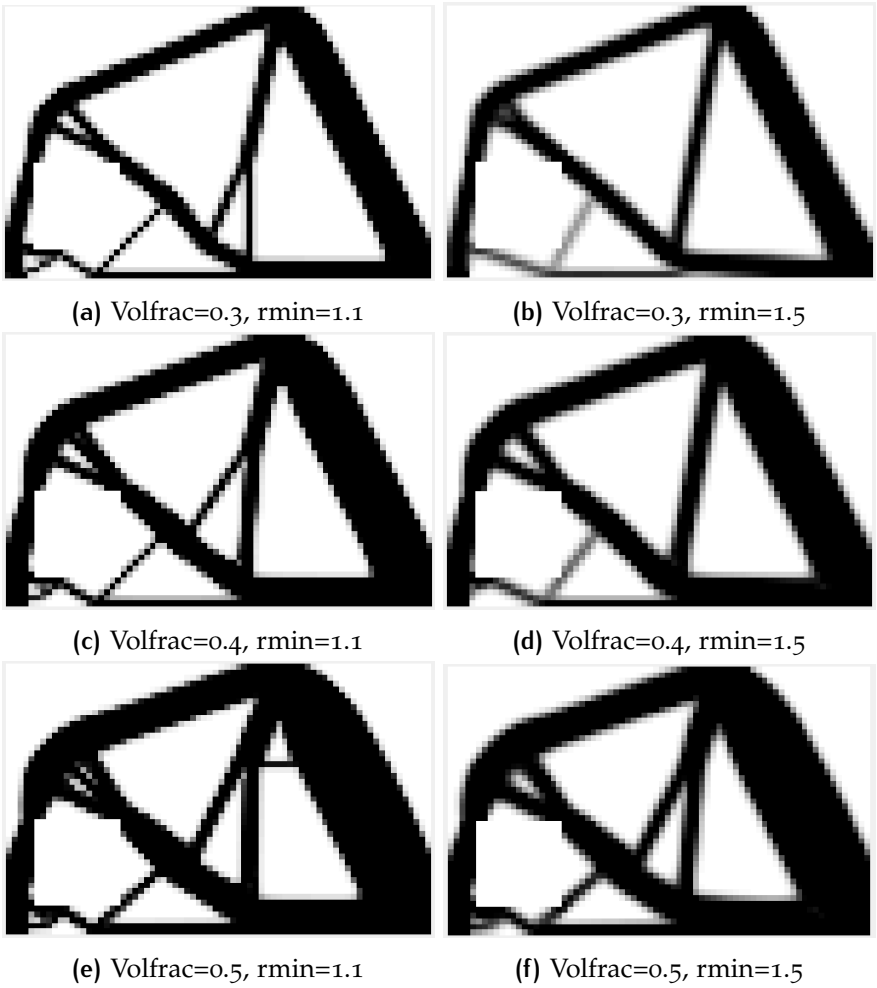

(a) Volfrac=0.3, rmin=1.1 **(b)** Volfrac=0.3, rmin=1.5

(c) Volfrac=0.4, rmin=1.1 **(d)** Volfrac=0.4, rmin=1.5

(e) Volfrac=0.5, rmin=1.1 **(f)** Volfrac=0.5, rmin=1.5

Figure 4.4: Results of Topology Optimization using SIMP approach Case 2.

cases, first the results from the same approach are compared among them, and then in a more general way, the results obtained using these approaches are compared with each other.

To see the effect of *rmin* on the results using the SIMP approach the following comparisons were made, Figure 4.6.a with Figure 4.6.b, Figure 4.6.c with Figure 4.6.d, and Figure 4.6.e with Figure 4.6.f. It is seen that there is almost no difference between these results, the biggest difference occurs when $volfrac = 0.4$, here the result of the optimization when $rmin = 1.1$ has one more internal path than the one when $rmin = 1.15$. For the rest of the values of *volfrac*, there is not a big difference between results. In the same manner, the corresponding comparisons are made to see the effect of *rmin* on the results of the BESO approach (Figure 4.7). Likewise, in the SIMP approach, here the only noticeable difference in the shape of the results are observed when of $volfrac = 0.4$. The result obtained using $rmin = 1.1$ has an additional internal path, and the inclination of another path differs from the result obtained using $rmin = 1.5$.

Now to check the effect that *volfrac* has on the results of the TO using the SIMP approach, the following comparisons were made, Figure 4.6.a, Figure 4.6.c, and Figure 4.6.e for a value of $rmin = 1.1$, and among Figure 4.6.b, Figure 4.6.d, and Figure 4.6.f for a value of $rmin = 1.5$. In contrast to the

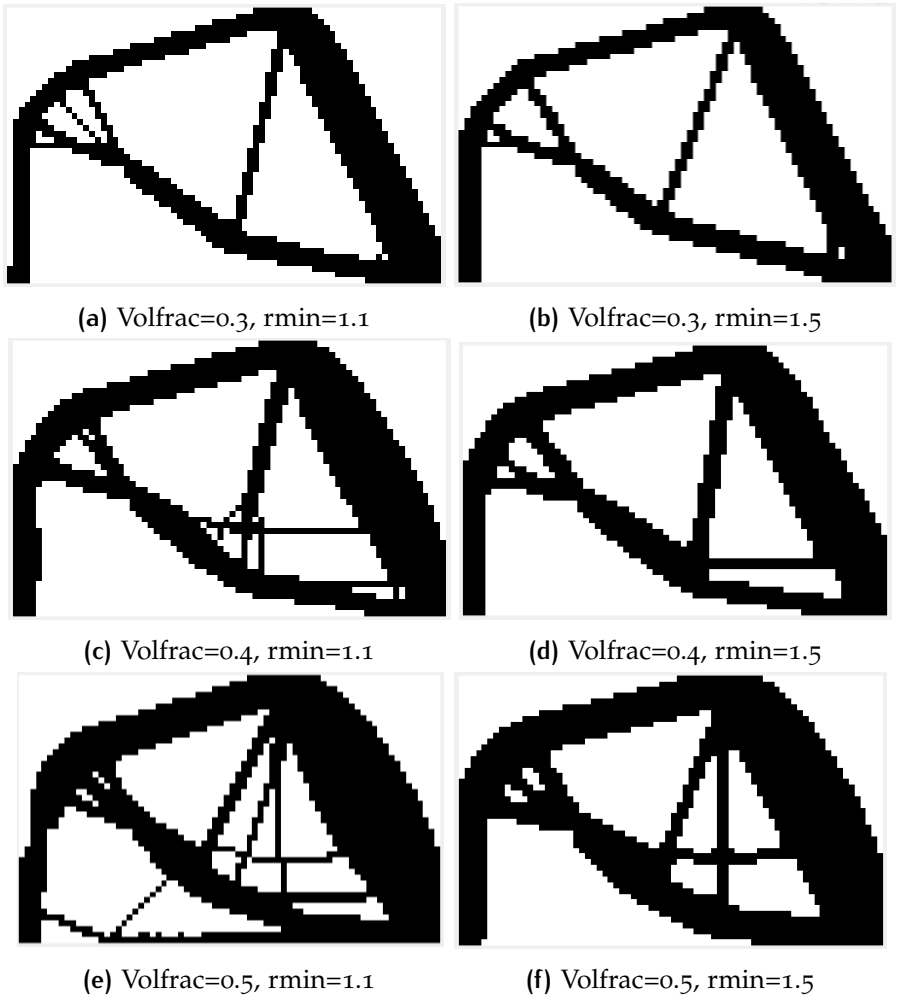

(a) Volfrac=0.3, rmin=1.1 **(b)** Volfrac=0.3, rmin=1.5

(c) Volfrac=0.4, rmin=1.1 **(d)** Volfrac=0.4, rmin=1.5

(e) Volfrac=0.5, rmin=1.1 **(f)** Volfrac=0.5, rmin=1.5

Figure 4.5: Results of Topology Optimization using BESO approach Case 2.

previous cases, in this case, the main difference occurred between the results of $volfrac = 0.3$ and $volfrac = 0.4$. This effect is also seen with the corresponding comparisons of the BESO approach. The results corresponding to $volfrac = 0.4$ have internal material paths, while the ones obtained using $volfrac = 0.3$ have only external ones. The difference between the results of $volfrac = 0.4$ and $volfrac = 0.5$ is almost only the thickness of the paths.

Comparing the results from the SIMP and BESO approaches, it is seen that there is no big difference in the material distribution between their results. In fact, for values of $volfrac = 0.3$, there is almost no visual difference in the results. The large similitude between these results of the two approaches is due to the small surface area of the beam that the hole and the dapped provoked. Although the discontinuities in the discrete model should cause different material distributions depending on the approach, it is seen that the small available surface area of the beam had a bigger influence on the results.

In this case, the variation of the input parameter *rmin* had almost no influence on the trusses for the Strut-and-Tie model. However, the difference in results is mostly observed for values of $volfrac = 0.3$, to values of $volfrac = 0.4$ and $volfrac = 0.5$ where the results are similar due to the

small surface area of the beam. The difference, in the results of the material distribution, would influence the trusses for the Strut-and-Tie model, this effect is analyzed in Section 4.3.

In this case the variation of results

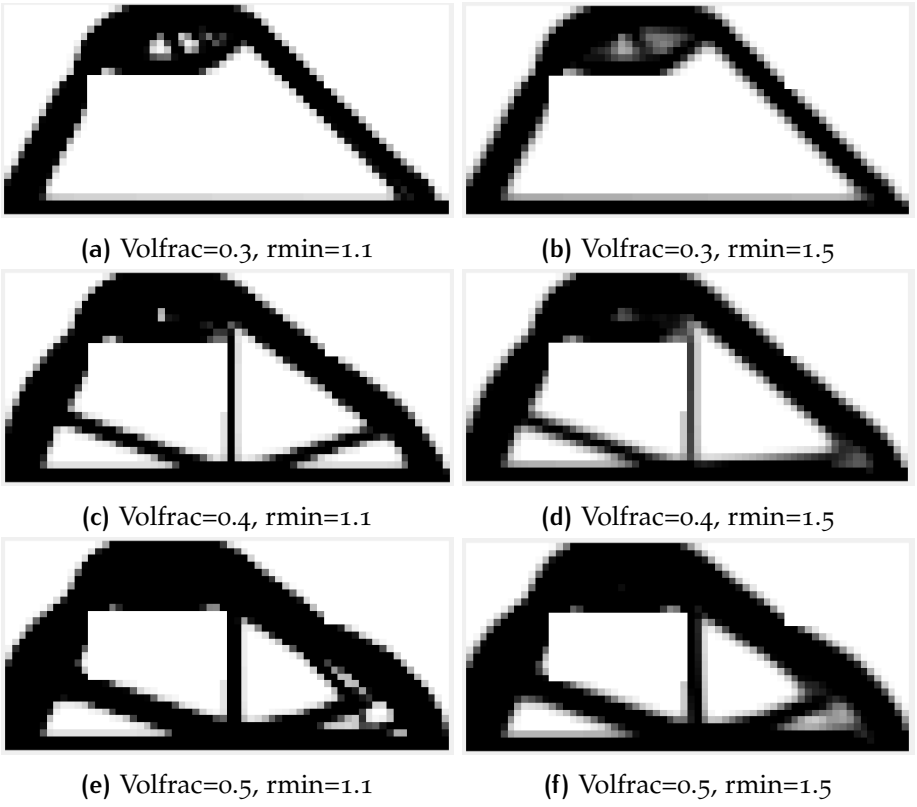

(a) Volfrac=0.3, rmin=1.1 **(b)** Volfrac=0.3, rmin=1.5

(c) Volfrac=0.4, rmin=1.1 **(d)** Volfrac=0.4, rmin=1.5

(e) Volfrac=0.5, rmin=1.1 **(f)** Volfrac=0.5, rmin=1.5

Figure 4.6: Results of Topology Optimization using SIMP approach Case 3.

4.2 PRINCIPAL STRESS CALCULATION

Once the new material distribution was obtained using the topology optimization, it was necessary to calculate the principal stresses of these results to see which paths are under compression and which of them under tension. Also, the principal stresses of the full domain of the beams were calculated using an FEA software. The results of the principal stresses of the new material distributions were compared with the results of the full beam domain, to check if the areas in compression or tension remain the same after the optimization process.

The principal stress diagrams of the results obtained during the optimization process were computed for every solution of all the three studied cases. Due to the similitude showed among the results of the same approach, only one stress diagram per approach per case is shown. Comparing one result per approach was enough to analyze the similarity between the principal stress over the results of the optimization with the results of the full domain.

Figure 4.8, Figure 4.9, and Figure 4.10 show the principal stress diagrams for Case 1, Case 2, and Case 3, respectively. Each figure consists of two sub-

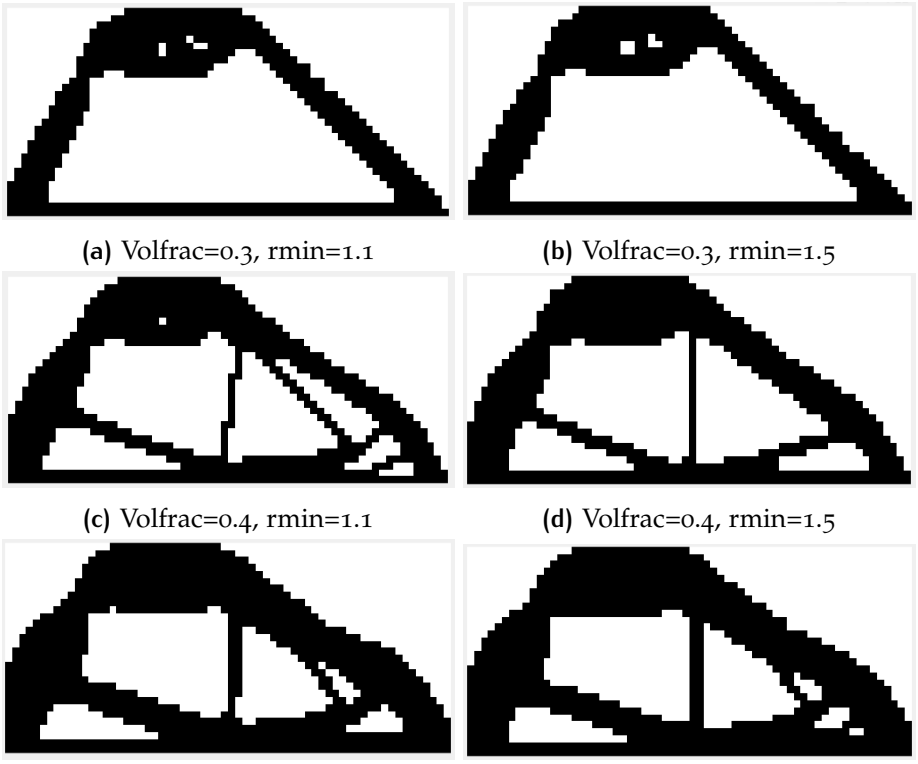

(a) Volfrac=0.3, rmin=1.1 **(b)** Volfrac=0.3, rmin=1.5

(c) Volfrac=0.4, rmin=1.1 **(d)** Volfrac=0.4, rmin=1.5

(e) Volfrac=0.5, rmin=1.1 **(f)** Volfrac=0.5, rmin=1.5

Figure 4.7: Results of Topology Optimization using BESO approach Case 3.

figures, one for the results obtained using the SIMP approach, and another one for the results of the BESO approach. In these figures, the areas in compression are blue, while the elements in tension are red. Appendix C shows the principal stress diagrams obtained using the software DIANA FEA.

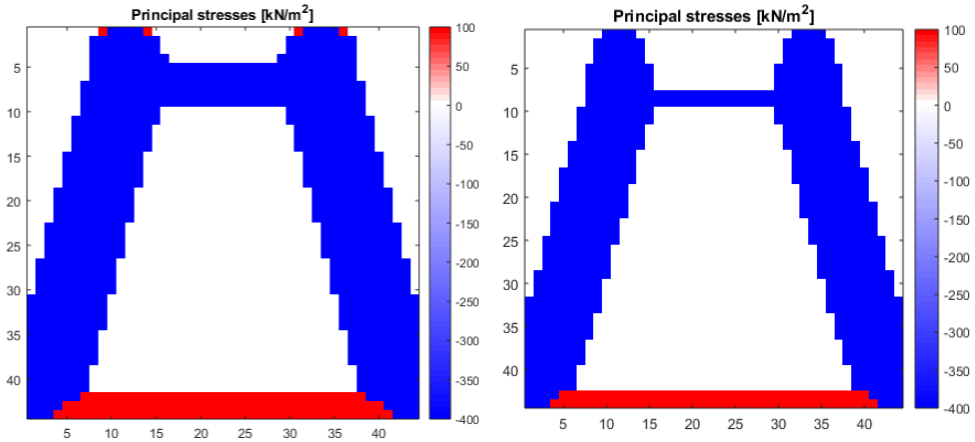

(a) SIMP Approach **(b)** BESO Approach

Figure 4.8: Principal Stress over the optimal material distribution Case 1.

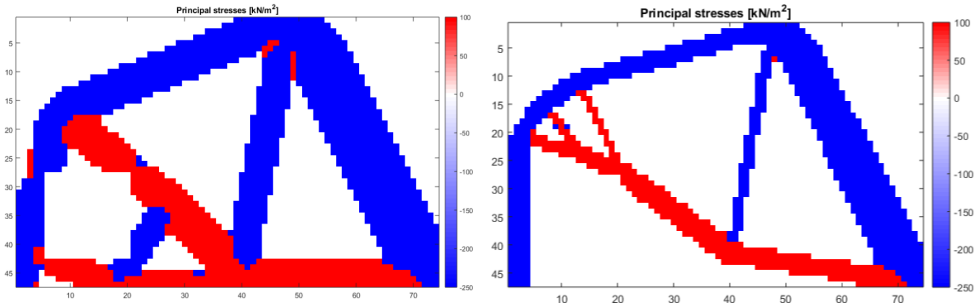

(a) SIMP Approach **(b)** BESO Approach

Figure 4.9: Principal Stress over the optimal material distribution Case 2.

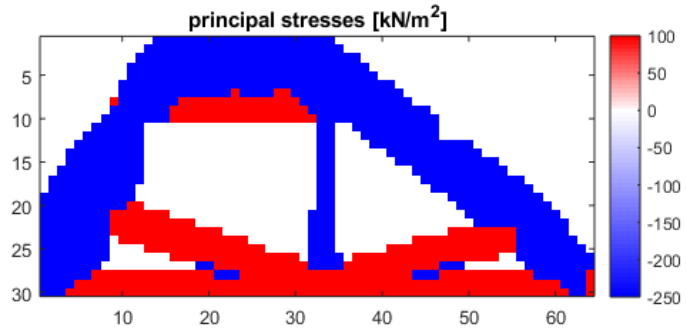

(a) SIMP Approach

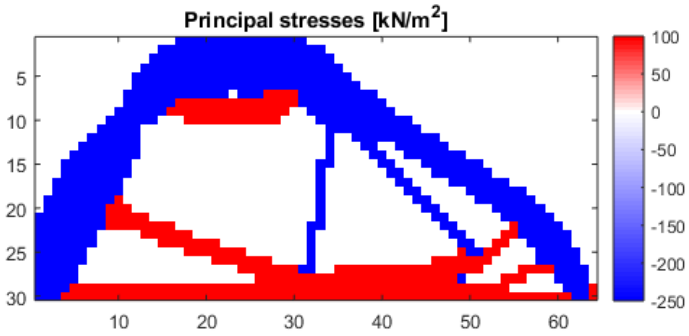

(b) BESO Approach

Figure 4.10: Principal Stress over the optimal material distribution Case 3.

4.2.1 Comparison of Results.

Figure 4.11 shows the overlay of the principal stress diagrams of the new material distribution and the full beam for both approaches in Case 1. In general terms, it could be said that the principal stress diagram of the material distribution after the optimization process are consistent with the ones of the full beam because they match the main areas in tension and compression. Comparing Figure 4.11.a and Figure 4.11.b, it was seen that the position of the top compression strut in the BESO approach is a little closer to the position of the of it on the full beam diagram. However, the thickness of this strut is more similar for the SIMP approach than for the BESO approach.

Figure 4.12 shows the overlay of the principal stress diagrams of the new material distribution and the full beam for both approaches in Case 2. First, analyzing Figure 4.12.a it is seen that the main areas in compression and

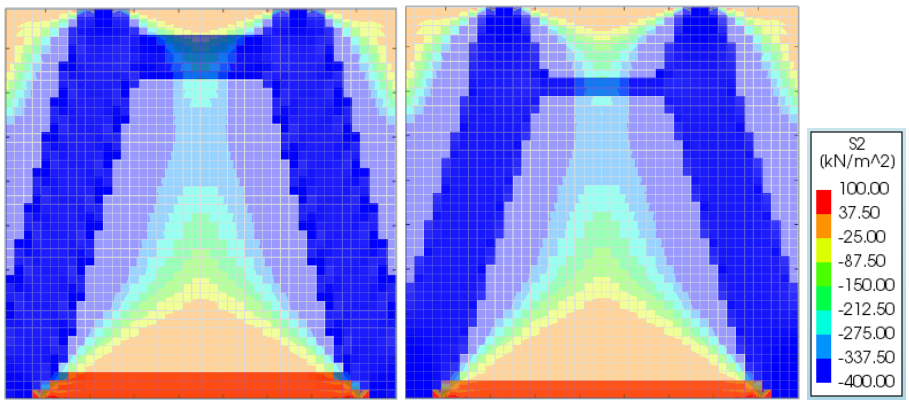

(a) SIMP Approach **(b)** BESO Approach **(c)**

Figure 4.11: Overlay of principal stress diagrams Case 1.

tension are consistent between the results of the SIMP approach and the full model. On the other hand, the result from the BESO approach (Figure 4.12.b) shows consistency in the most areas in compression but for the ones in tension it is seen that this model ignores some of them. This effect is seen especially in the elements around the hole. In the case, the principal stress diagrams obtained using the SIMP approach is closer to the results from the full beam.

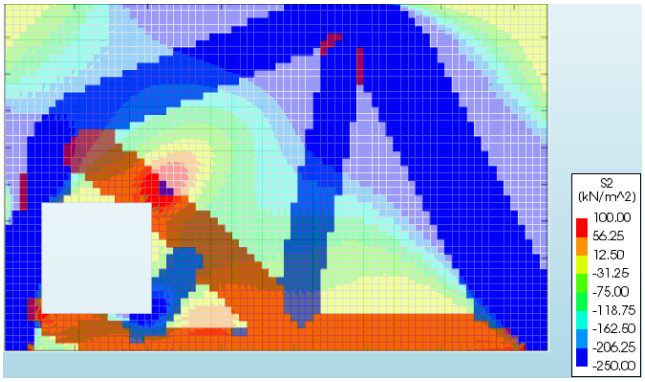

(a) SIMP Approach

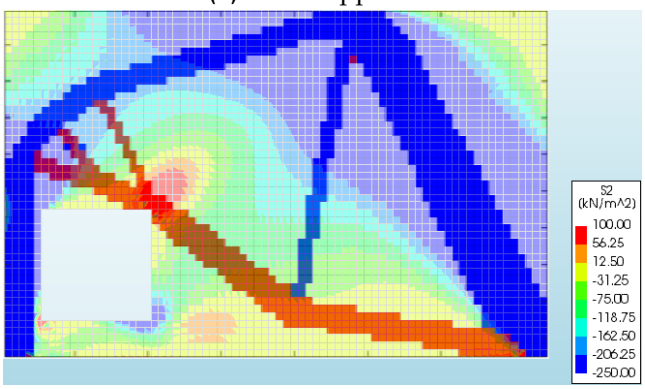

(b) BESO Approach

Figure 4.12: Overlay of principal stress diagrams Case 2.

Figure 4.13 shows the overlay of the principal stress diagrams of the new material distribution and the full beam for both approaches in Case 3. There

is a considerable similarity between the principal stresses diagrams obtained using the FEA software for the full domain and the ones obtained over the results of the topology optimization. It is considered that the results of the new material distributions are consistent with the one of the full beam because most of the areas in tension are also considered in both diagrams.

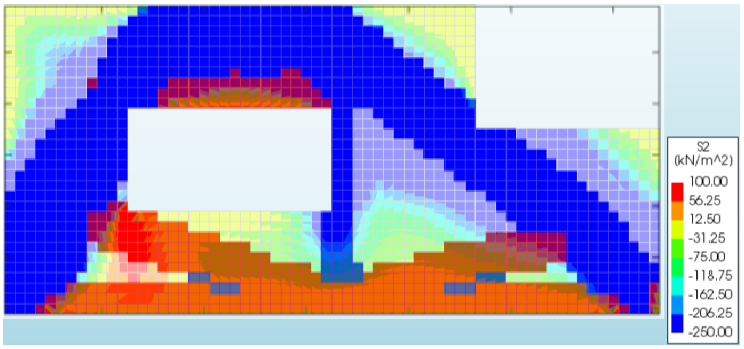

(a) SIMP Approach

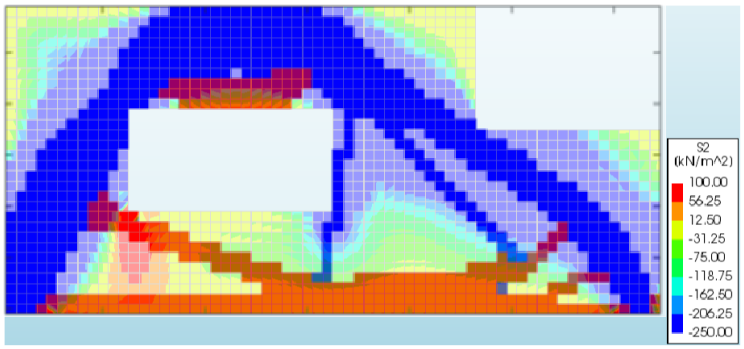

(b) BESO Approach

Figure 4.13: Overlay of principal stress diagrams Case 3.

Even though, in all of the cases, the results from the new material distribution are similar to the ones obtained from the full model, there are some areas in compression and tension that are ignored in these results. To create the truss structures these results were taken straight away, but in case that these results would be used to design a reinforcement layout additional conditions about the tensile areas that are not present in the results of the optimization process should be taking into account.

4.3 CREATION AND STABILIZATION OF TRUSS STRUCTURES

To find the truss structures that were used in the structural analysis the procedure described in Section 3.4 was followed.

4.3.1 Case 1

As it was stated in Section 4.1, for the Case 1 the variation of the input parameters does not have a notable influence in the trusses for the Strut-and-Tie model, so only one truss was analyzed for each approach. Figure 4.14 shows the resulting stable truss structures for Case 1 using the SIMP and BESO ap-

proaches, all the elements that were placed within the stress paths (green lines) of both approaches are considered as elements of the original structure. To stabilize these truss structures, the strategy that was followed was the addition of stabilizers. In this case for the SIMP and BESO approaches the stabilization process was simple because the necessary element to stabilize the structure (stabilizer) had only one possible position where it could be placed, that was from the bottom node to the opposite top one. A fast way to recognize which element is only acting as a stabilizer is that the stabilizer is the only element that is outside the stress paths (purple line).

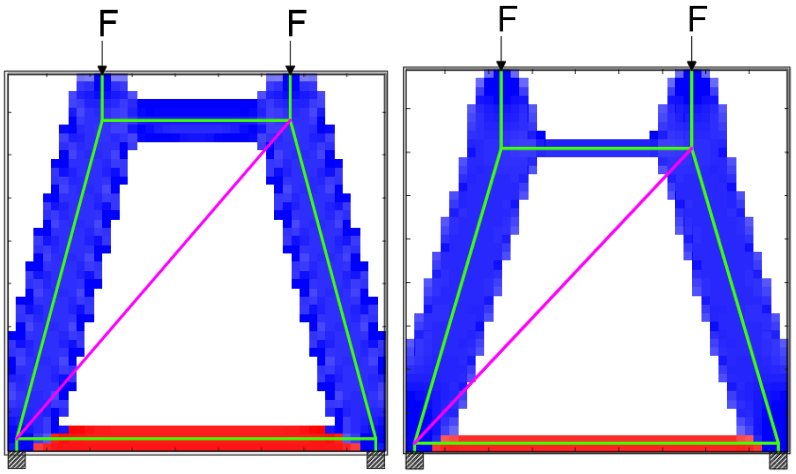

(a) SIMP Approach **(b)** BESO Approach

Figure 4.14: Stable Truss Structures for Case 1

4.3.2 Case 2

In this case, the variability of the material distributions results is noticeable, thus several trusses were created to analyzed the possible effect that the variation of the input parameter would have in the Strut-and-Tie model. Here the strategy followed for stabilizing a structure, and the color convention for the elements of the original structure (elements within the stress paths) and for stabilizer (elements outside of stress paths) was the same than the ones used in Case 1. Figure 4.15.a and 4.15.b shows the resulting stable structures for values of $volfrac = 0.3$ and $rmin = 1.5$ using the SIMP and BESO approaches. In this case, there were a couple of possible positions were the stabilizer could have been placed in every approach, but the position chosen position in both approaches was very similar. The stabilizer is connecting the node where the point load is applied (external node) with an internal node close to the hole, for the selected values of the input parameters the stabilization process was simple and only one stabilizer was needed. On the other hand, Figure 4.15.c and Figure 4.15.d shows the trusses created using a value $volfrac = 0.5$. In this case the stabilization process for large values of *volfrac* was more complicate than the one for a lower value of *volfrac*. To stabilize these structures was necessary the addition of three extra elements outside of the stress paths or the creation of one substructure and the addition of two extra elements.

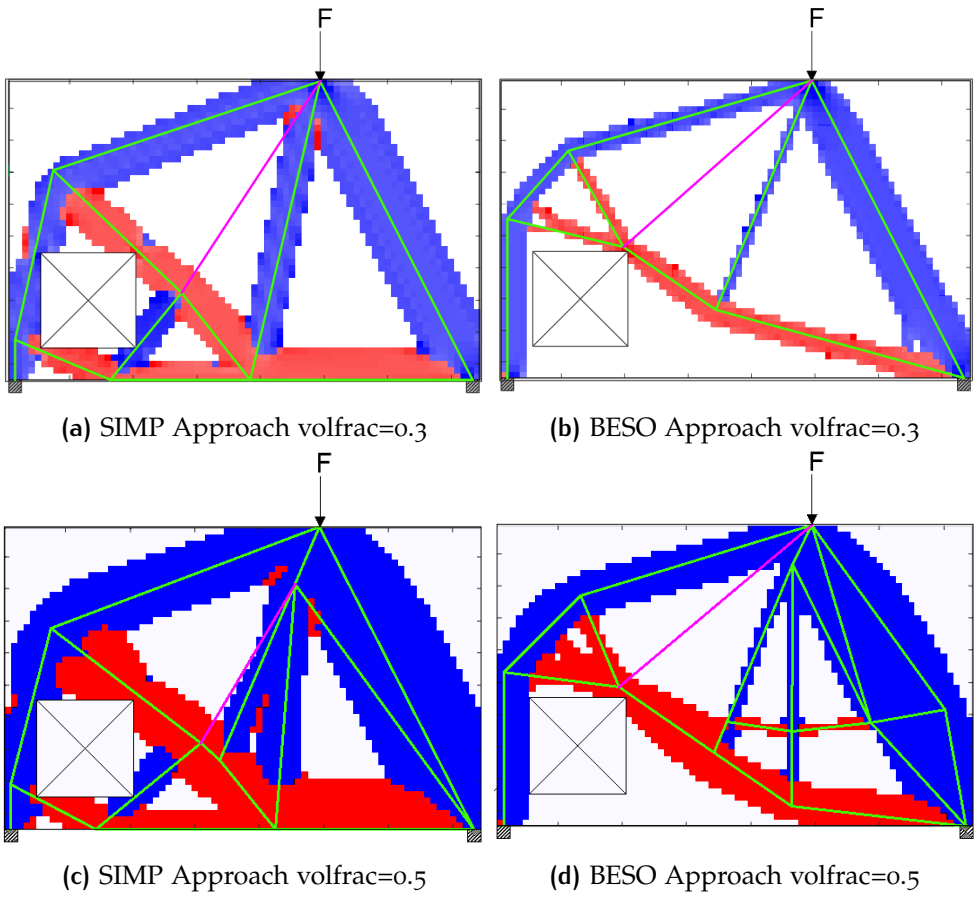

(a) SIMP Approach volfrac=0.3 **(b)** BESO Approach volfrac=0.3

(c) SIMP Approach volfrac=0.5 **(d)** BESO Approach volfrac=0.5

Figure 4.15: Stable Truss Structures for Case 2

4.3.3 Case 3

Figure 4.16 shows the resulting stable structures for Case 3 using the SIMP and BESO approaches. The same color convention depending on the type of elements used in the previous cases was used in Case 3, here for the stabilization process, two strategies were used, the addition of stabilizers, and the creation of substructures within the stress paths.

In the SIMP approach, the stabilizer (purple line) is connecting two internal nodes in the bottom part of the beam (Figure 4.16.a), there were other alternatives for the addition of the stabilizer but it was seen that this one is the one that interfered less with the stress diagrams form the topology optimization. In the case of the BESO approach (Figure 4.16.b) the stabilizer is connecting an internal node, with an external node that correspond to the rigth support of the beam.

The rest of alternatives where the stabilization strategy was creating substructures within the stress paths are shown in Figure 4.17 for the SIMP approach, and in Figure 4.17 for the BESO approach.

The stabilization process for truss structures created based on the results of $volfrac = 0.4$ and $volfrac = 0.5$ is similar due to the small surface area and the large value of *volfrac*, it makes that the created trusses do no differ much between them. On the other hand, using values of $volfrac = 0.3$ the resulting trusses are quite different, then, the stabilization process also differs. Figure 4.19 shows a stable truss structure for a value of $volfrac = 0.3$.

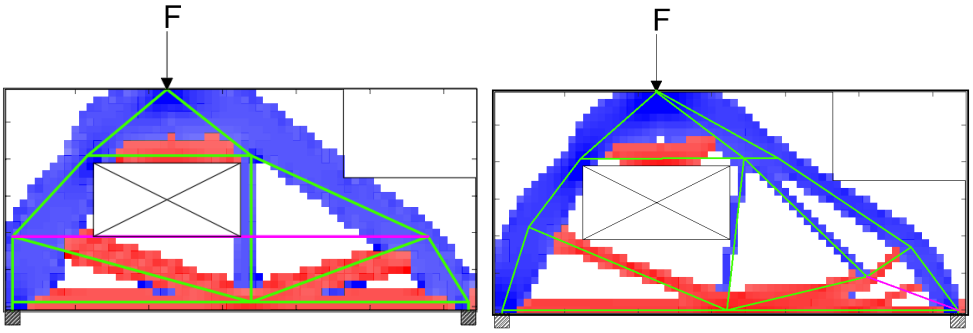

(a) SIMP Approach **(b)** BESO Approach

Figure 4.16: Stable Truss Structures for Case 3

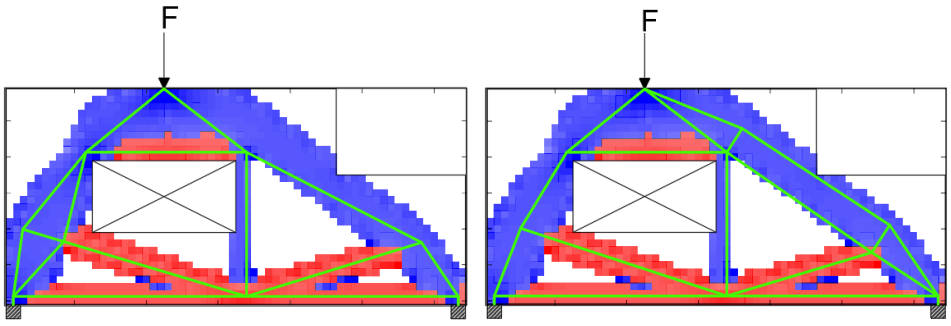

(a) Alternative truss 1 **(b)** Alternative truss 2

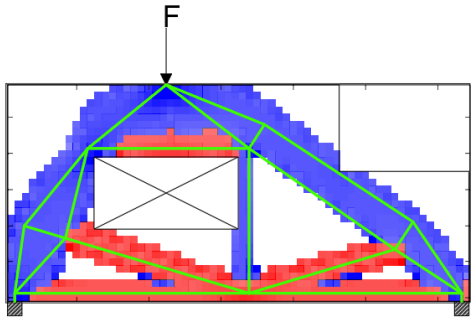

(c) Alternative truss 3

Figure 4.17: Alternatives for stable trusses using SIMP approach Case 3

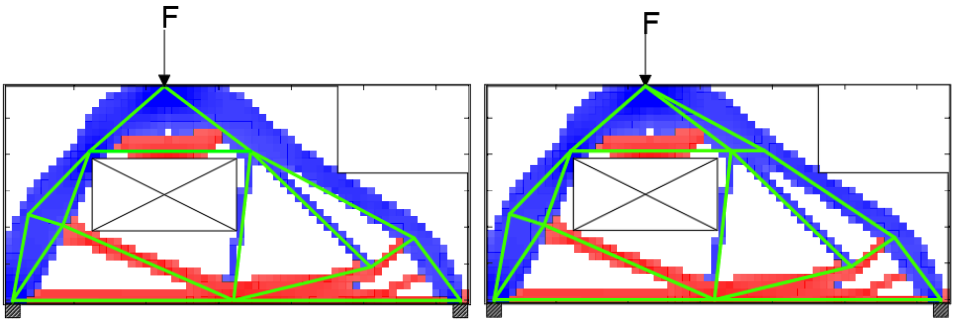

(a) Alternative truss 1 **(b)** Alternative truss 2

Figure 4.18: Alternatives for stable trusses using BESO approach Case 3

To stabilize this truss only one additional element was required, but it was not possible to find a position where this additional element has zero axial-

force (Section 4.4), consequently, with the addition of the stabilizer the stress diagram form the topology optimization changed.

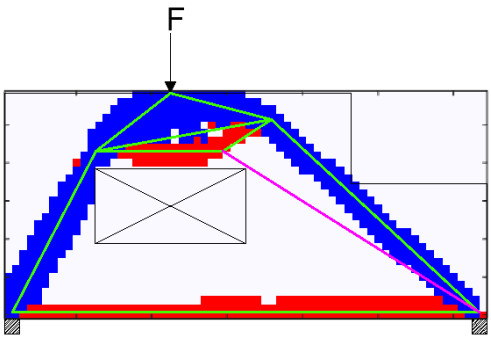

Figure 4.19: Stable truss for Case 3, volfrac=0.3

4.4 STRUCTURAL ANALYSIS OF TRUSSES

When the stable trusses have been found for each studied case, the structural analysis of these trusses was made using Rhinoceros with Grasshopper and Karamba plug-ins. The results of the structural analysis give the axial forces in all the members of the trusses.

4.4.1 Case 1

Figure 4.20 shows the results of the structural analysis for the proposed trusses in Case 1. It can be seen that the value of the axial force in the stabilizer for both approaches is zero. So, the stress diagrams found in Section 4.2 did not change. Also, it is seen that the axial forces in the elements of the trusses have the same sign than the stress diagrams over the results of the topology optimization.

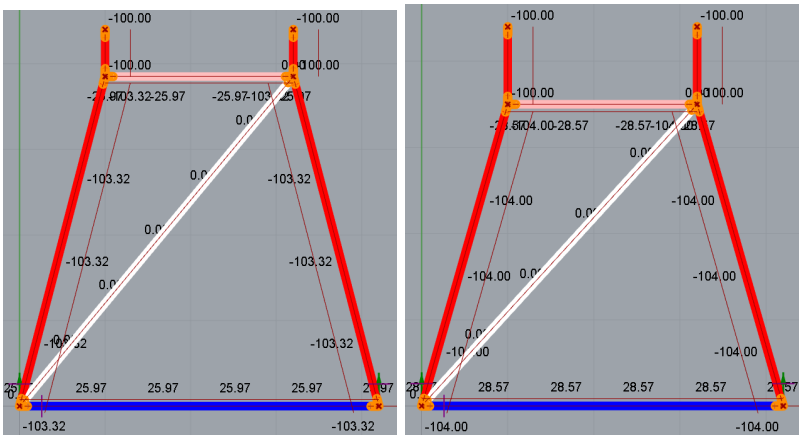

(a) SIMP Approach **(b)** BESO Approach

Figure 4.20: Truss Analysis for Case 1.

The resulting trusses obtained from this analysis are shown in Figure 4.21, in these structures, the stabilizers have been removed because they were

necessary just for the structural analysis of the trusses. Figure 4.21 also shows the small existing difference in the final trusses using SIMP and BESO approach. Table 4.1 shows a summary of the axial force in every element for the SIMP and BESO approaches. There is a small difference in the values of the axial force between the elements of the SIMP approach with their corresponding ones in the BESO approach.

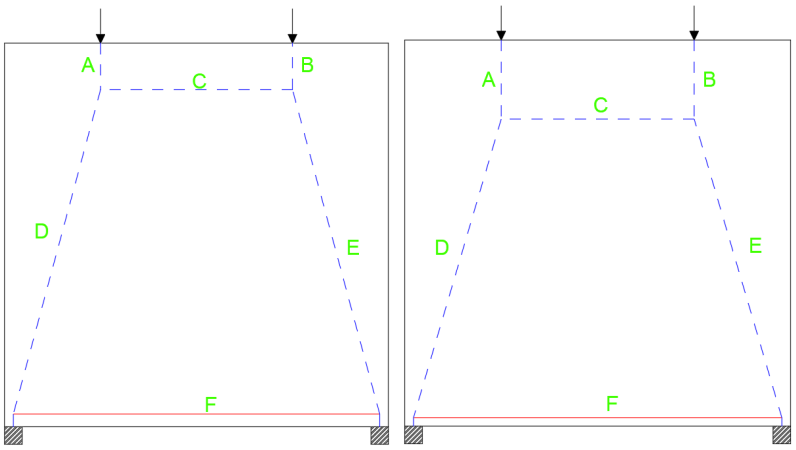

(a) SIMP Approach **(b)** BESO Approach

Figure 4.21: Final trusses for Case 1.

Table 4.1: Summary of axial forces for trusses of Case 1 (Figure 4.21)

	SIMP APPROACH		BESO APPROACH	
ELEMENT	FORCE (kN)	LENGTH (m)	FORCE (kN)	LENGTH (m)
A	-100.00	0.53	-100.00	0.9
B	-100.00	0.53	-100.00	0.9
C	-25.97	2.2	-28.57	2.2
D	-103.32	3.85	-104.00	3.55
E	-103.32	3.85	-104.00	3.55
F	**25.97**	**4.2**	**28.57**	**4.2**

4.4.2 Case 2

Figure 4.22 shows the results of the structural analysis for the proposed stable trusses corresponding to a $volfrac = 0.3$. In the same way, that in Case 1 the stress diagrams found in Section 4.2 did not change because for both approaches the force in the stabilizers is equal to zero. The final trusses resulting from this analysis are shown in Figure 4.23. In this case, the stabilizers were only required to obtain the forces in the elements of the original truss. Table 4.2 shows the axial forces in each member of the trusses for the SIMP and BESO approach. The highest values of tensile and compressive forces between the two trusses were found in elements **C** and **G** of the truss from the BESO approach, but this values alone said nothing

about the performance of the trusses, the performance of them according to the evaluation criteria is evaluated in Section 4.6.

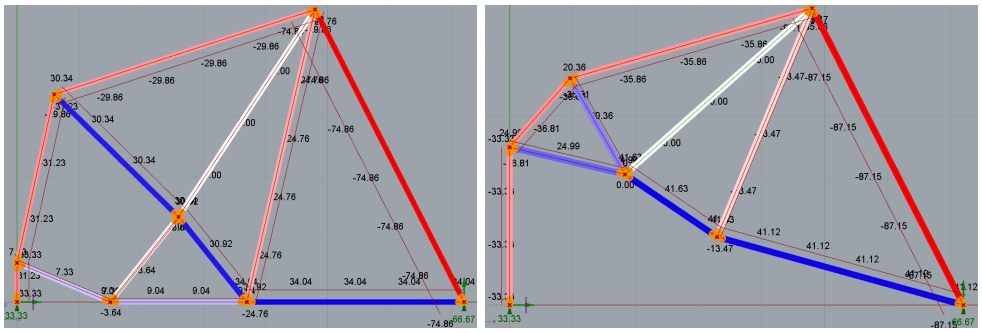

(a) SIMP Approach **(b)** BESO Approach

Figure 4.22: Truss Analysis for Case 2.

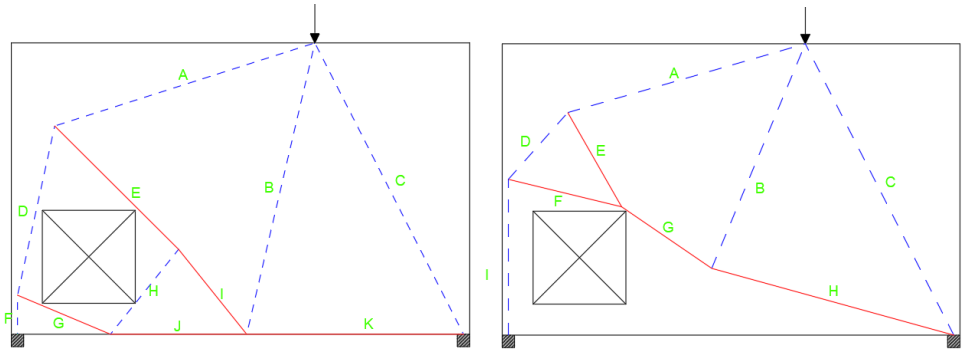

(a) SIMP Approach **(b)** BESO Approach

Figure 4.23: Final trusses for Case 2.

Table 4.2: Summary of axial forces for trusses of Case 2

SIMP APPROACH			BESO APPROACH		
Element	Force (kN)	Length (m)	Element	Force (kN)	Length (m)
A	-29.86	4.41	A	-35.86	4.00
B	-24.76	4.80	B	-13.47	3.93
C	-74.86	5.26	C	-87.15	5.28
D	-31.23	2.80	D	-35.86	1.44
E	**30.34**	**2.82**	**E**	**20.36**	**1.75**
F	-33.33	0.63	**F**	**24.99**	**1.88**
G	**7.33**	**1.63**	**G**	**41.63**	**1.76**
H	-3.64	1.76	**H**	**41.12**	**4.06**
I	**30.92**	**1.76**	I	-35.86	2.51
J	**9.04**	**2.20**			
K	**34.04**	**3.50**			

A structural analysis was performed also to the truss obtained using the BESO approach with a value of $volfrac = 0.5$ (Figure 4.15.d). The purpose of this analysis was to check if, even though the stabilization process of

this structure was more complicated than for trusses with lower values of *volfrac*, the total tension force in the structure is lower than the force in the other trusses. Figure 4.24 shows the results of the structural analysis for this structure, and Figure 4.25 shows the resultant truss structures.

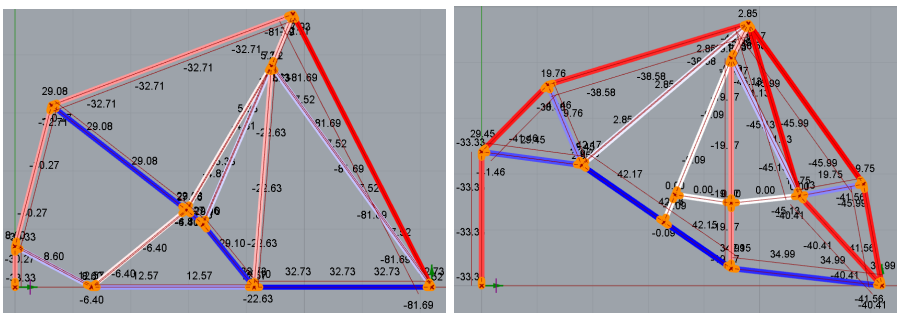

(a) SIMP Approach **(b)** BESO Approach

Figure 4.24: Truss analysis for stable structures $volfrac = 0.5$

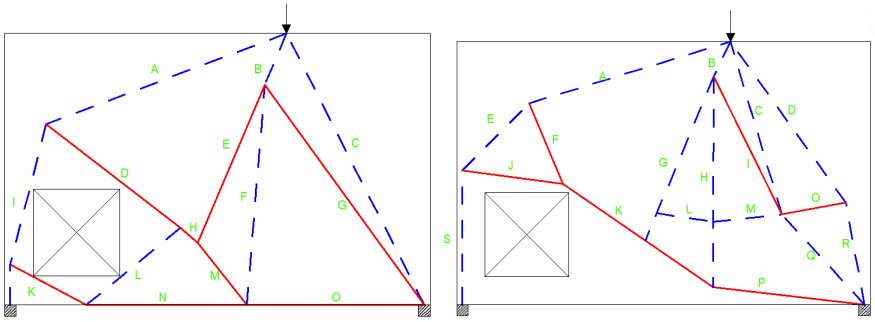

(a) SIMP Approach **(b)** BESO Approach

Figure 4.25: Stable truss structures using $volfrac = 0.5$

4.4.3 Case 3

Figure 4.26 shows the results of the structural analysis for the stable truss obtained using a volume of $volfrac = 0.3$, it is seen that even though, the stabilization process was simple, the truss does not fulfill the essential requirement for a stabilizer (zero axial force). Consequently, this truss is considered not valid for the evaluation criteria because it changes the stress diagram obtained in the topology optimization.

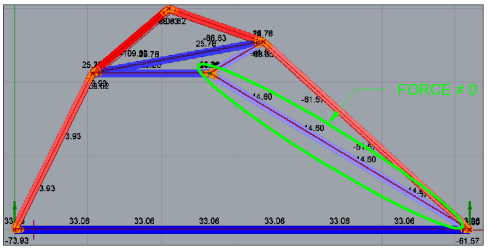

Figure 4.26: Truss analysis for stable structure $volfrac = 0.3$

Figure 4.27 shows the results of the structural analysis for all the proposed truss alternatives using the SIMP approach. In alternative one (Figure 4.27.a) is observed that the force in the stabilizer is very close to zero, so it was assumed that it did not change the stress diagrams of Section 4.2. Due to the difficulty to find this position where the stabilizer does not change the stress diagrams, other alternatives that did not require stabilizers were proposed (Figure 4.27.b to Figure 4.27.d), in these trusses, substructures were created in different parts of the stress diagrams. Figure 4.28 shows the final trusses proposed using the SIMP approach, the values of the axial forces in each member of this trusses are shown in Table 4.3 for the alternatives one and two, and in Table 4.4 for alternatives three and four.

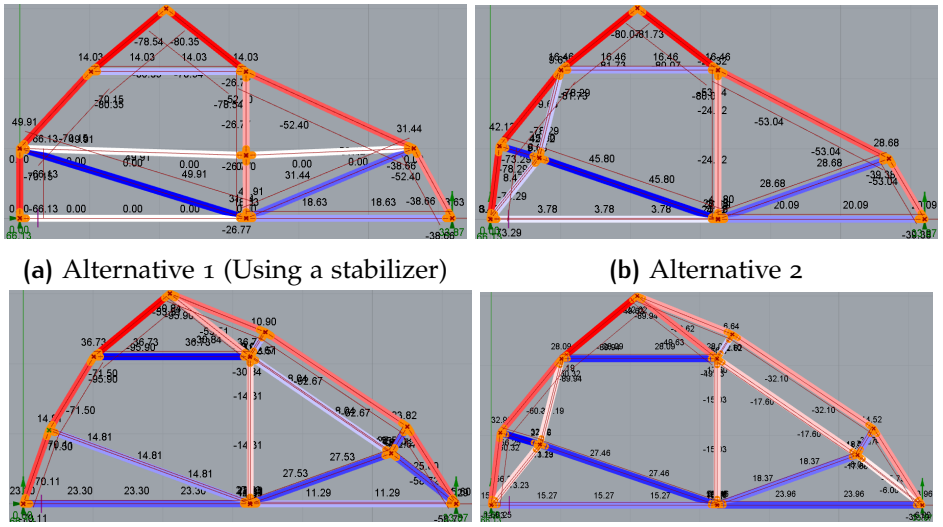

(a) Alternative 1 (Using a stabilizer) **(b)** Alternative 2

(c) Alternative 3 **(d)** Alternative 4

Figure 4.27: Truss Analysis for trusses obtained using SIMP approach Case 3

Similar to the SIMP approach, for the BESO approach the first alternative was stabilized adding one stabilizer and the other alternatives creating substructures within the stress path. Figure 4.29 shows the truss analysis for the alternatives proposed for the BESO approach, Figure 4.30 shows the final trusses corresponding to this analysis. Table 4.5 shows the axial forces for the truss elements of alternatives one and two, and Table 4.6 for alternative three.

From the results of the truss analysis, it is seen that in the trusses where substructures were created within the stress paths, although, the stress diagram showed areas in compression, some elements of the proposed trusses could be in tension. This effect of having one or more truss elements under tension in areas where the stress paths are in compression is due to the equilibrium of the extra node that is introduced when the substructure is created.

It is important to notice that, even though the strategy of creation substructures seems to work always stabilizing the truss structures, the angles formed between the elements near these substructures might not satisfy the requirements of the minimum angle between two elements for the Strut-and-Tie model. This criterion should be considered at the moment of dimension-

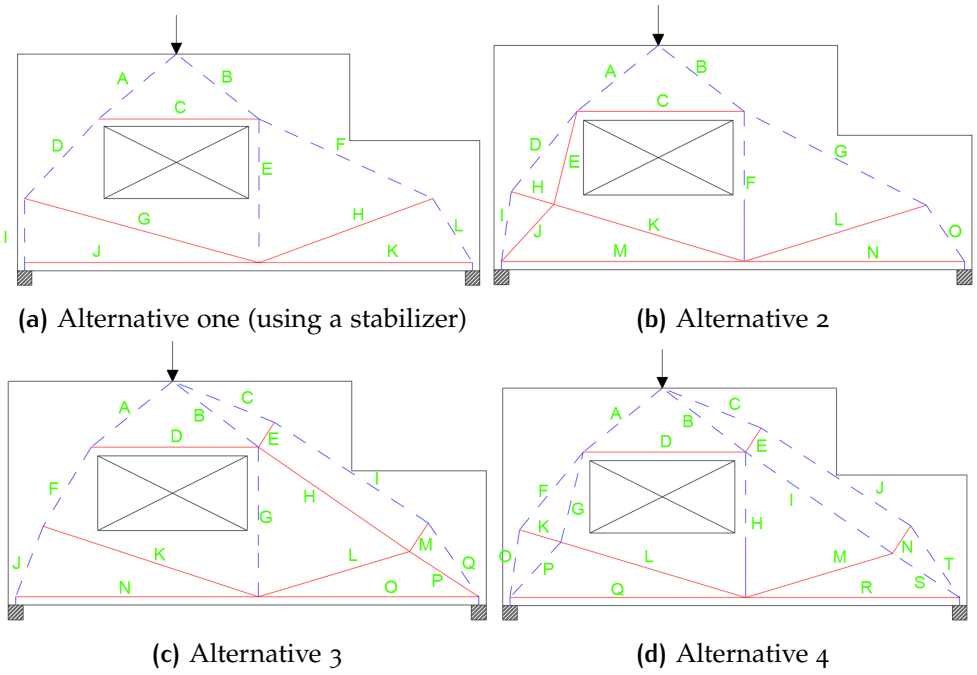

(a) Alternative one (using a stabilizer)

(b) Alternative 2

(c) Alternative 3

(d) Alternative 4

Figure 4.28: Alternatives of final trusses using SIMP approach for Case 3.

Table 4.3: Summary of axial forces for trusses using SIMP approach of Case 3 (1/2)

Alternative 1		
Element	Force (kN)	Length (m)
A	-80.35	1.41
B	-78.45	1.46
C	**14.03**	**2.23**
D	-70.15	1.5
E	-26.77	1.98
F	-52.40	2.65
G	**49.91**	**3.36**
H	**31.45**	**2.56**
I	-66.13	1
J	0.00	3.25
K	**18.63**	**2.96**
L	-38.66	1.05

Alternative 2		
Element	Force (kN)	Length (m)
A	-81.73	1.4
B	-80.07	1.45
C	**16.46**	**2.24**
D	-78.29	1.38
E	**9.63**	**1.28**
F	-24.32	2.01
G	-53.04	2.74
H	**42.12**	**0.6**
I	-73.29	0.94
J	**8.47**	**1.03**
K	**45.80**	**2.66**
L	**28.68**	**2.55**
M	**3.78**	**3.25**
N	**20.00**	**2.95**
O	-39.38	0.91

ing the Strut-and-Tie model, being necessary to verify it according to the specific design code that is being used.

Appendix E shows the tables with the summary of the axial forces for the truss structures taken from the literature (Figure 3.11).

Table 4.4: Summary of axial forces for trusses using SIMP approach of Case 3 (2/2)

Alternative 3			Alternative 4		
Element	Force (kN)	Length (m)	Element	Force (kN)	Length(m)
A	-95.90	1.4	A	-89.94	1.4
B	-30.84	1.45	B	-49.63	1.45
C	-53.51	1.47	C	-32.62	1.47
D	**36.73**	**2.24**	**D**	**28.09**	**2.24**
E	**10.90**	**0.4**	**E**	**6.64**	**0.4**
F	-71.50	1.24	F	-60.32	1.39
G	-14.31	2.01	G	-11.19	1.28
H	**8.04**	**2.46**	H	-15.03	2.01
I	-52.67	2.46	I	-17.60	2.46
J	-70.11	1.01	J	-32.10	2.46
K	**14.81**	**3.03**	**K**	**32.92**	**0.6**
L	**27.53**	**2.11**	**L**	**27.46**	**2.66**
M	**23.82**	**0.46**	**M**	**18.37**	**2.11**
N	**23.30**	**3.25**	**N**	**14.52**	**0.46**
O	**11.29**	**2.95**	O	-56.25	0.94
P	**25.60**	**1.11**	P	-13.23	1.04
Q	-58.72	1.2	**Q**	**15.27**	**3.25**
			R	**23.96**	**2.95**
			S	-6.00	1.11
			T	-45.8	1.2

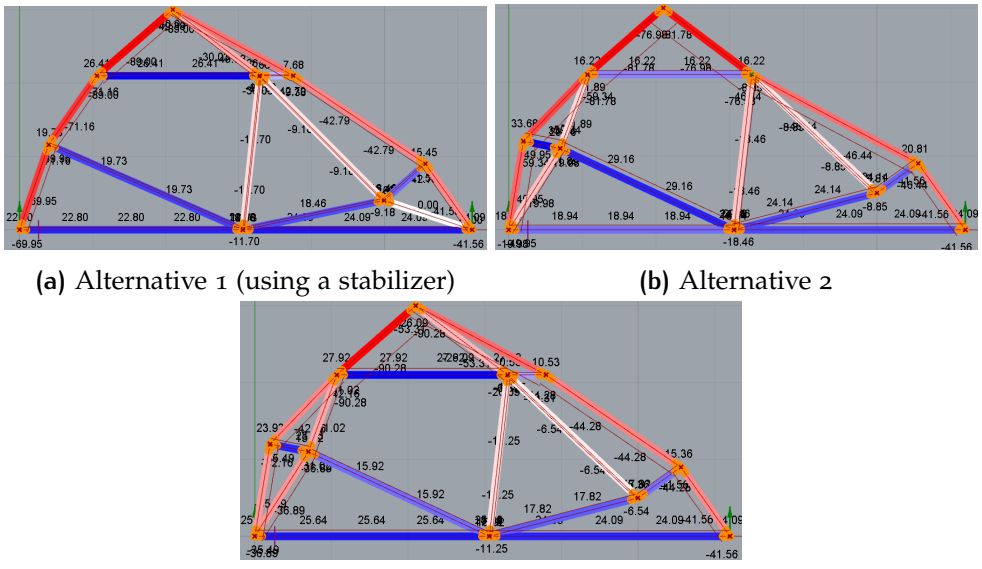

(a) Alternative 1 (using a stabilizer)

(b) Alternative 2

(c) Alternative 3

Figure 4.29: Truss Analysis for trusses obtained using BESO approach Case 3

4.5 SENSITIVITY ANALYSIS

Sensitivity analyses were performed in the trusses where stabilizers were used to check how the axial force in the stabilizer varies when the positions of the nodes change. In this section, all the results of these analyses are

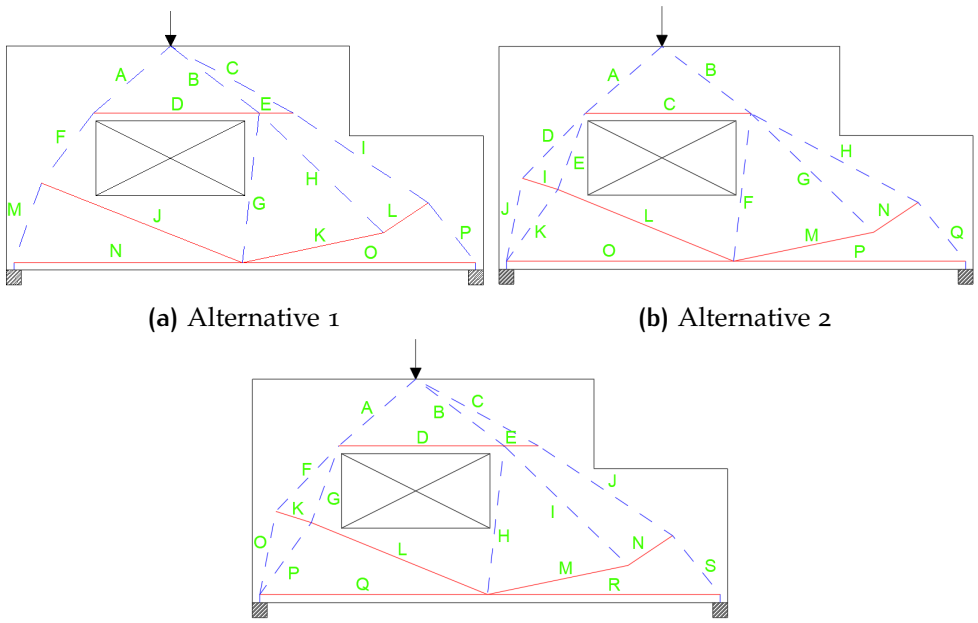

(a) Alternative 1

(b) Alternative 2

(c) Alternative 3

Figure 4.30: Alternatives of final trusses using BESO approach for Case 3

Table 4.5: Summary of axial forces for trusses using BESO approach of Case 3 (1/2)

Alternative 1			Alternative 2		
Element	Force (kN)	Length (m)	Element	Force (kN)	Length (m)
A	-89.00	1.38	A	-81.78	1.38
B	-30.03	1.49	B	-76.98	1.49
C	-49.38	1.89	**C**	**16.22**	**2.22**
D	**26.41**	**2.22**	D	-59.34	1.22
E	**7.68**	**0.45**	E	-11.89	1.1
F	-71.16	1.17	F	-18.46	2.08
G	-11.77	2.02	G	-8.85	2.32
H	-9.18	2.31	H	-46.44	2.57
I	-42.79	2.17	**I**	**33.68**	**0.5**
J	**19.73**	**2.90**	J	-49.95	1.14
K	**18.46**	**1.94**	K	-19.98	1.19
L	**15.45**	**0.72**	**L**	**29.16**	**2.56**
M	-69.95	1.13	**M**	**24.14**	**1.93**
N	**22.80**	**3.07**	**N**	**20.81**	**0.72**
O	**24.09**	**3.13**	**O**	**18.94**	**3.07**
P	-41.56	1.03	**P**	**24.09**	**3.13**
			Q	-39.35	1.02

presented in a graphical way, Appendix F shows all the combinations for Case 2 and Case 3 with the corresponding axial force in the stabilizer for the sensitivity analysis.

In cases two and three the analyzed nodes are free to move in both directions (x and y), so the variation of the coordinates of several points results in 4D graph. Due difficulty of interpretation of this type of graphs, in the sub-

Table 4.6: Summary of axial forces for trusses using BESO approach of Case 3 (2/2)

Alternative 3		
Element	Force (kN)	Length (m)
A	-90.28	1.38
B	-26.09	1.49
C	-53.31	1.88
D	**27.92**	**2.22**
E	**10.53**	**0.46**
F	-42.16	1.22
G	-31.02	1.1
H	-11.25	2.08
I	-6.54	2.32
J	-44.28	2.9
K	**23.92**	**0.5**
L	**15.92**	**2.56**
M	**1.82**	**1.93**
N	**15.36**	**0.72**
O	-35.49	1.14
P	-36.89	1.19
Q	**25.64**	**3.06**
R	**24.09**	**3.14**
S	-39.35	1.02

section corresponding to Case 2, the results of a example of the sensitivity analysis of a single point is presented.

4.5.1 Case 1

In this case, there was no variation in the axial force of the stabilizer for any possible position of the upper bar according to Table 1. Similar results were observed for the truss obtained using the BESO approach. Figure 1 shows the results of the sensitivity analysis for the SIMP and BESO approaches. It can be seen that for all the possible positions of the upper bar the force in the stabilizer remains as zero, in both approaches. Thus, the stabilizer added in Case 1 is considered to be non-sensitive, consequently, the stress diagram found for this case did not change when the position of the selected nodes changed.

4.5.2 Case 2

First the results of the sensitivity analysis only for point 2 are shown, then the results for the change in the position of the three analyzed nodes is present.

Figure 4.32 shows the variation of the force in the stabilizer when only one coordinate of the node varies. It is seen that for both coordinates (x and y) the variation of the force in the stabilizer is almost linear, with its

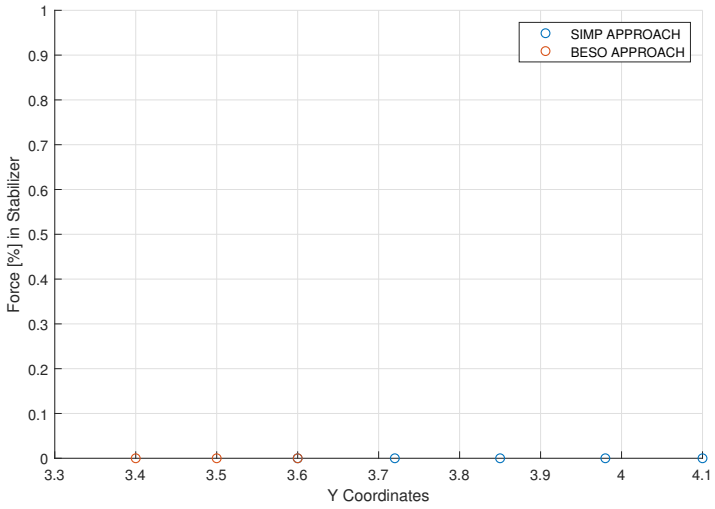

Figure 4.31: Sensitivity analysis results for trusses of Case 1.

minimum close to zero. The behavior of the stabilizer in both cases is similar because when the node moves away from its original position the force in the stabilizer started to increase, having Y coordinate a larger influence in the sensitivity of it.

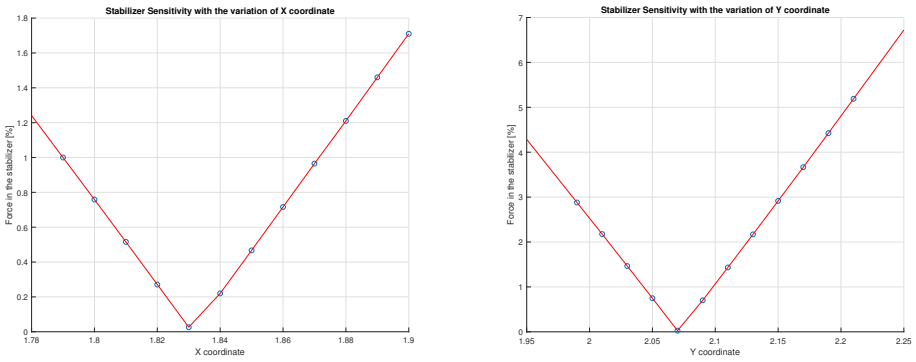

(a) Proposed truss **(b)** Alternative 1

Figure 4.32: Alternatives for final trusses using BESO approach for Case 3

Figure 4.33 shows the variation of the force in the stabilizer when only node two is moved from its original position. It is observed that in the line that the node is displaced there are two points where the force is minimum and two points where the force remains almost constant. In this example is seen that the variation of the force in the stabilizer is not linearly depending on the position of the node, the position of the node can be placed in more than one point without changing the principal stress diagram.

Finally, for the full sensitivity analysis of the trusses of Case 2, three nodes were considered to verify the effect that the change of their position would have on the force in the stabilizer. 60 possible combinations per each approach were analyzed. In the results, the x-axis corresponds to the positions of node one, and the y-axis corresponds to the positions of node three, both of them according to Table 3.5 for the SIMP approach, and Table 3.6 for the

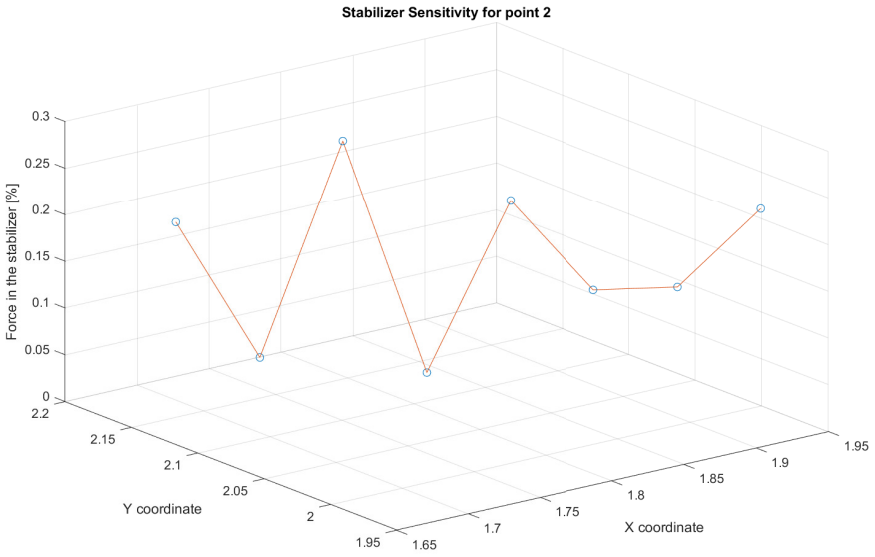

Figure 4.33: Sensitivity analysis results for trusses using BESO approach of Case 2.

BESO approach. The z-axis represents the percentage of the applied axial force ($100KN$) acting on the stabilizer, Figure 4.34 and Figure 4.35 show the results of the sensitivity analysis for the SIMP and BESO approaches, respectively.

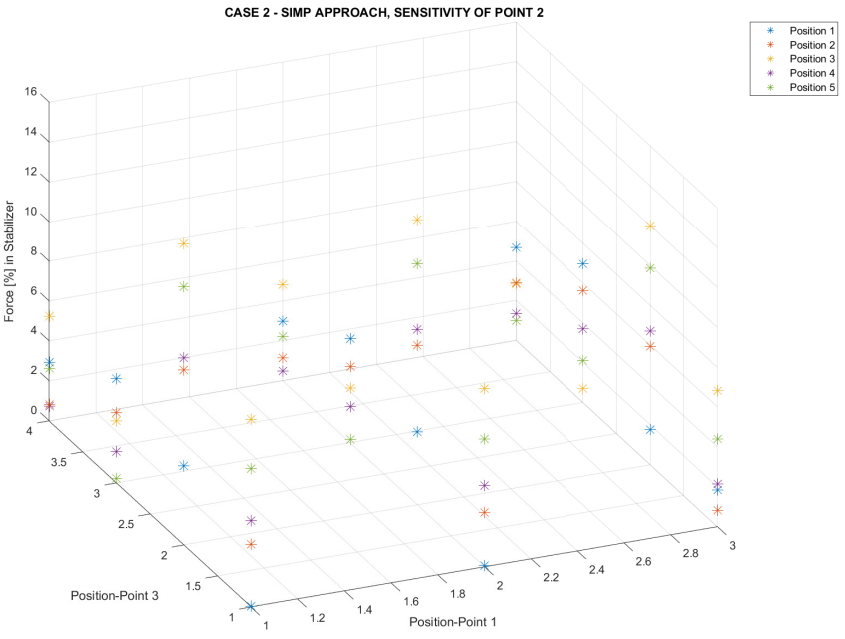

Figure 4.34: Sensitivity analysis results for trusses using BESO approach of Case 2.

It is observed that the force in the stabilizer of the truss obtained using the SIMP approach is very susceptible to change when the position of the nodes changed. In Figure 4.34, it is seen that there is not a specific position

of any node that provokes the largest force in the stabilizer for all positions of the two other nodes. The combination that gives the largest value of the force in the stabilizer (15.1%) for this truss is position one for node one, position three for node two, and position two for node three. It was found that there were ten different possible combinations (16% of the total amount of combinations) of nodes positions where it was assumed that the principal stress diagram did not change because the axial force present in the stabilizer is less than 1% of the applied force.

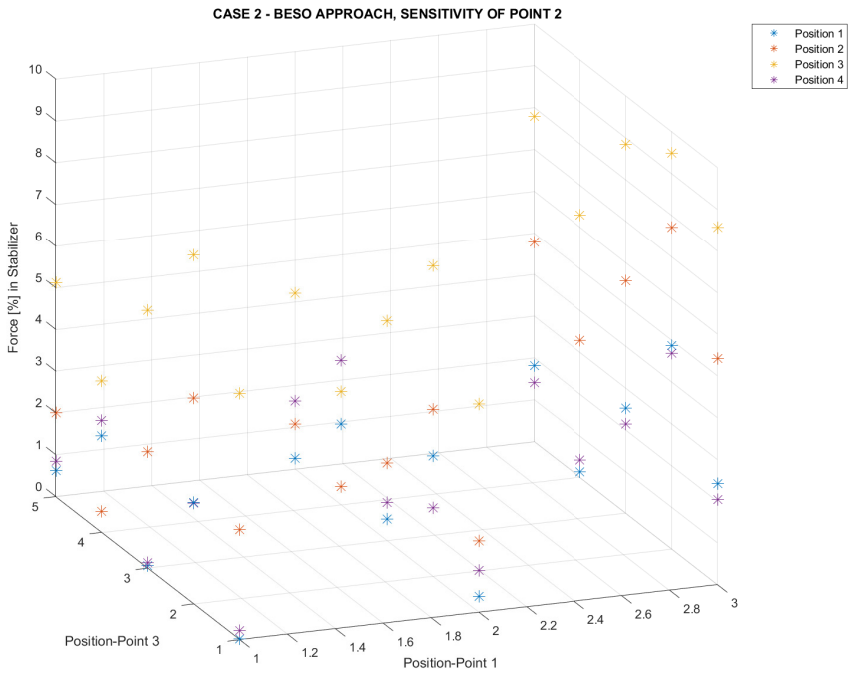

Figure 4.35: Sensitivity analysis results for trusses using SIMP approach of Case 2.

In the case of the truss obtaining using the BESO approach, Figure 4.34, it is seen that the force in the stabilizer is also very susceptible to change depending on the position of the nodes of elements that are connected to the stabilizer. Contrary to the results from the SIMP approach, in this case it was observed that position three of node two (yellow *) is the one that gives the largest forces in the stabilizer for all the other possible positions of the nodes, from them the combination that gives the largest global value of the axial force in the stabilizer (9.48%) is position three for nodes one and two, and position two for node three. There are 14 different possible combinations (23% of the total amount of combinations) of nodes positions where it was assumed that the principal stress diagram did not change because the axial force present in the stabilizer was less than 1% of the applied force.

4.5.3 Case 3

In the same way that in Case 2, 60 possible combinations were analyzed for the truss obtained using the SIMP approach, Figure 4.36 shows the variation of the force in the stabilizer expressed as a percentage of the external

applied force ($100KN$), using the same axis convention that the one used for Case 2, the x-axis corresponds to the position of point one, and the y-axis corresponds to the position of point three both of them according to Table 3.7.

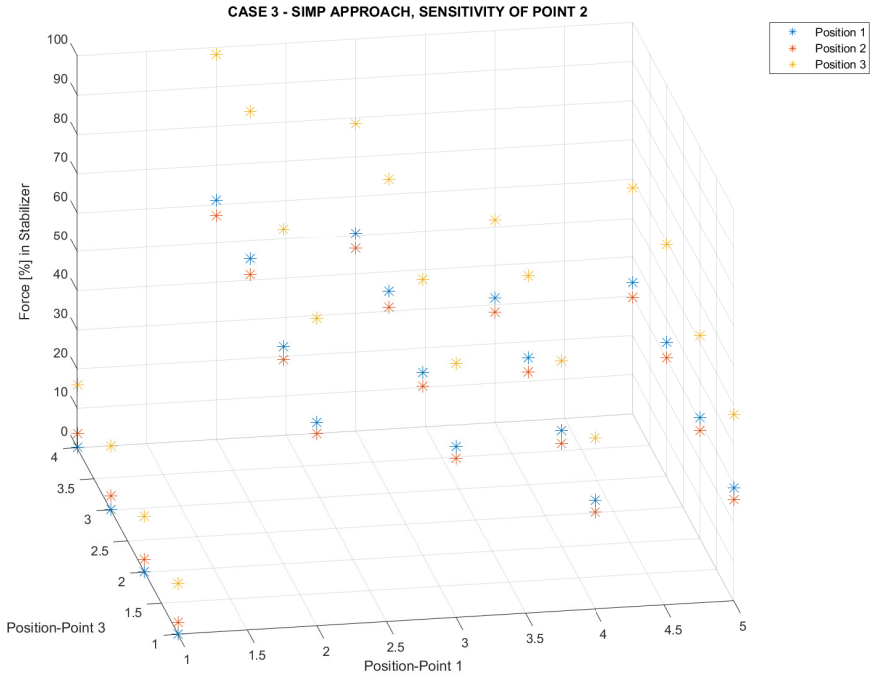

Figure 4.36: Sensitivity analysis results for trusses using SIMP approach of Case 3

It is seen that the force in the stabilizer is very susceptible to change when the positions of the nodes change. A similar situation that the one seen for the BESO approach of Case 2 is observed in this case. Position three of node two (yellow *) always gives the largest axial force in the stabilizer for all the other positions of the other two nodes. The combination that gave the largest axial force (99.57%) of all the possible combinations was position two for node one, and position three for nodes two and three. This model is extremely sensitive to change the principal stress diagrams, having only four possible solutions (0.07%) of the 60 combinations where the stress diagram was assumed to not changed because the force in the stabilizer was less than 1% of the applied load, all of these combinations corresponded to combinations where position of nodes one and two are located in position one.

4.6 EVALUATION OF TRUSSES

The evaluation criteria for the proposed trusses are divided into two parts, (i) the total amount of tension force in the truss elements, this force is given by the parameter H (Equation 3.1), and (ii) the compression stress in the struts. These parameters were computed for every proposed truss structure obtained in Section 3.5 and for all the trusses taken from the literature ac-

cording to Section 4.4. The selection of the most optimal truss structure will be based on the minimum value of H, the value of the compressive stress in the struts was used only to check that the concrete does not fail due to it.

4.6.1 Evaluation Criteria for Case 1

Table 4.7 shows the calculation of the H for truss obtained using the SIMP approach (Figure 4.21.a) because this structure has only one element under tension forces the total value of H for the truss is given only by this member. Likewise in the case of the BESO approach, the total value of H corresponding to Figure 4.21.b is given by Table 4.8, and Table 4.9 gives the total value of H for the STM taken from the literature (Figure 3.11.a).

Table 4.7: Computation of H, SIMP approach Case 1

Element	Force (kN)	Length (m)	H (kNm)
F	25.97	4.2	109.074

Table 4.8: Computation of H, BESO approach Case 1

Element	Force (kN)	Length (m)	H (kNm)
F	28.57	4.2	119.99

Table 4.9: Computation of H, model from literature [8] (Figure 3.11.a)

Element	Force (kN)	Length (m)	H (kNm)
F	42.74	4.2	179.51

These tables show that the truss with the lowest total tension force is the truss obtaining using the SIMP approach. In none of the struts of the trusses obtained using the SIMP and the BESO approaches or the ones from the truss from the literature, the compressive stress in the concrete was critical. The maximum compressive stress was found in the truss from literature, elements D and E (Figure 3.11.a) are under a compressive stress of $6MPa$. Considering these results, it is assumed that the best truss structure according to the evaluation criteria is, the one obtained using the SIMP approach (Figure 4.21.a). The small difference between the results of the SIMP and BESO approach (8.5%) was expected because, the results of the optimization process and the created truss are very similar, the small difference in the total tension force is due to the angle formed between the struts and the tie in the bottom of the beam.

4.6.2 Evaluation Criteria for Case 2

Analogous as Case 1, in this case, Table 4.10, Table 4.11, and Table 4.14 show the computation of H for the trusses generated using the SIMP (Figure 4.23.a and Figure 4.23.c) and BESO (Figure 4.23.b and Figure 4.23.d) approaches,

and for the truss of the STM taken from the literature (Figure 3.11.b), respectively.

Table 4.10: Computation of H, SIMP approach $volfrac = 0.3$ (Figure 4.23.a)

Element	Force (kN)	Length (m)	TiLi (kNm)
E	30.34	2.82	85.56
G	7.33	1.63	11.95
I	30.92	1.76	54.42
J	9.04	2.2	19.89
K	34.04	3.5	119.14
		H [kNm]	290.95

Table 4.11: Computation of H, BESO approach $volfrac = 0.3$ (Figure 4.23.b)

Element	Force (kN)	Length (m)	TiLi (kNm)
E	20.36	1.75	35.63
F	24.99	1.88	46.98
G	41.63	1.76	73.27
H	41.12	4.06	166.95
		H [kNm]	322.83

Table 4.12: Computation of H, SIMP approach $volfrac = 0.5$ (Figure 4.23.c)

Element	Force (kN)	Length (m)	TiLi (kNm)
D	29.08	2.94	85.50
H	27.06	0.39	10.55
M	29.10	1.38	40.16
O	32.73	3.07	100.48
K	8.60	1.5	12.90
N	12.57	2.79	35.07
G	7.52	4.71	35.42
E	5.33	2.97	15.83
		H [kNm]	335.91

The trusses created for this case have many members under the action of tension forces, then the total value of H was given by the summation of the partial H values of each member. The truss took from the literature (Figure 3.11.b) was determined to get a large value of stiffness (low displacement under the load), this structure was found splitting the point force in two forces of different magnitude, and then finding the individual trusses for each point loads [8]. For these reasons, it would not be a good point of reference comparing the value of H of this truss with the ones of the other trusses.

Comparing the trusses obtained using the topology optimization, the one that has a minimum value of H is the one obtained using the SIMP approach

Table 4.13: Computation of H, BESO approach $volfrac = 0.5$ (Figure 4.23.d)

Element	Force (kN)	Length (m)	TiLi (KN,m)
F	19.76	1.56	30.83
J	29.45	1.81	53.30
K	42.17	3.27	137.90
P	34.99	2.73	95.52
O	19.75	1.17	23.11
I	11.13	2.75	30.61
		H [kNm]	371.26

Table 4.14: Computation of H, model from literature [8] (Figure 3.11.b)

Element	Force (kN)	Length (m)	TiLi (kNm)
C.2	8.24	1.00	8.24
H	30.26	5.34	161.59
J	10.65	1.03	10.97
K	10.24	0.99	10.14
N	19.22	0.99	19.03
O	20.89	0.99	20.68
P	20.89	1.10	22.98
Q	19.22	0.99	19.03
U	9.73	1.13	10.99
V	10.95	1.10	12.05
X	8.31	1.81	15.04
Y	32.46	3.16	102.57
Z1.2	9.50	1.04	9.88
		H [kNm]	423.19

for a value of $volfrac = 0.3$ (Figure 4.23.a), in these trusses also all the elements in compression had stresses lower than the maximum admissible. Thus, for Case 2 the truss found using the SIMP approach is consider as the most optimal according to the chosen evaluation criterion, this truss has a value of H that is 9.9% smaller than the best option of the trusses obtained using the BESO approach.

Furthermore, it is observed that the trusses obtained using a value of $volfrac = 0.5$ had larger values of the total tension force than the ones using a value $volfrac = 0.3$. Thus, in this case, the trusses created using lower values of $volfrac$ for the topology optimization generated trusses that are easily stabilized and have a better performance according to the evaluation criterion.

4.6.3 Evaluation Criteria for Case 3

Several trusses were created for each approach of this case, therefore the value of H had to be calculated for every alternative. Table 4.15, Table 4.16, Table 4.17, Table 4.18 show the calculation of H for the four alternatives using

the SIMP approach, likewise Table 4.19, Table 4.20, Table 4.21 for the alternatives using the BESO approach, and finally Table 4.22, Table 4.23 show the calculation of H for the Novak-Sprenger and Zhong et al. models, respectively.

Table 4.15: Computation of H, SIMP approach Case 3 (Alternative 1 Figure4.28.a)

Element	Force (kN)	Length (m)	TiLi (kNm)
C	14.03	2.23	31.29
G	49.91	3.36	167.70
H	31.45	2.56	80.51
K	18.63	2.96	55.14
		H [kNm]	334.64

Table 4.16: Computation of H, SIMP approach Case 3 (Alternative 2 Figure4.28.b)

Element	Force (kN)	Length (m)	TiLi (kNm)
C	16.46	2.24	36.87
E	9.63	1.28	12.33
H	42.12	0.6	25.27
J	8.47	1.03	8.72
K	45.80	2.66	121.83
L	28.68	2.55	73.13
M	3.78	3.25	12.29
N	20.00	2.95	59.00
		H [kNm]	349.44

Table 4.17: Computation of H, SIMP approach Case 3 (Alternative 3 Figure4.28.c)

Element	Force (kN)	Length (m)	TiLi (kNm)
D	36.73	2.24	82.28
E	10.90	0.4	4.36
H	8.04	2.46	19.78
K	14.81	3.03	44.87
L	27.53	2.11	58.09
M	23.82	0.46	10.96
N	23.30	3.25	75.73
O	11.29	2.95	33.31
P	25.60	1.11	28.42
		H [kNm]	357.78

In this case also the two models taken from the literature have much higher values of H than any of the created trusses using the SIMP or BESO approaches. A possible explanation is that these models cover a bigger surface area than the ones created using the results of the topology optimization, it could also be argued that the trusses from the literature for all the studied

Table 4.18: Computation of H, SIMP approach Case 3 (Alternative 4 Figure4.28.d)

Element	Force (kN)	Length (m)	TiLi (kNm)
D	28.09	2.24	62.92
E	6.64	0.4	2.66
K	32.92	0.6	19.75
L	27.46	2.66	73.04
M	18.37	2.11	38.76
N	14.52	0.46	6.68
Q	15.27	3.25	49.63
R	23.96	2.95	70.68
		H [kNm]	324.12

Table 4.19: Computation of H, BESO approach Case 3 (Alternative 1 Figure4.30.a))

Element	Force (kN)	Length (m)	TiLi (kNm)
D	26.41	2.22	58.6302
E	7.68	0.45	3.456
J	19.73	2.90	57.217
K	18.46	1.94	35.8124
L	15.45	0.72	11.124
N	22.80	3.07	69.996
O	24.09	3.13	75.4017
		H [kNm]	311.64

Table 4.20: Computation of H, BESO approach Case 3 (Alternative 2 Figure4.30.b))

Element	Force (kN)	Length (m)	TiLi (kNm)
D	20.48	2.22	45.47
J	25.24	2.90	73.20
K	21.84	1.93	42.15
L	18.82	0.72	13.55
M	20.39	3.06	62.39
N	24.09	3.14	75.64
		H [kNm]	312.40

cases were created to get a maximum stiffness (minimum displacement) and the tension force was not a design parameter.

Table 4.21: Computation of H, BESO approach Case 3 (Alternative 3 Figure4.30.c))

Element	Force (kN)	Length (m)	TiLi (kNm)
D	27.92	2.22	61.98
E	10.53	0.46	4.84
K	23.92	0.5	11.96
L	15.92	2.56	40.76
M	1.82	1.93	3.51
N	15.36	0.72	11.06
Q	25.64	3.07	78.71
R	24.09	3.13	75.40
		H [kNm]	288.23

Table 4.22: Computation of H, STM by Novak-Sprenger [2] (Figure 3.11.c)

Element	Force (kN)	Length (m)	TiLi (kNm)
C	44.55	2.34	104.25
G	31.43	1.11	34.89
I	20.03	1.11	22.23
J	15.83	0.84	13.30
K	11.40	1.06	12.08
M	40.06	1.06	42.46
N	15.83	0.84	13.30
Q	59.14	0.95	56.18
R	15.83	0.84	13.30
U	78.21	2.18	170.50
X	34.17	0.84	28.70
Z	37.05	0.91	33.72
		H [kNm]	544.91

Table 4.23: Computation of H, STM by Zhong et al.[2] (Figure 3.11.d)

Element	Force (kN)	Length (m)	TiLi (kNm)
C	8.50	1.89	16.07
G	39.17	2.44	95.57
L	34.53	1.17	40.40
N	25.13	1.17	29.40
O	13.95	0.84	11.72
P	18.54	2.47	45.79
R	63.84	2.47	157.68
U	13.52	1.56	21.09
V	52.66	2.57	135.34
		H [kNm]	553.07

Among the four possible trusses obtained using the SIMP approach, it is seen that the maximum variation of H is 9.4% between alternatives two and three, being alternative three the one that has the minimum value of H, and

alternative two has the highest one. On the other hand, among the three alternatives obtained using the BESO approach, the maximum variation in H is 8.3% between alternative one and alternative three, being the best one with the lowest value of H alternative three and the one with the highest alternative one. It is also observed that every truss created using the BESO approach gives a lower value of H than any truss obtained using the SIMP approach. Thus, the extra internal element (branch in the stress diagram) gives a better response to the trusses in terms of minimum tension force.

From this relations, it could be assumed that in Case 3, the alternatives that give the lowest values of H are the ones where substructures were created within the stress paths in both sides of the structure. As well as, all the previous cases the compressive stress is lower than the maximum allowed, thus it is not a decisive factor at the moment of selecting the most optimal truss according to the evaluation criteria. In this case, the difference between the minimum value of H of the 2 approaches is 12.5%, being the best option according to the evaluation of the BESO approach, and the most optimal truss structure is the alternative three created using this approach.

For all the studied cases the difference in results between the two approaches was around 10%, the results with the stabilization methods were also similar. Thus, it is assumed that the two methods are suitable to created stable trusses that could be used in the STM.

5 CONCLUSIONS AND RECOMMENDATIONS

5.1 CONCLUSIONS

The objective of this thesis was to generate and compare truss structures based on the results of two approaches of topology optimization that could be used in Strut-and-Tie models. Three cases of deep concrete beams were selected for this study, the number of discontinuities in the domain of the beams increased gradually for each case. The scripts used for the topology optimization were based on educational scripts developed by Sigmund [9].

The main findings for the research questions are briefly described here:

a **Can suitable truss structures for the Strut-and-Tie model always be created from the results obtained in the topology optimization ?**

Considering all the results obtained in this thesis for the three studied cases, it is assumed that the SIMP and BESO approaches of the topology optimization are similarly efficient, and it would always be possible to obtain suitable truss structures for the Strut-and-Tie model.

b **What is the influence of the input parameters for each approach, and to what extent do these approaches differ in the results of the topology optimization, and truss generation ?**

The main influence of the input parameters on the results of the topology optimization are, (i) the thickness of the stress (material) paths, it was mainly observed with the variation of *volfrac*, the stress paths got thicker as the value of it increased, and (ii) the number of internal branches in the results, this effect had a opposite effect between the input parameters, the results were more branched when the value of *volfrac* increased, while, they were less branched for larger values of *rmin*. Even though, in most cases, the variation of the input parameters did not change the global topology of the results, the extra creation of internal branches, or having paths thicker stress paths made that, the stabilization process became more difficult and in some case not possible to do it without changing the stress paths of the topology optimization.

The small difference in the results according to the evaluation criterion for all the studied cases, the fact that there is no a big difference between the results of the two topology optimization approaches, also the global shape of the results did not change between the results of each approach, and that only some changes appeared in the areas surrounding the discontinuities of the models making that some truss structures differ from each other, lead to the assumption that the two approaches are equally suitable for the creation of stable truss structures that can be used in the STM.

c **Which aspects should be considered to stabilize the truss structures obtained using topology optimization?**

The stabilization of the trusses is necessary to perform a structural analysis of them and make it easier for the calculation of the axial forces in the elements. The first aspect that should be determined is the number of stabilizers that should be added to the original truss. After the stabilizers are placed, it is necessary to verify that the axial forces on them are zero, in case that the force in them is not zero, the proposed truss does not correspond anymore with the results of the topology optimization, thus the positions of some nodes should change to get a zero force on it, always considering that all the elements of the truss should be within the stress paths. If after this process, it is not possible to get a zero force in the stabilizers, additional elements within the stress paths instead of the stabilizers should be added to create substructures that help to stabilize the whole structure. This process was proved to works for all the proposed trusses of the three cases studied in this thesis.

d **How sensitive are the stabilizers of the trusses to change the stress diagrams obtained with the topology optimization?**

Even though, having a very sensitive truss does not mean that this structure will have a bad performance in the Strut-and-Tie, a very sensitive truss implies that with a small change on the position of the nodes the proposed structure will not correspond anymore to the stress paths obtained during the topology optimization. The sensitivity of the stabilizers depends completely on the complexity of the trusses. In Case 1, the truss is simple and there was only one possible position to add a stabilizer, thus there were no changes in the axial force of the stabilizer for all the analyzed positions of the nodes, then the stabilizers were assumed to be non-sensitive. On the other hand, the trusses of Case 2 and Case 3 are very sensitive because the axial force in the stabilizers changed easily when the positions of the nodes changed. For these two cases, it was proved that a better stabilization strategy to get a minimum tension force was the creation of substructures within the stress paths.

e **Which is the most optimal approach (SIMP or BESO) for topology optimization to create truss structures based on the results of the optimization process according to the evaluation criteria?**

Considering only the total amount of tension force in the structure, from the three cases, in two of them the most optimal truss was obtained using the SIMP approach, and in the third one, it was obtained using the BESO approach. Because the difference in results for all the cases was around 10 %, then it could not be said that one approach is better than the other just based on this criterion. Additional factors like the percentage of beam surface area cover by the proposed truss, stiffness of the structure, computational cost, etc. These factors, among others, should be included in the evaluation to assume that one approach is better.

5.2 RECOMMENDATIONS

1. **Dimensioning of the Strut-and-Tie model.**

   Making an accurate and complete dimensioning of the Strut-and-Tie model using the truss structures obtained in this thesis would be useful to see the real performance of the proposed trusses. It is also important to consider the minimum angles allowed between the elements of the truss according to an specific design code, this criterion would be specially important to check for the trusses that are stabilized using the creation of substructures within the stress paths.

2. **Adding the more parameters to the evaluation criteria.**

   The evaluation of only one parameter is not enough to decide if a determinate approach is better than others. The addition of more parameters to the evaluation criteria would give a better understanding of the global performance of the proposed truss structures. It would also help the comparisons with models from literature because they would be more representative.

3. **Comparing the results of the truss model with the discrete model**.

   Comparing the total amount of reinforcement needed for the created truss structure and the one for the discrete model (stress paths obtained form the topology optimization) would be a good way to validate the procedure used in this thesis.

4. **Automatizing the generation process of the truss structures.**

   In this thesis the creation of the truss structures was done in a manual way, implementing this process into the MATLAB scripts to make this an automatic process would save a lot of time at the moment of the creation of the trusses. Besides, the structural analysis could have been implemented in the same MATLAB script.

5. **Different formulation for the topology optimization approaches.**

   Using different formulations, like the hybrid approaches, for the topology optimization would lead to different final truss structures, comparing these trusses with the ones obtained using the SIMP and BESO approaches would give a better idea of the performance of the results obtained using

6. **Controlling the computational cost of each approach of topology optimization**.

   Controlling the time that each approach takes to solve the topology optimization, and the calculation of the principal stresses would give an idea of which approach is better to use in more complex structures from the computational cost point of view.

BIBLIOGRAPHY

[1] H.-G. Kwak and S.-H. Noh, "Determination of strut-and-tie models using evolutionary structural optimization," *Engineering Structures*, vol. 28, no. 10, pp. 1440–1449, 2006.

[2] J. Zhong, L. Wang, P. Deng, and M. Zhou, "A new evaluation procedure for the strut-and-tie models of the disturbed regions of reinforced concrete structures," *Engineering Structures*, vol. 148, pp. 660–672, 2017.

[3] J. Schlaich and K. Schafer, "Design and detailing of structural concrete using strut-and-tie models," *Structural Engineer*, vol. 69, no. 6, pp. 113–125, 1991.

[4] R. C. Hibbeler and K.-H. Tan, *Structural Analysis in SI Units*. Pearson Australia Pty Limited, 2016.

[5] A. Gebisa and H. Lemu, "A case study on topology optimized design for additive manufacturing," in *IOP Conference Series: Materials Science and Engineering*, vol. 276, no. 1. IOP Publishing, 2017, p. 012026.

[6] A. T. Gaynor, J. K. Guest, and C. D. Moen, "Reinforced concrete force visualization and design using bilinear truss-continuum topology optimization," *Journal of Structural Engineering*, vol. 139, no. 4, pp. 607–618, 2012.

[7] H. Hardjasaputra, "Evolutionary structural optimization as tool in finding strut-and-tie-models for designing reinforced concrete deep beam," *Procedia Engineering*, vol. 125, pp. 995–1000, 2015.

[8] S. El-Metwally and W.-F. Chen, *Structural Concrete: Strut-and-Tie Models for Unified Design*. CRC Press, 2017.

[9] O. Sigmund, "A 99 line topology optimization code written in matlab," *Structural and multidisciplinary optimization*, vol. 21, no. 2, pp. 120–127, 2001.

[10] M. Victoria, O. M. Querin, and P. Martí, "Generation of strut-and-tie models by topology design using different material properties in tension and compression," *Structural and Multidisciplinary Optimization*, vol. 44, no. 2, pp. 247–258, 2011.

[11] Q. Q. Liang, B. Uy, and G. P. Steven, "Performance-based optimization for strut-tie modeling of structural concrete," *Journal of structural engineering*, vol. 128, no. 6, pp. 815–823, 2002.

[12] A. R. Mohamed, M. S. Shoukry, and J. M. Saeed, "Prediction of the behavior of reinforced concrete deep beams with web openings using the finite element method," *Alexandria Engineering Journal*, vol. 53, no. 2, pp. 329–339, 2014.

[13] W.-F. Chen and D.-J. Han, *Plasticity for structural engineers*. J. Ross Publishing, 2007.

[14] M. Bruggi, "Generating strut-and-tie patterns for reinforced concrete structures using topology optimization," *Computers & Structures*, vol. 87, no. 23-24, pp. 1483–1495, 2009.

[15] J. Schlaich, K. Schafer, and M. Jennewein, "Towards a consistent design of reinforced concrete structures," *PCI Journal*, vol. 32, no. 3, pp. 74–150, 1987.

[16] W. C. Young, R. G. Budynas, A. M. Sadegh *et al.*, *Roark's formulas for stress and strain*. McGraw-Hill New York, 2002, vol. 7.

[17] S. Bhavikatti, *Finite element analysis*. New Age International, 2005.

[18] O. Sigmund and K. Maute, "Topology optimization approaches," *Structural and Multidisciplinary Optimization*, vol. 48, no. 6, pp. 1031–1055, 2013.

[19] Q. Q. Liang, Y. M. Xie, and G. P. Steven, "Topology optimization of strut-and-tie models in reinforced concrete structures using an evolutionary procedure," Ph.D. dissertation, American Concrete Institute, 2000.

[20] M. Bruggi, "A numerical method to generate optimal load paths in plain and reinforced concrete structures," *Computers & Structures*, vol. 170, pp. 26–36, 2016.

[21] H. A. Eschenauer and N. Olhoff, "Topology optimization of continuum structures: a review," *Applied Mechanics Reviews*, vol. 54, no. 4, pp. 331–390, 2001.

[22] G. I. Rozvany, "A critical review of established methods of structural topology optimization," *Structural and multidisciplinary optimization*, vol. 37, no. 3, pp. 217–237, 2009.

[23] X. Huang and Y.-M. Xie, "A further review of eso type methods for topology optimization," *Structural and Multidisciplinary Optimization*, vol. 41, no. 5, pp. 671–683, 2010.

[24] X. Yang, Y. Xei, G. Steven, and O. Querin, "Bidirectional evolutionary method for stiffness optimization," *AIAA journal*, vol. 37, no. 11, pp. 1483–1488, 1999.

[25] V. S. Almeida, H. L. Simonetti, and L. O. Neto, "Comparative analysis of strut-and-tie models using smooth evolutionary structural optimization," *Engineering Structures*, vol. 56, pp. 1665–1675, 2013.

[26] L. Mai and D.-L. Nguyen, "Density-based optimization for strut-tie modeling," in *2018 4th International Conference on Green Technology and Sustainable Development (GTSD)*. IEEE, 2018, pp. 802–805.

[27] *EN 1992-1-1 Eurocode 2: Design of concrete structures - Part 1-1: General ruels and rules for buildings*, EN. Brussels: CEN, 2005.

A MATLAB SCRIPT FOR SIMP APPROACH

```
%MATLAB Script for the calculation of the topology optimization and
%principal stress calculation
%Script Based on educational script developed by Sigmund [8]
%%Topology Optimization
function [x,sigma,sx,sy]= simp_2(nelx,nely,volfrac,penal,rmin,xdapped,
                            ydapped,xhole,yhole,xdistance,ydistance)
tic
% INITIALIZE
x(1:nely,1:nelx) = volfrac;
%HOLES DEFINITION
for ely = 1:nely
    for elx = 1:nelx
        if (elx > (nelx-xdapped)&& ely <= (ydapped)) || ((elx > xdistance &&
         elx <= xdistance + xhole) && (ely > ydistance && ely <= ydistance + yhole))
            passive(ely,elx) = 1;
            x(ely,elx) = 0.001;
        else
            passive(ely,elx) = 0;
        end
    end
end
loop = 0;
change = 1.;
% START ITERATION
figure
while change > 0.01
    loop = loop + 1;
    xold = x;
% FE-ANALYSIS
    [U]=FE(nelx,nely,x,penal);
% OBJECTIVE FUNCTION AND SENSITIVITY ANALYSIS
    [KE] = lk;
    c = 0.;
    for ely = 1:nely
        for elx = 1:nelx
            %upper left node number (global numbers)
            n1 = (nely+1)*(elx-1)+ely;
            %upper rigth node number (global numbers)
            n2 = (nely+1)* elx +ely;
            Ue = U([2*n1-1;2*n1; 2*n2-1;2*n2; 2*n2+1;2*n2+2; 2*n1+1;2*n1+2],1);
            c = c + x(ely,elx)^penal*Ue'*KE*Ue;
```

```
            dc(ely,elx) = -penal*x(ely,elx)^(penal-1)*Ue'*KE*Ue;
        end
    end
% FILTERING OF SENSITIVITIES
    [dc] = check(nelx,nely,rmin,x,dc);
% DESIGN UPDATE BY THE OPTIMALITY CRITERIA METHOD
    [x] = OC(nelx,nely,x,volfrac,dc,passive);
% PRINT RESULTS
    change = max(max(abs(x-xold)));
    disp([' It.: ' sprintf('%4i',loop) ' Obj.: ' sprintf('%10.4f',c) ...
    ' Vol.: ' sprintf('%6.3f',sum(sum(x))/(nelx*nely)) ...
    ' ch.: ' sprintf('%6.3f',change )])
% PLOT DENSITIES
    colormap(gray); imagesc(-x); axis equal; axis tight; axis off;pause(1e-6);
    if loop > 100
        break
    end
end
toc
%%Principal Stress calculation
tic
sigma=zeros(nelx,nely);
  for ely = 1:nely
        for elx = 1:nelx
            if x(ely,elx)>0.001
                n1 = (nely+1)*(elx-1)+ely;
                n2 = (nely+1)* elx +ely;
                Ue = U([2*n1-1;2*n1; 2*n2-1;2*n2; 2*n2+1;2*n2+2; 2*n1+1;2*n1+2],1);
                [sigma(elx,ely),sx(elx,ely),sy(elx,ely)]=stress(Ue);
            end
        end
  end
  toc
  sigma=-1*sigma';
  figure
  colormap default
  imagesc(sigma)
  colorbar
end
% OPTIMALITY CRITERIA UPDATE
function [xnew]=OC(nelx,nely,x,volfrac,dc,passive)
l1 = 0; l2 = 100000; move = 0.2;
while (l2-l1 > 1e-4)
    lmid = 0.5*(l2+l1);
    xnew = max(0.001,max(x-move,min(1.,min(x+move,x.*sqrt(-dc./lmid)))));
    xnew(find(passive))=0.001;
    if sum(sum(xnew)) - volfrac*nelx*nely > 0
        l1 = lmid;
    else
```

```
        l2 = lmid;
    end
end
end
%MESH-INDEPENDENCY FILTER
function [dcn]=check(nelx,nely,rmin,x,dc)
dcn=zeros(nely,nelx);
for i = 1:nelx
    for j = 1:nely
        sum=0.0;
        for k = max(i-round(rmin),1): min(i+round(rmin),nelx)
            for l = max(j-round(rmin),1): min(j+round(rmin), nely)
                fac = rmin-sqrt((i-k)^2+(j-l)^2);
                sum = sum+max(0,fac);
                dcn(j,i) = dcn(j,i) + max(0,fac)*x(l,k)*dc(l,k);
            end
        end
        dcn(j,i) = dcn(j,i)/(x(j,i)*sum);
    end
end
end
%FE-ANALYSIS
function [U]=FE(nelx,nely,x,penal)

[KE] = lk;
K = sparse(2*(nelx+1)*(nely+1), 2*(nelx+1)*(nely+1));
F = sparse(2*(nely+1)*(nelx+1),1); U = sparse(2*(nely+1)*(nelx+1),1);
for ely = 1:nely
    for elx = 1:nelx
        n1 = (nely+1)*(elx-1)+ely;
        n2 = (nely+1)* elx +ely;
        edof = [2*n1-1; 2*n1; 2*n2-1; 2*n2; 2*n2+1;2*n2+2;2*n1+1; 2*n1+2];
        K(edof,edof) = K(edof,edof) + x(ely,elx)^penal*KE;
    end
end

%Force location should be updated according to needs.
F(floor(nelx-nelx/3)*2*(nely+1)+2,1) = -100000;

%SIMPLY SUPPORTED BEAM
verts=union([2*(nely+1):2*(nely+1):3*2*(nely+1)],[4*(nely+1)-1]);
vertp=2*(nelx+1)*(nely+1):-2*(nely+1):2*(nelx+1)*(nely+1)-4*(nely+1);
fixeddofs = union(verts,vertp);
alldofs = 1:2*(nely+1)*(nelx+1);
freedofs = setdiff(alldofs,fixeddofs);
% SOLVING
U(freedofs,:) = K(freedofs,freedofs) \F(freedofs,:);
U(fixeddofs,:)= 0;

end
```

```
%ELEMENT STIFFNESS MATRIX
function [KE]=lk
E = 25000;
nu = 0.2;
k=[ 1/2-nu/6 1/8+nu/8 -1/4-nu/12 -1/8+3*nu/8 ...
-1/4+nu/12 -1/8-nu/8 nu/6 1/8-3*nu/8];
KE = E/(1-nu^2)*...
[ k(1) k(2) k(3) k(4) k(5) k(6) k(7) k(8)
k(2) k(1) k(8) k(7) k(6) k(5) k(4) k(3)
k(3) k(8) k(1) k(6) k(7) k(4) k(5) k(2)
k(4) k(7) k(6) k(1) k(8) k(3) k(2) k(5)
k(5) k(6) k(7) k(8) k(1) k(2) k(3) k(4)
k(6) k(5) k(4) k(3) k(2) k(1) k(8) k(7)
k(7) k(4) k(5) k(2) k(3) k(8) k(1) k(6)
k(8) k(3) k(2) k(5) k(4) k(7) k(6) k(1)];
end
%Principal Stress calcultaion
function [sigma1,sx,sy] = stress(u)
syms xi eta lambda
a=1; b=1; E=25000; nu=0.2; l=1;
x1=-1; y1=-1;
x2=1; y2=-1;
x3=1; y3=1;
x4=-1; y4=1;
%Symbolic shape functions
n1=1/(4*a*b)*(xi-x2)*(eta-y4);
n2=-1/(4*a*b)*(xi-x1)*(eta-y3);
n3=1/(4*a*b)*(xi-x4)*(eta-y2);
n4=-1/(4*a*b)*(xi-x3)*(eta-y1);
B=zeros(3,8);
N=[n1 n2 n3 n4;n1 n2 n3 n4];
D=E/(1-nu^2)*[1 nu 0; nu 1 0; 0 0 (1-nu)/2];
 gp     = zeros(3,4);
 gp(1,:) = 1.0;
 gp(2,1) = -1.0/sqrt(3.0); gp(3,1) = -1.0/sqrt(3.0);
 gp(2,2) =  1.0/sqrt(3.0); gp(3,2) = -1.0/sqrt(3.0);
 gp(2,3) =  1.0/sqrt(3.0); gp(3,3) =  1.0/sqrt(3.0);
 gp(2,4) = -1.0/sqrt(3.0); gp(3,4) =  1.0/sqrt(3.0);
x=n1*0+n2*1+n3*1+n4*0;
y=n1*0+n2*0+n3*1+n4*1;
J=[ diff(x,xi) diff(y,xi); diff(x,eta) diff(y,eta)];
%Numerical Integration
for k=gp
B=[diff(N(1,:),xi); diff(N(2,:),eta)];
x1  = k(2);
eta1 = k(3);
B=subs(B,xi,x1);
B=subs(B,eta,eta1);
J1=subs(J,xi,x1);
```

```
J1=subs(J1,eta,eta1);
B1=B'*inv(J);
B = zeros(3, 8);
for i=1:2
  B(i, i:2:end) = B1(:,i)';
  end
B(3, 1:2:end) = B1(:,2)'; B(3, 2:2:end) = B1(:,1)';
% Compute stress
stress(:,l) = D*B*u;
l = l +1;
end
sx=mean(stress(1,:));
sy=mean(stress(2,:));
sxy=mean(stress(3,:));
sigma=[sx-lambda sxy; sxy sy-lambda];
h=det(sigma);
sigma1=roots(sym2poly(h));
sigma1=sigma1(1);
end
```

B MATLAB SCRIPT FOR BESO APPROACH

```
%MATLAB Script for the calculation of the topology optimization and
%principal stress calculation
%Script Based on educational script developed by Huang and  Xie [23] which is
%based on the one proposed by Sigmund [8].
%%Topology Optimization
function [x,sigma]= sbeso_2(nelx,nely,volfrac,er,rmin,xdapped,ydapped,xhole,
                    yhole,xdistance,ydistance)
tic
% INITIALIZE
x(1:nely,1:nelx) = volfrac; vol=1; i=0; change=1;penal=3;
%HOLES DEFINITION
for ely = 1:nely
    for elx = 1:nelx
        if (elx > (nelx-xdapped)&& ely <= (ydapped)) ||((elx > xdistance &&
        elx <= xdistance + xhole) && (ely > ydistance && ely <= ydistance + yhole))
            passive(ely,elx) = 1;
            x(ely,elx) = 0.001;
        else
            passive(ely,elx) = 0;
        end
    end
end
figure
vol=1;
% START ITERATION
while change > 0.001
%while vol > volfrac
i = i + 1;
    vol=max(vol*(1-er),volfrac);
    if i>1
        olddc=dc;
    end
% FE-ANALYSIS
    [U]=FE(nelx,nely,x,penal);
% OBJECTIVE FUNCTION AND SENSITIVITY ANALYSIS
    [KE] = lk;
    c(i) = 0;
    for ely = 1:nely
        for elx = 1:nelx
            n1 = (nely+1)*(elx-1)+ely;
            n2 = (nely+1)* elx +ely;
```

```
            Ue = U([2*n1-1;2*n1; 2*n2-1;2*n2; 2*n2+1;2*n2+2; 2*n1+1;2*n1+2],1);
            c(i) = c(i) + 0.5*x(ely,elx)^penal*Ue'*KE*Ue;
            dc(ely,elx) = 0.5*x(ely,elx)^(penal-1)*Ue'*KE*Ue;
        end
    end
% FILTERING OF SENSITIVITIES
    [dc] = check(nelx,nely,rmin,x,dc);
%Stabilization of evolutionary process
    if i>1
        dc=(dc+olddc)/2;
    end
% BESO DESIGN UPDATE
    [x] = ADDDEL(nelx,nely,vol,dc,x,passive);
% PRINT RESULTS
    if i>10
    change = abs(sum(c(i-9:i-5))-sum(c(i-4:i)))/sum(c(i-4:i));
    end
    disp([' It.: ' sprintf('%4i',i) ' Obj.: ' sprintf('%10.4f',c(i)) ...
    ' Vol.: ' sprintf('%6.3f',sum(sum(x))/(nelx*nely)) ...
    ' ch.: ' sprintf('%6.3f',change )])
% PLOT DENSITIES
    colormap(gray); imagesc(-x); axis equal; axis tight; axis off;pause(1e-5);
    vol=sum(sum(x))/(nelx*nely);
end
toc
%%Principal Stress calculation
tic
sigma=zeros(nelx,nely);
  for ely = 1:nely
        for elx = 1:nelx
            if x(ely,elx)>0.001
                n1 = (nely+1)*(elx-1)+ely;
                n2 = (nely+1)* elx +ely;
                Ue = U([2*n1-1;2*n1; 2*n2-1;2*n2; 2*n2+1;2*n2+2; 2*n1+1;2*n1+2],1);
                sigma(elx,ely)=stress(Ue);
            end
        end
  end
  sigma=sigma';
  figure
  colormap default
  imagesc(-sigma)
  colorbar
  toc
end
%OPTIMALITY CRITERIA UPDATE
function [x]=ADDDEL(nelx,nely,volfra,dc,x,passive)
l1=min(min(dc));
l2=max(max(dc));
```

```
while ((l2-l1)/l2 > 1.0e-4)
    th=(l1+l2)/2;
    x=max(0.001,sign(dc-th));
    x(find(passive))=0.001;
    if sum(sum(x))-volfra*(nelx*nely) > 0;
        l1=th;
    else
        l2=th;
    end
end
end
%MESH-INDEPENDENCY FILTER
function [dcf]=check(nelx,nely,rmin,x,dc)
dcf=zeros(nely,nelx);
for i = 1:nelx
    for j = 1:nely
        sum=0.0;
        for k = max(i-floor(rmin),1): min(i+floor(rmin),nelx)
            for l = max(j-floor(rmin),1): min(j+floor(rmin), nely)
                fac = rmin-sqrt((i-k)^2+(j-l)^2);
                sum = sum+max(0,fac);
                dcf(j,i) = dcf(j,i) + max(0,fac)*dc(l,k);
            end
        end
        dcf(j,i) = dcf(j,i)/sum;
    end
end
end
%FE-ANALYSIS
function [U]=FE(nelx,nely,x,penal)
[KE] = lk;
K = sparse(2*(nelx+1)*(nely+1), 2*(nelx+1)*(nely+1));
F = sparse(2*(nely+1)*(nelx+1),1); U = zeros(2*(nely+1)*(nelx+1),1);
for elx = 1:nelx
    for ely = 1:nely
        n1 = (nely+1)*(elx-1)+ely;
        n2 = (nely+1)* elx +ely;
        edof = [2*n1-1; 2*n1; 2*n2-1; 2*n2; 2*n2+1;2*n2+2;2*n1+1; 2*n1+2];
        K(edof,edof) = K(edof,edof) + x(ely,elx)^penal*KE;
    end
end
%Loaction of forces should be updated according to needs.
F((nely+1)*2*22+2,1)=-100000;
%SIMPLY SUPPORTED BEAM
verts=union([2*(nely+1):2*(nely+1):2*3*(nely+1)],[4*(nely+1)-1]);
vertp=2*(nelx+1)*(nely+1):-2*(nely+1):2*(nelx+1)*(nely+1)-4*(nely+1);
fixeddofs = union(verts,vertp);
alldofs = 1:2*(nely+1)*(nelx+1);
freedofs = setdiff(alldofs,fixeddofs);
```

```
% SOLVING
U(freedofs,:) = K(freedofs,freedofs) \F(freedofs,:);
U(fixeddofs,:)= 0;
end
% ELEMENT STIFFNESS MATRIX
function [KE]=lk
E = 25000;
nu = 0.2;
k=[ 1/2-nu/6 1/8+nu/8 -1/4-nu/12 -1/8+3*nu/8 ...
-1/4+nu/12 -1/8-nu/8 nu/6 1/8-3*nu/8];
KE = E/(1-nu^2)*...
[ k(1) k(2) k(3) k(4) k(5) k(6) k(7) k(8)
k(2) k(1) k(8) k(7) k(6) k(5) k(4) k(3)
k(3) k(8) k(1) k(6) k(7) k(4) k(5) k(2)
k(4) k(7) k(6) k(1) k(8) k(3) k(2) k(5)
k(5) k(6) k(7) k(8) k(1) k(2) k(3) k(4)
k(6) k(5) k(4) k(3) k(2) k(1) k(8) k(7)
k(7) k(4) k(5) k(2) k(3) k(8) k(1) k(6)
k(8) k(3) k(2) k(5) k(4) k(7) k(6) k(1)];
end
%STRESS CALCULATION
function [sigma1] = stress(u)
syms xi eta lambda
a=1; b=1; E=25000; nu=0.2; l=1;
x1=-1; y1=-1;
x2=1; y2=-1;
x3=1; y3=1;
x4=-1; y4=1;
%Symbolic shape functions
n1=1/(4*a*b)*(xi-x2)*(eta-y4);
n2=-1/(4*a*b)*(xi-x1)*(eta-y3);
n3=1/(4*a*b)*(xi-x4)*(eta-y2);
n4=-1/(4*a*b)*(xi-x3)*(eta-y1);
B=zeros(3,8);
N=[n1 n2 n3 n4;n1 n2 n3 n4];
D=E/(1-nu^2)*[1 nu 0; nu 1 0; 0 0 (1-nu)/2];
 gp     = zeros(3,4);
 gp(1,:) = 1.0;
 gp(2,1) = -1.0/sqrt(3.0); gp(3,1) = -1.0/sqrt(3.0);
 gp(2,2) =  1.0/sqrt(3.0); gp(3,2) = -1.0/sqrt(3.0);
 gp(2,3) =  1.0/sqrt(3.0); gp(3,3) =  1.0/sqrt(3.0);
 gp(2,4) = -1.0/sqrt(3.0); gp(3,4) =  1.0/sqrt(3.0);
x=n1*0+n2*1+n3*1+n4*0;
y=n1*0+n2*0+n3*1+n4*1;
J=[ diff(x,xi) diff(y,xi); diff(x,eta) diff(y,eta)];
%Numerical Integration
for k=gp
B=[diff(N(1,:),xi); diff(N(2,:),eta)];
x1  = k(2);
```

```
eta1 = k(3);
B=subs(B,xi,x1);
B=subs(B,eta,eta1);
J1=subs(J,xi,x1);
J1=subs(J1,eta,eta1);
B1=B'*inv(J);

B = zeros(3, 8);
for i=1:2
  B(i, i:2:end) = B1(:,i)';
  end
B(3, 1:2:end) = B1(:,2)'; B(3, 2:2:end) = B1(:,1)';
% Compute stress
stress(:,l) = D*B*u;
l = l +1;
end
sx=mean(stress(1,:));
sy=mean(stress(2,:));
sxy=mean(stress(3,:));
sigma=[sx-lambda sxy; sxy sy-lambda];
h=det(sigma);
sigma1=roots(sym2poly(h));
sigma1=sigma1(1);
end
```

C PRINCIPAL STRESS DIAGRAMS FOR ALL THE STUDIED CASES

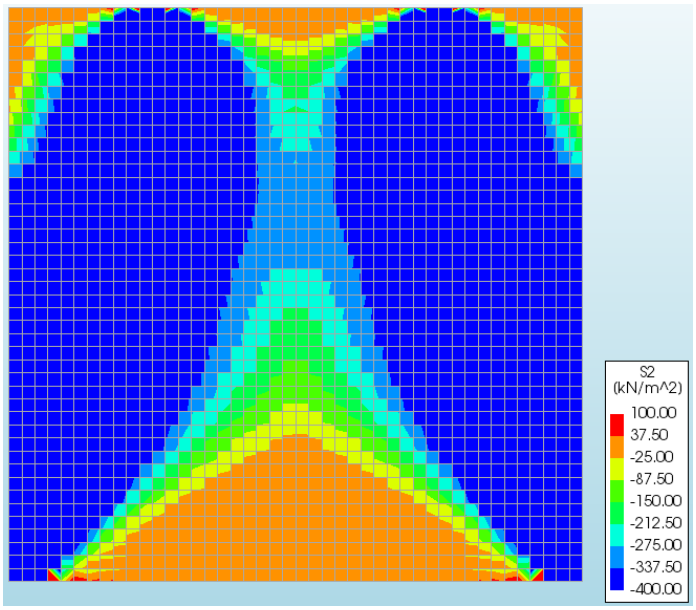

Figure C.1: Principal stresses Case 1

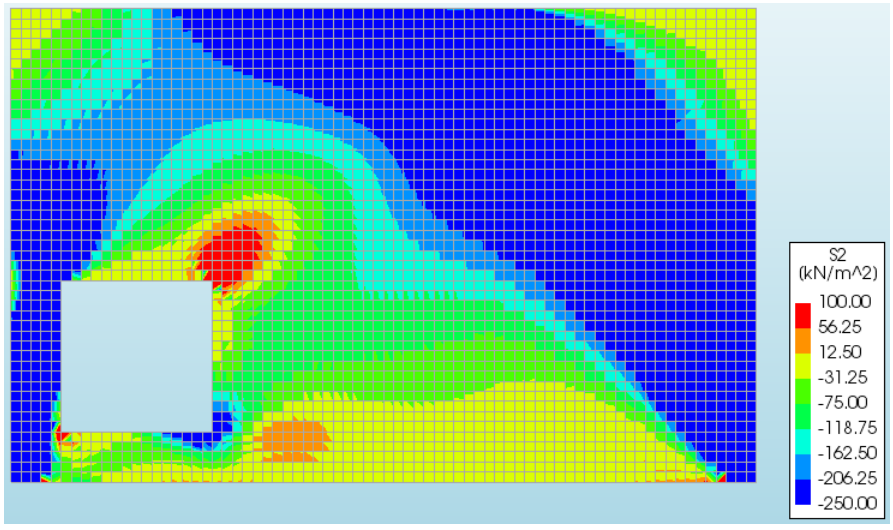

Figure C.2: Principal stresses Case 2

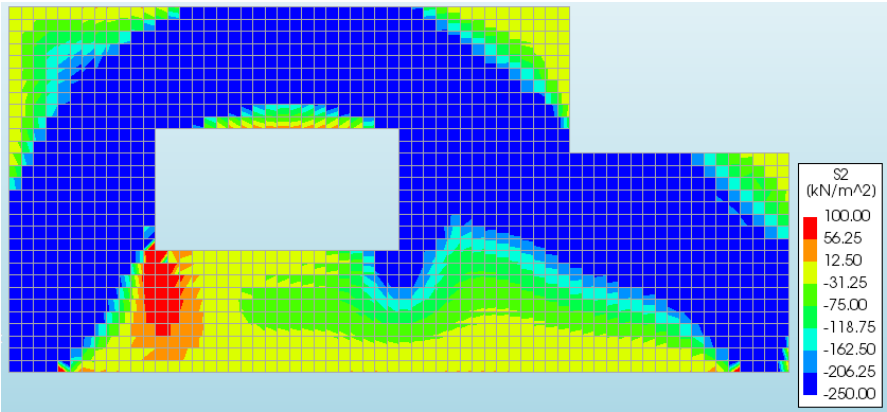

Figure C.3: Principal stresses Case 3

D TOTAL AMOUNT OF REINFORCEMENT FOR EACH CASE

Table D.1: Total amount of reinforcement steel for trusses Case 1

Case	**Total tension [KN]**	**Fy [MPA]**	**As (req) [mm2]**
SIMPApproach	25.97	420	71.11
BESO Approach	28.57	420	78.23
STM	42.74	420	117.03

Table D.2: Total amount of reinforcement steel for trusses Case 2

Case	**Total tension [KN]**	**Fy [MPA]**	**As (req) [mm2]**
SIMP Approach	111.67	420	305.76
BESO Approach	128.10	420	350.75
STM	210.56	420	576.53

Table D.3: Total amount of reinforcement steel for trusses Case 3

	Case	Total tension [kN]	Fy [MPA]	As (req) [mm2]
SIMP	Alternative 1	114.02	420	312.20
	Alternative 2	174.94	420	479.00
	Alternative 3	182.02	420	498.39
	Alternative 4	167.23	420	457.89
BESO	Alternative 1	134.62	420	368.60
	Alternative 2	130.86	420	358.31
	Alternative 3	145.20	420	397.57
LITERATURE	STM N-S	403.53	420	1104.90
	STM Zhong et al.	269.84	420	738.85

E AXIAL FORCES FOR STM FROM THE LITERATURE.

Table E.1: Summary of axial forces for STM from the Literature [8]. Case 1

Element	Force (KN)	Length (M)
A	-100.00	2.05
B	-100.00	2.05
C	-42.74	2.2
D	-108.75	2.4
E	-108.75	2.4
F	42.74	4.2

Table E.2: Summary of axial forces for STM from the Literature [8]. Case 2

Element	Force (KN)	Length (M)	Element	Force (KN)	Length (M)
A	-21.54	4.39	K	10.24	0.99
B	-7.77	1.62	L	-10.65	0.99
B.1	-7.32	1.61	M	-14.48	1.4
B.2	-3.09	0.51	N	19.22	0.99
C	-23.78	1.54	O	20.89	0.99
C.1	-25.74	1.5	P	20.89	1.1
C.2	8.24	1	Q	19.22	0.99
D	-8.81	1.04	R	-14.73	1.48
D.1	-7.32	0.91	S	-9.25	0.99
D.2	-14.73	1.48	T	-34.38	2.23
E	-21.61	4.31	U	9.73	1.13
F	-23.47	4.85	V	10.95	1.1
F.1	-26.38	2	W	-12.52	1.57
F.2	-24.03	2	X	8.31	1.81
G	-24.15	1.61	Y	32.46	3.16
H	30.26	5.34	Z	-23.62	1.49
I	-14.77	1.43	Z.1	-25.84	1.52
J	10.65	1.03	Z1.2	9.50	1.04

Table E.3: Summary of axial forces for STM proposed by Novak-Sprenger [2]. Case 3

Element	Force (KN)	Length (M)	Element	Foce (KN)	Length (M)
A	-90.95	1.4	N	15.83	0.84
B	-90.95	1.4	O	-8.63	0.95
C	44.55	2.34	P	-24.79	1.26
D	-59.06	1.6	Q	59.14	0.95
E	-59.06	1.6	R	15.83	0.84
F	-50.00	0.84	S	-27.71	1.09
G	31.43	1.11	T	-24.79	1.37
H	-25.53	1.38	U	78.21	2.18
I	20.03	1.11	V	-37.05	1.09
J	15.83	0.84	W	-53.5	1.37
K	11.40	1.06	X	34.17	0.84
L	-25.53	1.34	Y	-50.4	1.23
M	40.06	1.06	Z	37.05	0.91

Table E.4: Summary of axial forces for STM proposed by Zhong et al. [2]. Case 3

Element	Force (KN)	Length (M)	Element	Force (KN)	Length (M)
A	0.00	1.99	M	-21.22	1.44
B	-82.84	0.23	N	25.13	1.17
C	8.50	1.89	O	13.95	0.84
D	-12.48	1.1	P	18.54	2.47
E	-96.76	1.3	Q	-41.15	2.61
F	-96.76	1.3	R	63.84	2.47
G	39.17	2.44	S	-7.60	0.84
H	-67.93	1.51	T	-25.83	1.31
I	-22.28	1.26	U	13.52	1.56
J	-47.48	2.04	V	52.66	2.57
K	-50.00	0.84	W	-63.81	1.51
L	34.53	1.17			

F POSITION OF NODES FOR THE SENSITIVITY ANALYSIS.

All the possible combinations of coordinates that were analyzed in the sensitivity analysis with their corresponding force are presented in this section. The coordinates correspond to the analyzed positions of nodes given in Section 3.5

Table F.1: Coordinates for sensitivity analysis using the SIMP approach Case 2 (1/2)

Coordinates point 1		Coordinates point 2		Coordinates point 3		Force
X	Y	X	Y	X	Y	[%]
0.6	3.33	2.6	1.37	3.7	0	0.037
0.6	3.33	2.6	1.37	3.46	0	3.96
0.6	3.33	2.6	1.37	3.86	0.18	5.22
0.6	3.33	2.6	1.37	3.93	0	2.93
0.6	3.33	2.86	1.24	3.7	0	3.14
0.6	3.33	2.86	1.24	3.46	0	8.77
0.6	3.33	2.86	1.24	3.86	0.18	3.51
0.6	3.33	2.86	1.24	3.94	0	0.81
0.6	3.33	2.85	1.51	3.7	0	9.4
0.6	3.33	2.85	1.51	3.46	0	15.1
0.6	3.33	2.85	1.51	3.86	0.18	3.11
0.6	3.33	2.85	1.51	3.94	0	5.23
0.6	3.33	2.77	1.39	3.7	0	4.33
0.6	3.33	2.77	1.39	3.46	0	9.38
0.6	3.33	2.77	1.39	3.86	0.18	1.58
0.6	3.33	2.77	1.39	3.94	0	0.73
0.6	3.33	2.89	1.36	3.7	0	6.92
0.6	3.33	2.89	1.36	3.46	0	12.94
0.6	3.33	2.89	1.36	3.86	0.18	0.21
0.6	3.33	2.89	1.36	3.94	0	2.64
0.66	3.19	2.6	1.37	3.7	0	0.06
0.66	3.19	2.6	1.37	3.46	0	3.66
0.66	3.19	2.6	1.37	3.86	0.18	5.22
0.66	3.19	2.6	1.37	3.94	0	2.98
0.66	3.19	2.86	1.24	3.7	0	2.71
0.66	3.19	2.86	1.24	3.46	0	8

Table F.2: Coordinates for sensitivity analysis using the SIMP approach Case 2 (2/2)

Coordinates point 1		Coordinates point 2		Coordinates point 3		Force
X	Y	X	Y	X	Y	[%]
0.66	3.19	2.86	1.24	3.86	0.18	3.81
0.66	3.19	2.86	1.24	3.94	0	1.15
0.66	3.19	2.85	1.51	3.7	0	8.92
0.66	3.19	2.85	1.51	3.46	0	14.3
0.66	3.19	2.85	1.51	3.86	0.18	2.75
0.66	3.19	2.85	1.51	3.94	0	4.82
0.66	3.19	2.77	1.39	3.7	0	4.07
0.66	3.19	2.77	1.39	3.46	0	8.78
0.66	3.19	2.77	1.39	3.86	0.18	1.8
0.66	3.19	2.77	1.39	3.94	0	0.48
0.66	3.19	2.89	1.36	3.7	0	6.4
0.66	3.19	2.89	1.36	3.46	0	12.07
0.66	3.19	2.89	1.36	3.86	0.18	0.17
0.66	3.19	2.89	1.36	3.94	0	2.21
0.74	3.29	2.6	1.37	3.7	0	1.84
0.74	3.29	2.6	1.37	3.46	0	1.76
0.74	3.29	2.6	1.37	3.86	0.18	6.96
0.74	3.29	2.6	1.37	3.94	0	4.68
0.74	3.29	2.86	1.24	3.7	0	0.82
0.74	3.29	2.86	1.24	3.46	0	5.93
0.74	3.29	2.86	1.24	3.86	0.18	5.62
0.74	3.29	2.86	1.24	3.94	0	2.9
0.74	3.29	2.85	1.51	3.7	0	6.8
0.74	3.29	2.85	1.51	3.46	0	12
0.74	3.29	2.85	1.51	3.86	0.18	0.7
0.74	3.29	2.85	1.51	3.94	0	2.83
0.74	3.29	2.77	1.39	3.7	0	2.14
0.74	3.29	2.77	1.39	3.46	0	6.69
0.74	3.29	2.77	1.39	3.86	0.18	3.68
0.74	3.29	2.77	1.39	3.94	0	1.34
0.74	3.29	2.89	1.36	3.7	0	4.38
0.74	3.29	2.89	1.36	3.46	0	9.86
0.74	3.29	2.89	1.36	3.86	0.18	2.11
0.74	3.29	2.89	1.36	3.94	0	1

Table F.3: Coordinates for sensitivity analysis using the BESO approach Case 2 (1/2)

Coordinates point 1		Coordinates point 2		Coordinates point 3		Force
X	Y	X	Y	X	Y	[%]
0.96	3.59	1.83	2.07	3.29	1.08	0.026
0.96	3.59	1.83	2.07	3.24	0.99	2.42
0.96	3.59	1.83	2.07	3.21	1.13	0.064
0.96	3.59	1.83	2.07	3.32	1.17	2.31
0.96	3.59	1.83	2.07	3.38	1.05	0.62
0.96	3.59	1.76	2.19	3.29	1.08	2.63
0.96	3.59	1.76	2.19	3.24	0.99	4.93
0.96	3.59	1.76	2.19	3.21	1.13	2.79
0.96	3.59	1.76	2.19	3.32	1.17	0.5
0.96	3.59	1.76	2.19	3.38	1.05	2.01
0.96	3.59	1.93	2.16	3.29	1.08	5.89
0.96	3.59	1.93	2.16	3.24	0.99	8.36
0.96	3.59	1.93	2.16	3.21	1.13	6.17
0.96	3.59	1.93	2.16	3.32	1.17	3.62
0.96	3.59	1.93	2.16	3.38	1.05	5.13
0.96	3.59	1.94	1.99	3.29	1.08	0.22
0.96	3.59	1.94	1.99	3.24	0.99	2.41
0.96	3.59	1.94	1.99	3.21	1.13	0.13
0.96	3.59	1.94	1.99	3.32	1.17	2.68
0.96	3.59	1.94	1.99	3.38	1.05	0.85
1.06	3.66	1.83	2.07	3.29	1.08	0.38
1.06	3.66	1.83	2.07	3.24	0.99	2.88
1.06	3.66	1.83	2.07	3.21	1.13	0.51
1.06	3.66	1.83	2.07	3.32	1.17	1.94
1.06	3.66	1.83	2.07	3.38	1.05	0.26
1.06	3.66	1.76	2.19	3.29	1.08	1.7
1.06	3.66	1.76	2.19	3.24	0.99	4
1.06	3.66	1.76	2.19	3.21	1.13	1.86
1.06	3.66	1.76	2.19	3.32	1.17	0.43
1.06	3.66	1.76	2.19	3.38	1.05	1.07
1.06	3.66	1.93	2.16	3.29	1.08	4.99
1.06	3.66	1.93	2.16	3.24	0.99	7.45
1.06	3.66	1.93	2.16	3.21	1.13	5.26
1.06	3.66	1.93	2.16	3.32	1.17	2.71
1.06	3.66	1.93	2.16	3.38	1.05	4.21
1.06	3.66	1.94	1.99	3.29	1.08	1
1.06	3.66	1.94	1.99	3.24	0.99	1.64
1.06	3.66	1.94	1.99	3.21	1.13	0.91
1.06	3.66	1.94	1.99	3.32	1.17	3.46
1.06	3.66	1.94	1.99	3.38	1.05	1.63

Table F.4: Coordinates for sensitivity analysis using the BESO approach Case 2 (2/2)

Coordinates point 1		Coordinates point 2		Coordinates point 3		Force [%]
X	Y	X	Y	X	Y	
1.04	3.5	1.83	2.07	3.29	1.08	2.42
1.04	3.5	1.83	2.07	3.24	0.99	4.87
1.04	3.5	1.83	2.07	3.21	1.13	2.51
1.04	3.5	1.83	2.07	3.32	1.17	0.13
1.04	3.5	1.83	2.07	3.38	1.05	1.82
1.04	3.5	1.76	2.19	3.29	1.08	5.41
1.04	3.5	1.76	2.19	3.24	0.99	7.7
1.04	3.5	1.76	2.19	3.21	1.13	5.56
1.04	3.5	1.76	2.19	3.32	1.17	3.28
1.04	3.5	1.76	2.19	3.38	1.05	4.78
1.04	3.5	1.93	2.16	3.29	1.08	8.56
1.04	3.5	1.93	2.16	3.24	0.99	9.48
1.04	3.5	1.93	2.16	3.21	1.13	8.84
1.04	3.5	1.93	2.16	3.32	1.17	6.29
1.04	3.5	1.93	2.16	3.38	1.05	7.79
1.04	3.5	1.94	1.99	3.29	1.08	2.04
1.04	3.5	1.94	1.99	3.24	0.99	4.68
1.04	3.5	1.94	1.99	3.21	1.13	2.13
1.04	3.5	1.94	1.99	3.32	1.17	0.42
1.04	3.5	1.94	1.99	3.38	1.05	1.41

Table F.5: Coordinates for sensitivity analysis using the SIMP approach Case 3 (1/2)

Coordinates point 1		Coordinates point 2		Coordinates point 3		Force
X	Y	X	Y	X	Y	[%]
0	1	3.24	0	5.65	1	0.1
0	1	3.24	0	5.36	0.89	0.11
0	1	3.24	0	5.5	0.73	0.12
0	1	3.24	0	5.81	0.74	0.12
0	1	3.04	0	5.65	1	3.03
0	1	3.04	0	5.36	0.89	3.24
0	1	3.04	0	5.5	0.73	3.58
0	1	3.04	0	5.81	0.74	3.52
0	1	3.1	0.25	5.65	1	13.02
0	1	3.1	0.25	5.36	0.89	14.23
0	1	3.1	0.25	5.5	0.73	16.35
0	1	3.1	0.25	5.81	0.74	15.99
0.39	0.81	3.24	0	5.65	1	51.85
0.39	0.81	3.24	0	5.36	0.89	55.28
0.39	0.81	3.24	0	5.5	0.73	61.82

Table F.6: Coordinates for sensitivity analysis using the SIMP approach Case 3 (2/2)

Coordinates point 1		Coordinates point 2		Coordinates point 3		Force
X	Y	X	Y	X	Y	[%]
0.39	0.81	3.24	0	5.81	0.74	61.19
0.39	0.81	3.04	0	5.65	1	49.02
0.39	0.81	3.04	0	5.36	0.89	52.04
0.39	0.81	3.04	0	5.5	0.73	57.74
0.39	0.81	3.04	0	5.81	0.74	57.2
0.39	0.81	3.1	0.25	5.65	1	78.38
0.39	0.81	3.1	0.25	5.36	0.89	85.38
0.39	0.81	3.1	0.25	5.5	0.73	99.57
0.39	0.81	3.1	0.25	5.81	0.74	98.17
0.43	0.98	3.24	0	5.65	1	43.56
0.43	0.98	3.24	0	5.36	0.89	46.48
0.43	0.98	3.24	0	5.5	0.73	51.35
0.43	0.98	3.24	0	5.81	0.74	50.55
0.43	0.98	3.04	0	5.65	1	40.63
0.43	0.98	3.04	0	5.36	0.89	43.15
0.43	0.98	3.04	0	5.5	0.73	47.3
0.43	0.98	3.04	0	5.81	0.74	46.62
0.43	0.98	3.1	0.25	5.65	1	64.68
0.43	0.98	3.1	0.25	5.36	0.89	70.29
0.43	0.98	3.1	0.25	5.5	0.73	80.11
0.43	0.98	3.1	0.25	5.81	0.74	78.45
0.4	1.15	3.24	0	5.65	1	27.67
0.4	1.15	3.24	0	5.36	0.89	29.57
0.4	1.15	3.24	0	5.5	0.73	32.38
0.4	1.15	3.24	0	5.81	0.74	31.72
0.4	1.15	3.04	0	5.65	1	24.79
0.4	1.15	3.04	0	5.36	0.89	26.35
0.4	1.15	3.04	0	5.5	0.73	28.65
0.4	1.15	3.04	0	5.81	0.74	28.11
0.4	1.15	3.1	0.25	5.65	1	43.64
0.4	1.15	3.1	0.25	5.36	0.89	47.4
0.4	1.15	3.1	0.25	5.5	0.73	53.16
0.4	1.15	3.1	0.25	5.81	0.74	51.78
0.27	0.97	3.24	0	5.65	1	28.75
0.27	0.97	3.24	0	5.36	0.89	30.73
0.27	0.97	3.24	0	5.5	0.73	34.06
0.27	0.97	3.24	0	5.81	0.74	33.53
0.27	0.97	3.04	0	5.65	1	25.8
0.27	0.97	3.04	0	5.36	0.89	27.45
0.27	0.97	3.04	0	5.5	0.73	30.2
0.27	0.97	3.04	0	5.81	0.74	29.77
0.27	0.97	3.1	0.25	5.65	1	47.36
0.27	0.97	3.1	0.25	5.36	0.89	51.59
0.27	0.97	3.1	0.25	5.5	0.73	59.11
0.27	0.97	3.1	0.25	5.81	0.74	57.89